TECHNISCHE UNIVERSITÄT
ILMENAU

Radio Resource Allocation for Overlay D2D-based Vehicular Communications in Future Wireless Networks

PhD Thesis

BY

Dariush Mohammad Soleymani

Reviewers

Prof. Dr.-Ing. Giovanni Del Galdo

Prof. Dr.rer.nat. Jochen Seitz

Prof. Dr.-Ing. Jens Mückenheim

A dissertation to obtain the academic degree Doktoringenieur (Dr.-Ing.)
Electrical Engineering and Information Technology, TU Ilmenau

submitted on: 19.10.2021
defended on: 25.03.2022

urn:nbn:de:gbv:ilm1-2022000083
DOI: 10.22032/dbt.51719

TECHNISCHE UNIVERSITÄT
ILMENAU

Radio Resource Allocation for Overlay D2D-based Vehicular Communications in Future Wireless Networks

Dissertation

von

Dariush Mohammad Soleymani

Gutachter

Prof. Dr.-Ing. Giovanni Del Galdo

Prof. Dr.rer.nat. Jochen Seitz

Prof. Dr.-Ing. Jens Mückenheim

Dissertation zur Erlangung des akademischen Grades Doktoringenieur (Dr.-Ing.)
Fakultät für Elektrotechnik und Informationstechnik, TU Ilmenau

eingereicht am: 19.10.2021
verteidigt am: 25.03.2022

urn:nbn:de:gbv:ilm1-2022000083
DOI: 10.22032/dbt.51719

Abstract

Next-generation cellular networks are envisioned to enable widely Device-to-Device (D2D) communication. For many applications in the D2D domain, deterministic communication latency and high reliability are of exceptionally high importance. The proximity service provided by D2D communication is a promising feature that can fulfill the reliability and latency requirements of emerging vertical applications. One of the prominent vertical applications is vehicular communication, in which the vehicles disseminate safety messages directly through D2D communication, resulting in the fatality rate reduction due to a possible collision.

Radio resource allocation techniques in D2D communication have recently gained much attention in industry and academia, through which the valuable radio resources are allocated more efficiently. In addition to the resource allocation techniques, energy sustainability is highly important and is usually considered in conjunction with the resource allocation approach. This dissertation is dedicated to studying different avenues of the radio resource allocation and energy efficiency techniques in Long Term Evolution (LTE) and New Radio (NR) Vehicle-to-Everthings (V2X) communications. In the following, we briefly describe the core ideas in this study.

Mostly, the D2D applications are characterized by relatively small traffic payload size, and in LTE, due to coarse granularity of the subframe, the radio resources can not be utilized efficiently. Particularly, in the case of semi-persistent scheduling when a radio resource is scheduled for a longer time in the overlay D2D, the radio resources are underutilized for the such applications. To address this problem, a hierarchical radio resource management scheme, i.e., a sub-granting scheme, is proposed by which nearby cellular users, i.e., beneficiary users, are allowed to reuse the unused radio resource indicated by sub-granting signaling. The proposed scheme is evaluated and compared with shortening Transmission Time Interval (TTI) schemes in terms of cell throughput. Then, the beneficiary user selection problem is investigated and is cast as a maximization problem of uplink cell throughput subject to reliability and latency requirements. A heuristic centralized, i.e., dedicated sub-granting radio resource Dedicated Sub-Granting Radio Resource (DSGRR) algorithm is proposed to address the original beneficiary user selection problem. The simulation results and analysis show the superiority of the proposed DSGRR algorithm over the random beneficiary user selection algorithm in term of the cell throughput in a scenario with stationary users. Further, the beneficiary user selection problem is investigated in a scenario that all users are moving in a dynamic environment. We evaluate the sub-granting signaling overhead due to mobility in the DSGRR, and then a distributed heuristics algorithm, i.e., Open Sub-Granting Radio Resource (OSGRR), is proposed and compared with the DSGRR algorithm and no sub-granting case. Simulation results show improved cell throughput for the OSGRR compared with other algorithms. Besides, it is observed that the overhead incurred by the OSGRR is less than the DSGRR while the achieved cell throughput is yet close to the maximum achievable uplink cell throughput.

Also, joint resource allocation and energy efficiency in autonomous resource selection in NR, i.e. Mode 2, is examined. The autonomous resource selection is formulated as a ratio of sum-rate and energy consumption. The objective is to minimize the energy efficiency of the power-saving users subject to reliability and latency requirements. A heuristic algorithm, density of traffic-based resource allocation (DeTRA), is proposed to solve the problem. The proposed algorithm splits the resource pool based on the traffic

density per traffic type. The random selection is then mandated to be performed on the dedicated resource pool upon arrival of the aperiodic traffic is triggered. The simulation results show that the proposed algorithm achieves the same packet reception ratio (PRR) value as the sensing-based algorithm. In addition, per-user power consumption is reduced, and consequently, the energy efficiency is improved by applying the DeTRA algorithm.

The research in this study leverages radio resource allocation techniques in LTE based D2D communications to be utilized radio resources more efficiently. In addition, the conducted research paves a way to study further how the power-saving users would optimally select the radio resources with minimum energy consumption in NR V2X communications.

Zusammenfassung

Mobilfunknetze der nächsten Generation ermöglichen einen weitverbreiteten Einsatz von Device-to-Device Kommunikation, der direkten Kommunikation zwischen zellularen Endgeräten. Für viele Anwendungsfälle zur direkten Kommunikation zwischen Endgeräten sind eine deterministische Latenz und die hohe Zuverlässigkeit von zentraler Bedeutung. Dienste zur direkten Kommunikation (D2D) für in der Nähe befindliche Endgeräte sind vielversprechend die hohen Anforderungen an Latenz und Zuverlässigkeit für zukünftige vertikale Anwendungen zu erfüllen.

Eine der herausragenden vertikalen Anwendungen ist die Fahrzeugkommunikation, bei der die Fahrzeuge sicherheitskritische Meldungen direkt über D2D-Kommunikation austauschen, die dadurch zur Reduktion von Verkehrsunfällen und gleichzeitig von Todesfällen im Straßenverkehrt beiträgt. Neue Techniken zur effizienteren Zuweisung von Funkressourcen in derD2D-Kommunikation haben in letzter Zeit in Industrie und Wissenschaft große Aufmerksamkeit erlangt. Zusätzlich zur Allokation von Ressourcen, wird die Energieeffizienz zunehmend wichtiger, die normalerweise im Zusammenhang mit der Ressourcenallokation behandelt wird. Diese Dissertation untersucht verschiedener Ansätze der Funkressourcenzuweisung und Energieeffizienztechniken in der LTE und NR V2X Kommunikation. Im Folgenden beschreiben wir kurz die Kernideen der Dissertation.

Meist zeichnen sich D2D-Anwendungen durch ein relativ geringes Datenvolumen aus, die über Funkressourcen übertragen werden. In LTE können diese Funkressourcen aufgrund der groben Granularität für die Ressourcenzuweisung nicht effizient genutzt werden. Insbesondere beim semi-persistenten Scheduling, bei dem eine Funkressource über einen längeren Zeitraum im Overlay D2D festgelegt wird, sind die Funkressourcen für solche Anwendungen nicht ausgelastet. Um dieses Problem zu lösen, wird eine hierarchische Form für das Management der Funkressourcen, ein sogenanntes Subgranting-Schema, vorgeschlagen. Dabei kann ein nahegelegener zellularer Nutzer, der sogenannte begünstigte Nutzer, ungenutzten Funkressourcen, die durch Subgranting-Signalisierung angezeigt werden, wiederzuverwenden. Das vorgeschlagene Schema wird bewertet und mit "shortening TTI", einen Schema mit reduzierten Sendezeitintervallen, in Bezug auf den Zellendurchsatz verglichen. Als nächster Schritt wird untersucht, wie der begünstigten Benutzer ausgewählt werden kann und als Maximierungsproblem des Zellendurchsatzes im Uplink unter Berücksichtigung von Zuverlässigkeits- und Latenzanforderungen dargestellt. Dafür wird ein heuristischer zentralisierter, d.h. dedizierter Sub-Granting-Radio-Ressource DSGRR-Algorithmus vorgeschlagen. Die Simulationsergebnisse und die Analyse ergeben in einem Szenario mit stationären Nutzern eine Erhöhung des Zelldurchsatzes bei dem Einsatz des vorgeschlagenen DSGRR-Algorithmus im Vergleich zu einer zufälligen Auswahl von Nutzern. Zusätzlich wird das Problem der Auswahl des begünstigten Nutzers in einem dynamischen Szenario untersucht, in dem sich alle Nutzer bewegen. Wir bewerten den durch das Sub-Granting durch die Mobilität entstandenen Signalisierungs-Overhead im DSGRR. Anschließend wird ein verteilter Heuristik-Algorithmus (OSGRR) vorgeschlagen und sowohl mit den Ergebnissen des DSGRR-Algorithmus als auch mit den Ergebnissen ohne Sub-Granting verglichen. Die Simulationsergebnisse zeigen einen verbesserten Zellendurchsatz für den OSGRR im Vergleich zu den anderen Algorithmen. Außerdem ist zu beobachten, dass der durch den OSGRR entstehende Overhead geringer ist als der durch den DSGRR, während der erreichte Zellendurchsatz nahe am maximal erreichbaren Uplink-Zellendurchsatz liegt.

Zusätzlich wird die Ressourcenallokation im Zusammenhang mit der Energieeffizienz bei autonomer Ressourcenauswahl in NR Mode 2 untersucht. Die autonome Auswahl der Ressourcen wird als Verhältnis von Summenrate und Energieverbrauch formuliert. Das Ziel ist den Stromverbrauch der akkubetriebenen Endgeräte unter Berücksichtigung der geforderten Zuverlässigkeit und Latenz zu minimieren. Der heuristische Algorithmus "Density of Traffic-based Resource Allocation (DeTRA)" wird als Lösung vorgeschlagen. Bei dem vorgeschlagenen Algorithmus wird der Ressourcenpool in Abhängigkeit von der Verkehrsdichte pro Verkehrsart aufgeteilt. Die zufällige Auswahl erfolgt zwingend auf dem dedizierten Ressourcenpool beim Eintreffen aperiodischer Daten. Die Simulationsergebnisse zeigen, dass der vorgeschlagene Algorithmus die gleichen Ergebnisse für die Paketempfangsrate (PRR) erreicht, wie der sensing-basierte Algorithmus. Zusätzlich wird der Stromverbrauch des Endgeräts reduziert und damit die Energieeffizienz durch die Anwendung des DeTRA-Algorithmus verbessert.

In dieser Arbeit werden Techniken zur Allokation von Funkressourcen in der LTE-basierten D2D-Kommunikation erforscht und eingesetzt, mit dem Ziel Funkressourcen effizienter zu nutzen. Darüber hinaus ist der in dieser Arbeit vorgestellte Ansatz eine Basis für zukünftige Untersuchungen, wie akkubasierte Endgeräte mit minimalem Stromverbrauch in der NR V2X-Kommunikation Funkressourcen optimal auswählen können.

To Mina, Sara, and Saina
and to my parents

"All our dreams can come true, if we have the courage to pursue them."

Walt Disney

Acknowledgments

I would like to take the opportunity, to thank all the people for the outstanding support I received during my entire Ph.D. work. This Ph.D. thesis was carried out in Electronic Measurement and Signal Processing group and Fraunhofer Institute for Integrated Circuits IIS. A part of the study was funded by the BMBF organization under the name of the FAST2020 wireless project.

I would like to express my most sincere thanks to my advisor, Professor Giovanni Del Galdo, for the guidance and mentorship he provided to me and encouraged me to start by completing this work. At the same time, I thank Professor Jochen Seitz and Professor Jens Mückenheim for all their valuable advice and time to review my thesis.

It was a pleasure to work with colleagues from the Integrated Communication system group in computer engineering. I would like to thank all of them for their supports, especially Professor Andreas Mitschele-Thiel, the head of the group. Last but not least, I would like to thank Dr. Elke Roth-Mandutz and Bernhard Niemann from the broadband and broadcasting communication department in Fraunhofer IIS for their friendly support, which enables me to complete my thesis.

Most importantly, I thank my family, parents, wife Mina, and my children Sara and Saina for their immense confidence in my work and unconditional support. Above all, Mina's support was fantastic, as she was always fully behind me and motivated me to keep going.

Contents

List of Figures

List of Tables

CHAPTER 1

Introduction

Contents

4G and 5G wireless networks are barely developed and commercialized targeting to achieve low latency, high reliability, and high capacity for various use cases, e.g., a massive number of connected devices with stringent requirements. New emerging applications and an increasing number of connected devices ask for further enhancement, which is foreseen to be achieved by 6G architecture. The 6G architecture and its components pave the way to promise ultra-high-speed and save valuable energy sources for the new emerging use cases. Besides, it is foreseen to overcome the deficit of current networks and enhance the existing technology design further by applying artificial intelligence or other advanced techniques.

For example, some critical applications like self-driving cars need low latency requirements, while enterprises will require capacity improvement more than latency reduction (*See Table* 1.1). In addition, it is worthy to note that many of these applications are typically characterized by small traffic payload, e.g., $50 \sim 100B$, and have certain reliability and latency requirements. Thereby, there is a consensus that future cellular networks need to be designed to satisfy all demanding requirements for all applications kind.

One of the features that were initially introduced in 4G and are foreseen to be used in future networks is a direct communication of nearby entities, say, D2D communications.

Table 1.1: Example of uRLLC applications requirements [1].

Use Case	Data Size [byte]	Latency [ms]	Reliability [Packet Loss Rate]
Printing Machines	30	1	10^{-9}
Machine Tools	16	0.25	10^{-9}
Packaging Machines	15	2.5	10^{-9}
Road safety Urban	500	$10 \sim 100$	$10^{-3} \sim 10^{-5}$

The idea of incorporating D2D communication into the cellular network has been a topic of considerable interest for a long time. As a result, many types of research have been conducted to examine the viability and benefit of D2D communication concerning proximity service and public safety needs. Multicasting communication [2] and machine-to-machine communication [3] are two types of use cases in which a user equipment benefits from proximity service of D2D communications to transceive data packets with a specific quality of service requirements. Besides, a short-range communication in D2D communication can provide a better power efficiency applying heuristic algorithms [4], [5] and improves the quality of service performance considering power constraints [6].

Along with academia, D2D communication has also been considered by 3GPP as an important radio enabler for future wireless communications, and corresponding use cases have been specified in [7]. One of the prominent use cases is vehicular communication which is specified for both LTE and NR technologies. Vehicular communication is recently revolutionized by introducing many different types of direct communications [8] between vehicular users and power-saving users, e.g., pedestrians, e-Bike, and electric cars, which are usually equipped with a battery. Thus the related procedures need to be enhanced considering their power constraints.

Resource allocation and power control have been the main research topics in D2D communications, where the goal is to optimize spectral efficiency, reliability, latency, and energy efficiency. In resource allocation, two techniques, so-called *underlay* and *overlay* resource allocation mechanisms, are considered for D2D integration in the cellular network. In the underlying method, cellular users share their radio resources with other D2D under the control of the cellular network. Intuitively, spectral efficiency is improved by sharing the bandwidth between cellular users and D2D communication, provided that appropriate interference reduction [9], [10] or interference avoidance techniques [11], [12] are applied. Another way to avoid the interference arise from sharing the resources between the cellular users and D2D communications is to apply the overlay approach, where a separate bandwidth is allocated to the cellular users and D2D communications. Although overlay D2D communication can eliminate the interference between the cellular users and D2D communication, the potential interference among D2D communications can treat the overall performance of the D2D communications. Some works have been conducted to mitigate the interference between D2D communications in a dense scenario [13], [14].

Finally, it is worthy to note that existing works in D2D communications also provide precious insight into joint power control and resource allocation optimization problem [15], [16]. Detailed overview on D2D communication can be found in [17], [18].

1.1 Problem Statement

The realization of ultra Reliable Low Latency Communication (uRLLC) use cases brings about several transformations in the current wireless technology in order to fulfill the requirements of those applications. Table 1.1 depicts a few examples of these applications in terms of reliability and latency requirements. As discussed in underlay D2D communications, cellular users share resources with D2D users, which may cause severe interference. Even though the underlay D2D is an appealing solution to increase spectra efficiency in D2D communication, stringent algorithms are needed to mitigate interference among the users sharing the radio resources. One solution to avoid the inferences arising from sharing radio resources is to assign orthogonal radio resources between cellular users and D2D users, i.e., overlay. In the overlay D2D communication, the base station may schedule radio resources for D2D users in a semi-persistent manner to reduce the control overhead and delay due to the scheduling procedure. However, in the overlay resource allocation, the number of available resources for cellular users is reduced, whereby the achieved throughput by the cellular users is deteriorated. In addition, the LTE subframe with normal cyclic prefix comprises 14 Orthogonal Frequency Division Multiple Access (OFDMA), which seems too coarse for uRLLC applications with small packets, and can further worsen the achieved cell throughput, especially in semi-persistent scheduling of the overlay radio resources. For example, given that the smallest scheduled radio resource in LTE (i.e., one resource block) and the highest modulation scheme, about 90 B, can be carried by the subframe. Therefore, for example, in the case of printing machine applications with 30 B, two-third of the allocated resources are being wasted.

Continuing progress on waveform leads to introducing the fifth generation (5G) of access technology, known as NR technology, to address a variety of use cases vertical applications from enhanced mobile broadband to ultra-reliable and low-latency communication to vehicular communications. Key features in NR include ultra-lean, support for low-latency communication, spectrum flexibility operation with different numerology. Recently, NR over sidelink communication is specified to be used for vehicular communications by which latency and reliability, required by new use cases specified in [8] are addressed. The vehicular users with an unlimited energy source were assumed. However, due to the increasing number of power-saving users with a limited energy source, e.g., e-bikes and electric cars, using NR sidelink communication, some enhancement to the specified procedures, e.g., resource allocation, concerning the energy consumption should be taken into account.

In the autonomous resource allocation procedure, i.e., Mode 2, vehicular user equipment performs sensing continuously before each data transmission triggering time interval. This sensing procedure is essential prior to any resource selection triggering time instance at the transmitter V-UE to ensure the reliability of the transmission and avoid any collision. However, this increases the energy consumption of the transmitter users. Two resource selection procedures, partial sensing and random resource selection, were introduced in LTE V2X to cater for the power-saving users [19]. Random resource selection is the procedure where a power-saving UE does not carry out sensing but randomly selects resources for its intended transmission from the configured radio resource pool. Another power-saving resource selection method specified in the LTE V2X is partial-sensing. It allows power-saving UEs to perform sensing for defined time intervals, resulting in energy saving. Note that in LTE V2X, periodic traffic is dominant, but

only the traffic with specific periodicities is supported. Thus, a power-saving UE only needs to perform the sensing at specific time intervals. However, traffic with different periodicities in NR V2X poses a significant challenge to the resource selection strategy for the power-saving users. The introduction of aperiodic traffic in conjunction with periodic traffic in NR V2X intensifies the problem. Therefore, in 3GPP plenary meeting [20], it was decided to leverage the existing resource allocation procedures in NR V2X considering both periodic and aperiodic traffic types for the power-saving users.

1.2 Proposed Solution

In this study, we first propose a radio resource allocation strategy, i.e., sub-granting, in overlay D2D-based LTE V2X communication in which whole or a part of unutilized radio resources that allocated to a D2D user, i.e., sub-grant provider, is granted to a selected cellular user in the vicinity, i.e., the beneficiary user. Then, two centralized and distributed algorithms are developed to select the beneficiary users aiming to maximize the uplink cell throughput (See Chapter 3 - 6). In the sub-granting scheme proposed in this work, the following fundamental functionalities are used:

1. **Sub-grant provider user:** Each original holder of the radio resource can broadcast the number of free resources over time and frequency domains. An additional field, say, the beneficiary user identity, is added to indicate the selected beneficiary user identity in case of a centralized approach.

2. **Beneficiary user:** In general, a beneficiary user needs an algorithm to perform energy sensing and decoding of the sub-grant signaling information in order to derive the number of free resources and beneficiary user identity, when it is available, indicated in the sub-granting signaling. In addition, the beneficiary user can assist in the selection process by exchanging some control information in a distributed approach.

3. **Beneficiary user selection algorithm:** In the sub-granting scheme, a part of unused radio resources can be granted to a beneficiary user. Therefore, assigning the sub-granted resources to a beneficiary user with a better radio channel condition can increase the overall uplink cell throughput. To this aim, here, a centralized and a distributed beneficiary user selection algorithms are developed, wherein the best beneficiary users are selected to achieve the maximum cell throughput.

Then, in this work, we examine the problem of joint radio resource selection and energy consumption in NR V2X communication. To this target, the energy efficiency problem is formulated as a ratio of the sum-rate to power consumption for the power-saving users subject to reliability and latency requirements (See Chapter 7). In addition, the power consumption in autonomous resource selection of NR V2X is modeled, and the energy consumption of sensing procedure in the radio resource selection procedure is taken into consideration. Finally, a heuristic of traffic density-based random resource selection on a dedicated pool algorithm (DeTRA) is proposed. The algorithm splits the resource pool based on the traffic density per traffic type. The random resource selection is then mandated to be performed on the dedicated resource pool upon arrival of the aperiodic traffic is triggered. This way, the energy efficiency is improved while the sum-rate value similar to the baseline algorithm is achieved.

1.3 Novelty and Contribution

The four major contributions of this thesis are

1. to **Propose the sub-granting radio resource scheme SGRR**.
2. to **Compare of the sub-granting and shortening TTI schemes**.
3. to **Propose a flexible subframe in the sub-granting scheme to reduce overhead and latency in D2D communication**.
4. to **Develop a distributed and centralized beneficiary user selection algorithms**.
5. to **Develop an energy-efficient radio resource allocation for NR Vehicle-to-Vehicle (V2V) communication**.

The proposed approaches are significant steps forward to make the radio resource allocation more efficient in overlay D2D-based V2V communication in LTE and NR technologies. Still, it does not preclude to widely be used for any other use cases, or technologies. The overriding goal of this work is, however, to reduce the radio resource wastage in overlay radio resource allocation and power consumption for vehicular and battery-based users. Besides the contributions, the following benefits can be deduced, although not all of them are evaluated in detail in this thesis:

- **Cross Network Technologies Applications:**

  The sub-granting approach is evaluated for LTE. However, the framework is applicable for legacy networks as well as for future cellular network generations, e.g., next radio NR. Recently, in NR V2X communication, inter-UE coordination is introduced in autonomous resource selection where a user assists the nearby users with sensing information or additional information to avoid collision or re-utilize the radio resource more efficiently. The initial observations show the benefit of the inter-UE coordination in terms of reliability and spectral efficiency. The concept of the inter-UE coordination is very similar to the sub-granting scheme, and thus the principle of the sub-granting can be exploited by the inter-UE approach in NR V2X communication.

  Energy efficiency was one of the key features in 5G NR, and it will be a fundamental design challenge in 6G [21]. The wireless information and particularly resource allocation procedures need to be reconsidered such that consume the valuable source of energy more efficiently and prolong the battery life of the connected devices. In this sense, introducing new metrics as energy efficiency studied in the **DeTRA** my thesis can provide a framework for joint optimization problems, e.g, energy and sum-rate optimization, also can pave the way for future advances considering the artificial intelligence progresses.

The following papers, articles, and the patent have been published based on this work.

1. Dariush M. Soleymani, Elke Roth-Mandutz, Andre Puschmann, Jens Mueckenheim, Andreas Mitschele-Thiel: "Transfer of Access Rights in the Form of Radio Resource Blocks in Wireless Communication Devices," 2016, Patent [22].

2. Dariush M. Soleymani, Andre Puschmann, Elke Roth-Mandutz, Jens Mueckenheim, and Andreas Mitschele-Thiel: "A Hierarchical Radio Resource Management Scheme for Next Generation Cellular Networks," In IEEE Wireless Communications and Networking Conference (WCNC), Doha, Qatar, April 2016 [23].

3. Dariush M. Soleymani, Jens Mueckenheimi, Mehdi Harounabadi, Abubaker Matovu Waswa, Zubair Shaik, and Andreas Mitschele-Thiel:" Implementation Aspects of Hierarchical Radio Resource Management Scheme for Overlay D2D," in IEEE International Conference on Ultra Modern Telecommunications and Control Systems, pages 154–161, 2017 [24].

4. Dariush M. Soleymani, Abubaker Matovu Waswa, Jens Mueckenheim, Andreas Mitschele-Thiel: "Study on Uplink Throughput of Radio Resource Sub-granting and Shortening TTI Schemes for Overlay D2D ," 23. ITG Fachtagung Mobilkommunikation, 6 Pages, Osnabrück, May 2018 [25].

5. Dariush M. Soleymani, M. Reza Ghomali, Jens Mueckenheimi, and Andreas Mitschele-Thiel:"Dedicated Sub- Granting Radio Resource in Overlay D2D Communication," in IEEE International Symposium on Personal, Indoor and Mobile Radio Communication, Istanbul, Turkey, September 2019 [26].

6. Dariush M. Soleymani, M. Reza Ghomali, Giovanni Del Galdo, Jens Mueckenheimi, and Andreas Mitschele-Thiel: "Open Sub-Granting Radio Resources in Overlay D2D-Based V2V Communications," EURASIP Journal on Wireless Communications and Networking, March 2022 [27].

7. Dariush M. Soleymani, M. Reza Ghomali, Giovanni Del Galdo: "Energy-Efficient Autonomous Resource Selection for Power-Saving Users in NR V2X," in IEEE PIMRC Conference 2021, Oulu, Finland, September 2021 [28].

The part of the thesis are incorporated in the following papers in collaboration with others:

1. Philipp Schulz, Albrecht Wolf, Gerhard P Fettweis, Abubaker Matovu Waswa, Dariush Mohammad Soleymani, Andreas Mitschele-Thiel, Torsten Dudda, Markus Dod, Marco Rehme, Jens Voigt, et al. Network archiectures for demanding 5g performance requirements: "Tailored toward specific needs of efficiency and flexibility," IEEE Vehicular Technology Magazine, 14(2):33– 43, 2019 [29].

2. Abubaker Matovu Waswa, Dariush M. Soleymani, Zubair Shaik, Jens Mückenheim, Andreas Mitschele-Thiel: "D2D Communication Implementation for Future Cellular Networks (5G)," 22. VDE/ITG Fachtagung Mobilkommunikation: Technologien und Anwendungen , Osnabrueck, Germany, May 2017 [30].

3. J. Mueckenheim, A. Puschmann, D.M. Soleymani, E. Roth-Mandutz, A.M. Waswa, A. Mitschele-Thiel: "On D2D-Communication for Resource Efficient Data Transmission of Delay-Critical Services," 21. ITG Mobilfunk-Fachtagung, Osnabrück, Mai 2016 [31].

As an additional activity, I was honored to be one of the main organizers and technical chairs of NR V2X communication workshop in Personal, Indoor and Mobile Radio Communications (PIMRC) conference in 2021 [32].

Besides, the following conference paper, patents, technical report, and article are published in collaboration with others during my dissertation:

1. Waswa, Abubaker M. and Soleymani, Dariush M. and Mwanje, Stephen and Mueckenheim, Jens and Mitschele-Thiel, Andreas, "Multiple Resource Reuse for D2D Communication with Uniform Interference in 5G Cellular Networks," 2017 IEEE 28th Annual International Symposium on Personal, Indoor, and Mobile Radio Communications (PIMRC), 2017 [33].

2. Dariush M. Soleymani et al.: "Method and Apparatus for Zone Adaption in a Network," April 2019 [34].

3. Dariush M. Soleymani et al.: "Radio Resource Management to Enhance Reliability in Mobility Scenarios," July 2019 [35].

4. Dariush M. Soleymani et al.: "NR Sidelink Control Message Design," August 2019 [36].

5. Dariush M. Soleymani et al.: "Enhanced Exceptional Pool Design for NR V2X Sidelink," 2019 [37].

6. Dariush M. Soleymani et al.: "User Devices for a Wireless Communication System and Methods for Communicating in a Wireless Communication system," October, 2019 [38].

7. TDoc R1-2008817,"NR Sidelink Resource Allocation for UE Power Saving," 3GPP TSG RAN WG1 Meeting 103-e-Meeting, October, 2020 [39].

8. M. Harounabadi, D. M. Soleymani, S. Bhadauria, M. Leyh and E. Roth-Mandutz, "V2X in 3GPP Standardization: NR Sidelink in Release-16 and Beyond," in IEEE Communications Standards Magazine, vol. 5, no. 1, pp. 12-21, March 2021 [40].

1.4 Thesis Organization

In the previous sections, the subject of the thesis, problems, and corresponding solutions are introduced. We now conclude this chapter with a summary of the remaining chapters as follows.

Chapter 2 introduces the radio resource allocation approach and assesses the corresponding state of the art. First uRLLC and D2D communication in LTE are introduced, and then the overlay and underlay radio resource in D2D communication are explained. As previously discussed, the granularity of LTE subframe is too coarse for many new emerging applications, e.g., uRLLC. Therefore, a shortening TTI scheme as a viable solution in LTE for the early mentioned applications is explained here. The rest of the chapter is focused on overlay radio resource allocation and the corresponding state of the art. Primarily, NR V2V communication are described the related scenarios are explained. Then, autonomous and controlled resource allocation techniques are explained, and some state-of-the-art in this area are overviewed. Finally, other key enablers like graph and auction theories and the corresponding state of the art are summarized.

Chapter 3 describes the sub-granting scheme concept and the principle of operation. Also, the sub-grant provider, the beneficiary user, and the beneficiary user selection algorithm are explained, and a new flexible subframe inspiring from shortening TTI is introduced. Finally, the beneficiary user selection problem is discussed, and two dedicated and open sub-granting algorithms employing the maximum matching in the Bipartite graph and the Auction theory are proposed.

In **Chapter 4** evaluates the sub-granting radio resource scheme with numerical analysis and simulation study in terms of uplink throughput.

Chapter 5 compares the sub-granting radio resource scheme with the shortening TTI in terms of transmission delay, overhead, and the uplink cell throughput

Chapter 6 attempts to evaluate the dedicated sub-granting algorithm performance by comparing it with a random selection algorithm. Then, dedicated and open sub-granting schemes are compared wherein the performance of both algorithms in a dynamic scenario is evaluated.

Chapter 7 formulates energy-efficient resource allocation problem for NR V2V communications and develops a heuristic algorithm to resolve the issue and compares the proposed algorithm with the baseline algorithm in terms of the sum-rate and energy efficiency.

Finally, **Chapter 8** summarizes all the works that have been undertaken in this thesis and an outlook on what future studies on the subject should entail. The potential areas are discussed in which the proposed algorithms could be improved and be applied to other open problems currently a discussion in academia and industry.

CHAPTER 2

Context and Related Work

Contents

uRLLC services refer to the applications which require reliable communication with a specific latency from one end to another. In the chapter, first, the uRLLC requirements, challenges, and use cases are introduced. Then, two radio key enablers, shortening TTI technique and D2D communication, in LTE are explained. *Overlay* D2D radio resource allocation in D2D communication is discussed, and the related state of the art is overviewed. Also, vehicular communication as one of the vertical applications of D2D communication in LTE and NR is described. Finally, different radio resource allocation algorithms with a focus on graph and auction theories are explained.

2.1 Ultra Reliable Low Latency Communication

New emerging use cases demanding for low-latency or higher-reliability or both, i.e., uRLLC, are foreseen as one of the critical objectives of the current, i.e., LTE, and future wireless communications [41]. These requirements bring a plethora of challenges in terms of system design into the current LTE and NR technologies in order to fulfill two contradicting requirements, i.e., low-latency and high-reliability, for the different vertical applications, e.g., V2X, Machine Type Communication (MTC). On the one hand, low-latency mandates to transfer the packets with a shorter subframe size, which in turn causes to have a new design in the channel coding and the physical layer structure. On the other hand, ensuring reliability calls for more resources over time and frequency domain, for example, in the case of re-transmission, packet duplication [41] and [42] .

As explained earlier, one way is to use a subframe with shorter granularity, e.g., 2, 7 symbols per subframe, say shortening TTI [43]. Reducing subframe duration may reduce delay as the data can be decoded in a shorter time at the receiver side. However, this may introduce more overhead on the network, whereby the cell throughput is reduced.

In addition to the shortening TTI, the D2D communication due to proximity of devices and one-hop communication is envisioned as a prominent key-enabler over which uRLLC requirements could be fulfilled. Further latency improvement can be achieved when the radio resources are scheduled for D2D communication in a semi-persistent manner by which the delay arising from dynamic scheduling is avoided.

In the following sections, these two key-enablers are explained, and state of the art in this context will be further discussed.

2.2 Shortening TTI Concept in LTE

Studying the sub-granting scheme requires a perception of the not only structure of LTE but also shortening TTI. This chapter reviews the shortening TTI concept, particularly on uplink Single Carrier Frequency Division Multiple Access (SC-FDMA), setting a basis for understanding the rest of the content in this thesis.

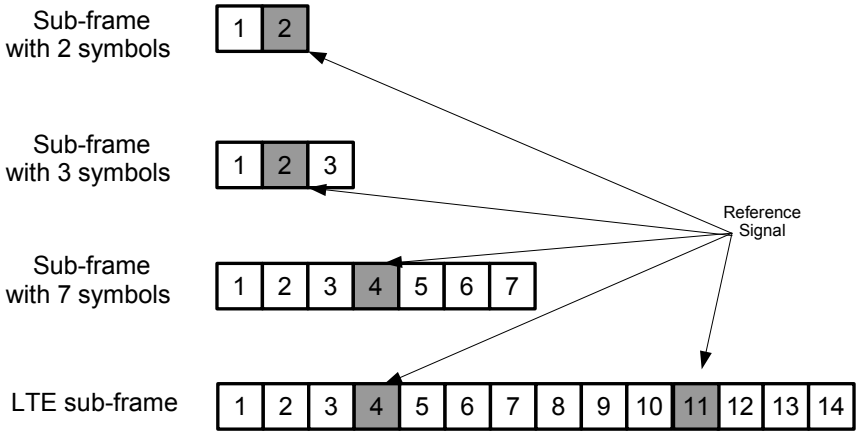

FIGURE 2.1: Illustration of different shortening TTI schemes and legacy LTE subframe.

In recent years, researchers have undertaken many types of researches to find avenues satisfying the latency requirements in emerging applications like Internet of Things (IoT). Focusing primarily on latency requires a different approach to the deigns of wireless communication. As the first step, it is crucial to understand the primary sources of delay in the LTE air interface.

In the uplink, the primary sources of delay for uplink data are as follows: scheduling delay, TTI delay due to subframe size of 1ms, and Hybrid Automatic Repeat Request (HARQ) feedback delay. Detail aspects of latency reduction were being studied and standardized in 3GPP [44]. The main characteristic of the low latency design is the reduction in TTI. A significant requirement of enabling shorter TTI is backward compatibility, such that the implementation impacts can be easily moderated. Besides, since the legacy LTE and shorter TTI coexist, thus they should easily convertible to each other. Generally, LTE subframe consists of two slots where each slot contains seven symbols, i.e., normal cyclic prefix, as illustrated in figure 2.1.

Note that the shorter TTI length is an integer number of symbols. As an example, the shorter TTI may contain two symbols, three symbols, or seven symbols. Having different subframe sizes would increase flexibility such that the latency requirement for the different applications is fulfilled. Figure 2.1 shows an illustrative example of shortening TTI schemes with different subframe sizes.

Due to a shorter transmission duration, the shortening TTI schemes can achieve higher throughput. Besides, since the processing delay is linearly proportional to the length of data, the processing delay is expected to be reduced in line with the length of the subframe. However, the shorter duration of TTI brings about some challenges. For instance, the necessity of the reference signals in every uplink subframe imposes significant overhead. Note that DeModulation Reference Signal (DMRS) is used by every receiver to estimate the radio channel for demodulation. Typically, in LTE, one DMRS is placed in every slot of the subframe. However, in a high Doppler scenario, e.g., V2X communications, a single DMRS might not be sufficient, and the number of DMRSs may increase. Notably, for a shorter subframe size, the higher overhead is expected. For example, in a subframe with two symbols, the overhead due to DMRS can be up to 50%. Exceptionally, for a subframe with seven symbols, the overhead is as same as the subframe with 14 Orthogonal Frequency Division Multiplexing (OFDM) symbols. The reason is that the overhead is measured on a slot basis, and the size of both slots are the same in a subframe. Several techniques are proposed in academia and industry through which the overhead arising from shortening TTI can be reduced. In the following, we briefly overview some of them.

In [45], the authors proposed a DMRS sharing method, by which the imposed overhead owning to having a DMRS in every slot of subframe can be reduced [45]. In the DMRS sharing method, the DMRS is not transmitted in every consecutive shortening TTI slots. This way, the overhead due to DMRS, for example, for short TTI with two symbols is reduced from 1/2 to 1/4. However, the overhead reduction by DMRS sharing is achieved at the cost of a lower channel estimation accuracy, especially when the coherence time is shorter than DMRS transmission interval. Thus the receiver can not track fast changes in the radio channel, and the channel estimation information becomes obsolete.

To address the problem mentioned above, DMRS multiplexing is proposed, wherein different UEs share the same DMRS for channel estimation. In the DMRS multiplexing

method, it is essential to ensure the orthogonality between different UE in order to estimate the radio channel properly. One way to provide such orthogonality is to assign the same base sequence with different cycle shifts for every UE [46]. However, multiplexing DMRS may increase the likelihood of the interference among UEs with same DMRS sequence. Consequently, DMRS multiplexing may not work efficiently in case of using high modulation and coding schemes due to inter DMRS interference.

Finally, it is noteworthy to mention that the backward compatibility with LTE subframe structure also needs to be considered in the shortening TTI schemes. To this aim, the different short TTI schemes are combined, such that to be fit into the legacy LTE subframe structure, i.e., 14 OFDMA symbols. For instance, two subframes with two-symbols along with one subframe with three-symbols can be embedded into one slot in LTE subframe structure [44]. The evaluation in [47] illustrates that shortening TTI schemes can achieve the end-to-end delay demanded by a certain group of applications, e.g., the automation industry.

2.3 Device-to-Device Communication

Following the brief introduction to shortening TTI in LTE, this section overviews a basic concept of D2D communication in LTE and NR networks. First, we describe enhancement in 3GPP standardization for D2D communication and explain some concepts used in D2D communication, e.g., different coverage scenarios, spectrum sharing and, power control mechanism. Also, V2X communications as a vertical application for D2D communication is explained, and some of the resource allocation techniques are then briefly described.

2.3.1 Overview of D2D Communication

D2D communication enables direct communication between two peer entities was defined as part of Proximity Service (ProSe) service and emerged first time in 3GPP standard Release 12 for a public safety use case.

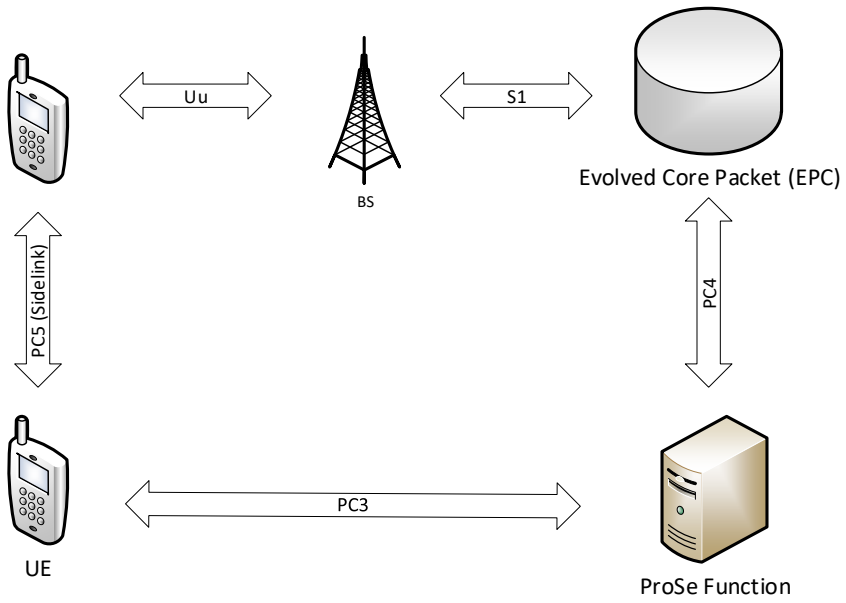

FIGURE 2.2: Architecture of sidelink communication, i.e., D2D communication in 3GPP.

The underlying architecture of D2D communication is shown in Figure 2.2, wherein a UE can establish a connection to ProSe application server through an interface, say PC3, to receive information that needed to initiate a discovery procedure. When a nearby device was discovered, two peer UEs communicate over the sidelink interface, i.e., PC5.

In LTE, the following reasons make the uplink waveform, i.e., Single Carrier Frequency Division Multiple Access (SCFDMA), as an appropriate candidate for the sidelink waveform:

- These radio resources are often less utilized compared to the downlink radio resources.
- Less control information is available in the uplink resources compared with downlink resources, which may facilitate sharing the uplink resources.
- In the case of sharing the uplink resources, the interference arises from D2D on the cellular network can be minimized since Base Station (BS) is more powerful and thus can better dealt with the raised interference.
- Reusing the downlink resources would increase hardware complexity due to regulatory concerns since the D2D communication should be capable of transmitting on the downlink bandwidth considering the regulatory rules.

Different coverage scenarios are considered in D2D communication [48], wherein the radio resource are allocated differently. When D2D users are in the coverage area, the radio resources are scheduled by a eNB, i.e., Mode 1. In the out of coverage, where D2D

users are not in eNB coverage area, and the radio resources are autonomously be selected from a list of configured radio resources by every D2D users, i.e., Mode 2.

In case the D2D transmitter is in coverage and D2D receiver is in out of coverage area, i.e., in a partial coverage scenario, the part of D2D communication that is in coverage area receives radio resources configuration from eNB and assists the other part of D2D communication in configuring the radio resources for a direct-communication. This way, D2D communication avoids the interference either on nearby D2D communications or the cellular network and besides aids the eNB to extend network coverage. Figure 2.3 illustrates the different coverage scenarios for D2D communication.

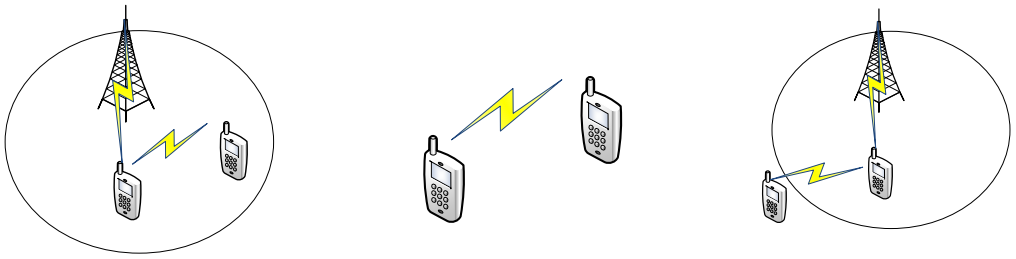

FIGURE 2.3: D2D communication coverage scenarios.

Figure 2.4 shows the milestones and progress in D2D communication on the 3GPP standardization. Briefly, in the initial phase, the main focus was on the public safety services on LTE based D2D communication. Service requirements related to the 5G system consider D2D in two different ways. The first one uses a direct device connection without any network entity in the middle. In the second approach, a relay UE is between a UE and the 5G network. This type of communication is called an indirect network connection mode, which mainly targeting coverage extension and service continuity. The relay concept in D2D communication was added into the technical specifications Rel. 13. One of the prominent vertical applications that were based on D2D communications, is vehicular communications, which was first time introduced in Release 14. Further enhancement and support for V2X services are discussed in 3GPP Release 15 wherein safety-related V2X scenarios, such as automated and remote driving and platooning, where vehicles form a platoon or a line traveling together, were included. Finally, the main focus of the standardization groups in 3GPP Release 16 is to enhance systems specifically for advance V2X communications, i.e., NR-V2X, and beyond to support the needs of future V2X use cases.

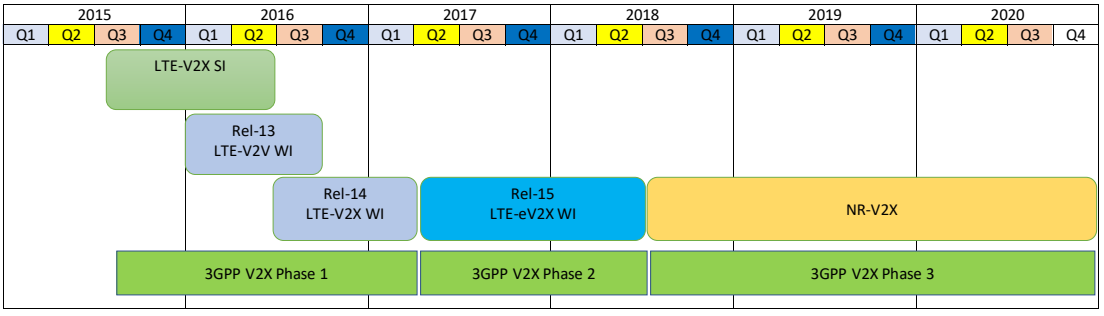

FIGURE 2.4: Illustration of D2D communication enhancement in 3GPP [49].

To be more specific, in the following, we name a few of the use cases in V2X communication that are specified in 3GPP:

- Vehicle-to-Vehicle (V2V): Two vehicular users are in proximity can exchange information, e.g., location, velocity, direction, wherein this information is predominantly broadcast-based traffic but not precluded to be any other cast communication type, e.g., unicast and multicast. The primary purpose of V2V communication is to avoid the possible accident and allowing vehicles in transient to relay data received from other vehicles. By exploiting the V2V communication, every vehicle exchanges the data with other nearby vehicles to reach the intended destination. Depending on how the technology is developed, a vehicle can receive a warning message such as emergency braking to react appropriately to any dangerous situations based on specific parameters detected by the devices/sensors placed on the vehicle. Some of these devices are as follows:
  - Blind-spot monitoring: It is a system that can monitor the blind spot's exterior rear-view mirrors employing radar sensors.
  - Forward collision warning: This system uses a radar sensor to detect the objects and estimate the distance between the obstacles and the vehicle.
  - Automatic emergency braking: It is an assisted braking system by which the speed of the vehicle is controlled to reduce the severity of the impact when the collision is avoidable.
  - Lane departure warning system: it is a device that warns the distracted driver of exceeding the line that delimits its lane.

  The V2V communication, thanks to the cooperation with already existing sensors, will yield efficient management of possible pitfalls in the roadways all over the world.

- Vehicle-to-Infrastructure (Vehicle-to-Infrastructure (V2I)): In this type of communication, a UE supporting V2I application can transmit the message to an infrastructure, e.g., Road Side Unit (RSU), which may accommodate a or multiple geographical area(s). Generally, V2I communications are wireless, bidirectional using radio resources, which are scheduled by the BS in an orthogonal manner to transfer data. This information is sent from the elements of the infrastructure data and provides travelers with real-time advice, sending information on road conditions, traffic congestion, accident in the road, and availability of parking places. Besides, traffic information collected from the vehicles and infrastructure system can be used to set different speed limits to facilitate traffic flows. Note that the communication is based on the sidelink on the PC5 interface and works also in out-of-coverage scenarios

- Vehicle-to-Network (Vehicle-to-Network (V2N)): A vehicle is able to communicate with the application server using uplink interface, i.e., U_u, in the network.

- Vehicle-to-Pedestrian (Vehicle-to-Pedestrain (V2P)): The majority of victims in road accidents account for pedestrian, cyclists classified as vulnerable road users. Therefore, it is essential to design a warning system to protect the pedestrian users against road accidents. One of the main goals of V2P is precisely to enhance the communication between vehicles and pedestrians aimed at reducing fatal accidents. In this use case, a pedestrian can warn/inform other nearby vehicles about possible

risk/threat using some embedded sensor modules. Identical to V2V and V2I, V2P is based on direct communication using the sidelink working also in out-of-coverage scenarios.

It is also noteworthy to mention MTC as another prominent vertical application for D2D communication which has recently drawn much attention. The MTC refers to a IoT where a large number of static sensors are deployed and report sporadically to an application server or cloud. As one of the critical technical enablers for 5G networks, D2D can guarantee the service requirements needed for MTC services. For example, as mentioned earlier, D2D relay is introduced in 3GPP release 13 to assist in the network coverage. Sensors can use this technique in MTC to convey the data between two machines. This way, a sensor in cell borders as remote sensors can establish a direct communication via D2D interface, i.e., sidelink, to relay the data to the intended D2D receiver. In the sequel, we will take a brief look at the state-of-the-art, focusing on the benefit of using the D2D communication, especially in MTC and IoT applications.

Authors in [50] proposed a smart transmission mode in MTC wherein a remote sensor transmits its data to another machine that relays the data to the intended machine or network infrastructure. They proposed a signaling scheme that a relay MTC device can collect and transfer the incoming message without imposing too much signaling overhead on the network.

A drastic increase in IoT devices produces enormous demands for data transmission over wireless networks, namely smart metering, remote health care, industrial automation. The proximity service in D2D communication has been attracted much attention from the scholars as an enabler to fulfill the earlier mentioned requirements, e.g., [51], [50], [52], to name a few of them.

Authors in [51] proposed D2D communication as a viable solution to reduce energy consumption. Particularly, they divided the D2D user to different clusters wherein a IoT smart device is appointed as collector acting to gather information of all cluster members toward the BS. It is shown that If the MCS is adopted properly on the communication link, the overall utilization rate can be maximized. Further improvement concerning the transmission power can be achieved when a lower modulation order is selected. In [50], service availability, and power consumption for MTC were discussed. The authors suggested to provide a better service for MTC applying D2D communication. To this aim, a context-aware algorithm is applied wherein the content of multiple communicating devices are taken into consideration. Besides, some additional signaling information is used to adapt configuration for both cellular and D2D users such that service availability and power saving are guaranteed.

One of the key features that ensure the reliability and latency for uRLLC application is re-transmission of control and data information when transmission link between the transmitter and receiver is in poor condition. However, this technique may degrade the resource utilization efficiency and energy consumption. Authors in [52] proposed a D2D strategy where an intelligent deterministic relay D2D communication selection algorithm is used to ensure reliability of D2D communication link while reducing energy consumption. The proposed algorithm shows a better performance in terms of packet delivery rate and end-to-end delay compared with an opportunistic method.

2.3.2 Spectrum based D2D Communication Taxonomy

This section overviews different resource allocation techniques for D2D communication, considering spectrum allocation methods. The interference among users in out-band communication, i.e., unlicensed band, is not controllable, and it is difficult to provision QoS required by uRLLC. Therefore, in our study, we only consider in-band communication. The in-band communication is further divided into underlay and overlay modes. In the underlay mode, cellular and D2D communications share the same radio resources. In contrast, in the overlay, the radio resources are divided into two parts, in which a part of radio resources is dedicated to the D2D users.

2.3.2.1 Underlay D2D Communication

To date, the majority of state of the art is related to the D2D communication underlying cellular users. By exploiting the underlay D2D, the spectral efficiency is increased. However, interference between the cellular users and D2D users is the most important issue that need to be considered. Premium interference mitigation techniques can increase the spectral efficiency and thus have attracted many scholar attention [53], [54], [9], [55], [11], [56] to name few.

One approach is to share the uplink radio resources between the cellular and D2D users. In the most state of the art, this approach is more preferred as it is easier to coordinate interference arising from the users on the cellular network due to lower transmission power of D2D users. Different techniques are proposed to mitigate such interference, for example, the authors in [53] proposed to use the measured signal of downlink control information to estimate the downlink path loss between the BS and the D2D communication. This way, D2D user will transmit with a lower transmission power to maintain the imposed interference on the BS below a specific threshold. In other words, the D2D is not allowed to transmit beyond a certain power level to avoid interference on the cellular network. However, the interference from the cellular users on the D2D is not considered. Mutual interference between D2D communication and the cellular user is considered in [54] wherein the authors proposed two mechanisms to control interference between the cellular users and D2D users. First, D2D users can read control information to identify the radio resources that are used by cellular users. Besides, D2D users can share their minimum interference requirements with other nearby D2D. This way, the D2D users can adapt their transmission power to maintain interference on the cellular network below a specific threshold.

In [9], a location-based interference mitigation technique is suggested, wherein all D2D users use a common, dedicated control channel. The cellular users measure this control channel Signal to Interference and Noise Ratio (SINR) strength and inform the measured signal to the BS. The BS then schedules the radio resources that not occupied by D2D users for the cellular users based on the collected SINR measurements. A similar solution is proposed in [55], wherein D2D users measure the received signal strength of nearby cellular users, and the BS 's database is updated by the collected measurements in a specific time interval. The BS then avoids to schedule the same resource block(s) for the D2D and cellular users that are in proximity. This way, the interference from the cellular users to the D2D user is mitigated.

A Uniform Interference Power (UIP) allocation scheme is proposed in [56], wherein the radio resources are shared between D2D users and cellular users. In the proposed algorithm, the power is assigned to D2D users to impose equal interference into the cellular users. For this target, all D2D users in a spatial area are mandated to transmit with specific power to avoid interference beyond a certain threshold on the cellular user. This way, the spectral efficiency is increased due to multiple reuses of radio resources while the reliability of the cellular users is guaranteed.

Finally, in [11], a new geographical area, say Interference Limited Area (ILA), is proposed wherein the resource reuse is not allowed in the hypothetical geographical area. This way, the cellular users can not share the same resources with D2D users within the ILA, and thus interference between the D2D and cellular users is deteriorated.

In this section, we have explained different underlay resource allocation techniques proposed by some literature aiming to mitigate interference among the cellular users and D2D users. Another approach is to split the radio resources between the cellular users and D2D users to avoid such interference. The next session discusses the overlay resource allocation, particularly in D2D communication and describes some state of the art.

2.3.2.2 Overlay D2D Communication

In underlay D2D communications, cellular users share the resource with D2D users, which may cause severe interference on the cellular network and D2D users. One way to avoid such interference is to split the bandwidth between the cellular users D2D users, i.e., overlay, and allocate a dedicated part of the bandwidth to the D2D users. Compared to the underlay resource allocation, less attention was paid to the overlay resource allocation. In this section, we overview some state of the art, focusing on the overlay resource allocation in D2D communication [57], [58], [59], [60], [61].

In [57], authors considered a multi-cast communication scenario and use D2D communication to improve network performance. Due to channel impairment, a cluster head in the multi-cast communication may not receive the data. To address this problem, every D2D user assists the cluster head user with re-transmission of its measured received signal. In this work, the number of of D2D communications involving the re-transmission dynamically changes to maximize the spectral efficiency. The results showed that the proposed algorithm could improve the spectral efficiency by 90% compared with other studied scenarios.

Authors in [58] proposed relay D2D communication to extend the coverage and improve the network spectral efficiency. To this end, an incremental relay is suggested wherein every D2D communication transmits the message to both the BS and the D2D receiver simultaneously. In case, the receiver could not decode the message, due to errors, the BS re-transmits a copy of the message to the receiver. Therefore, this method would decrease the outage probability of D2D transmission. Although this method uses some of the downlink resources for re-transmission purpose, the results show that the cell throughput improves by 40% compared with thereof in the underlay mode.

In D2D communication, different techniques, e.g., mode selection, power control, and discovery, can play a vital role in service continuity and spectrum efficiency—however, better performance yields at the cost of the comprehensive measurement information.

Fodor et al. in [59] examined the challenges in D2D communication and proposed to use network-assisted resource allocation in D2D communication to mitigate the interference between the cellular network and the D2D communication. Besides, it is claimed that the network-assisted resource allocation could decrease the inefficiencies of D2D communication in service continuity and peer discovery. In the conventional discovery method, D2D users disseminate the message in a short interval and monitor multiple channels, whereby power consumption in D2D communication is increased. To reduce energy consumption, the BS can configure optimum values for the message broadcast interval and sensing time window to address inefficiency in the peer discovery and service continuity. Also, the BS can assist the D2D communication in scheduling and power control by which the interference among the cellular users and D2D communications is mitigated.

Authors in [60] adopted overlay D2D communication and proposed a centralized and distributed location-based radio resource allocation. In the centralized scheme, a central scheduler orchestrates resource allocation for all D2D users. Due to half-duplex communication, in D2D communication, no more than one user sends information at a one-time instance; otherwise, the D2D transmitters may lose information transmitted by D2D users in communicating range. Besides, orthogonal resources are allocated to the D2D transmitters to avoid co-channel interference. However, this way, the centralized approach poses significant overhead on the cellular network. To avoid such an overhead, the authors proposed to use several schedulers in different BSs instead of a single centralized scheduler. Every scheduler can then assign radio resources to D2D users in specific cells without considering location information of users in other cells. In addition, the available radio resources are divided between different cells to mitigate inter-cell interference among nearby D2D transmitters in different cells. Both algorithms are evaluated in terms of resource utilization, time delay, and communication accuracy while considering the latency and packet errors required by D2D communication. It is observed that the distributed algorithm performance is slightly worse than the centralized algorithm in terms of resource utilization.

In [61], Feki et al. proposed a resource allocation algorithm in which Quality of Service (QoS) parameters are taken into consideration. The ant colony optimization method was adopted and applied to fulfill the QoS requirements. Simulation results reveal the superiority of the proposed algorithm in terms of sum rate and packet delivery rate in less-dense traffic scenarios compared with the location-based resource allocation algorithm as a baseline. However, in the case of a dense traffic scenario, the algorithm performance is degraded in terms of the packet delivery rate and sum-rate compared with the baseline algorithm.

2.3.3 D2D-based Vehicular Communication

Vehicular communication is one of the prominent vertical applications for D2D communication and has attracted much attention from the research community recently. In LTE, D2D-based V2X communication is a cornerstone for the realization of an intelligent transport system (ITS) and also facilitates autonomous driving in the future. In [62], different use cases are defined as for V2X services in which the services are classified into safety and non-safety messages. According to 3GPP standardization in [62], the safety based use cases are classified into different categories concerning the following parameters:

- Velocity: the maximum velocity of 500km/h is supported.
- Communication range: an effective distance wherein enable a driver to avoid collision according to relative velocity.
- Latency and reliability: Maximum end-to-end delay which can be supported by the application layer. The reliability is capability of communication link wherein two communicating users can transmit and receive a message without re-transmission according to application latency requirements.
- Message size: variable size of periodic and non-periodic traffic that the application layer generates between two communicating users.

The safety applications aim at reducing the probability of collision and accident for vehicular and vulnerable users, e.g., pedestrian and cyclist, and thus demanding high-reliability and low-latency communication. On the other hand, the non-safety applications focus on the applications whose service provides an efficient driving experience and comfort for the users. For example, it can facilitate traffic density or assist vehicular users in different driving situations.

2.3.3.1 Physical Channels Structure in LTE and NR V2X

As explained earlier, SC-FDMA has been chosen as a waveform for the LTE V2X wherein up to 20MHz bandwidth is supported. The bandwidth is divided into subframes, resource blocks (RBs), and subchannels. The subframe is 1ms long, and an RB is the smallest unit of resources in the time and frequency domain that can be assigned to every user. In the frequency domain, the RB spans 180kHz, i.e., 12 subcarriers of 15kHz, and a group of RBs is defined as a subchannel assigned to every user depending on the traffic payload and radio channel conditions. The traffic data is transmitted in Transport Blocks (TBs) over Physical Sidelink Shared Channel (PSSCH), and Physical Sidelink Control Channels are used to transmit the Sidelink Control Information (SCI) from the transmitter user to the intended receiver users [19]. This control information is essential to be received by the intended receiver so that the receiver be able to decode the TB correctly. To be more specific, in LTE V2X, depending on the location of the SCI and its associated TB, two physical sub-channel structures are defined (See Figure 2.5):

- **Adjacent PSCCH + PSSCH:** The first two RBs of the configured sub-channel are dedicated to SCI. The remaining RBs within the sub-channels are utilized for TB transmission, wherein the sub-channel size varies depending on the traffic size.
- **Non-Adjacent PSCCH + PSSCH:** The RBs are divided into two pools, where the first pool size consists of two RBs to be used for SCI transmission only. The second pool is reserved for TBs transmission and may comprise several sub-channels when it is configured.

Quadrature Phase-Shift Keying (QPSK) and 16-Quadrature Amplitude Modulation (16-QAM) are used for the TB transmission, whereas the SCI is transmitted on QPSK modulation. Also, LTE V2X uses turbo coding and normal cyclic prefix. And, one RB, i.e.,12 subcarriers, has 14 symbols in the subframe, which between two and four symbols

are dedicated to Demodulation Reference Signal (DMRS) depending on the velocity of the vehicle to combat the Doppler effect [19].

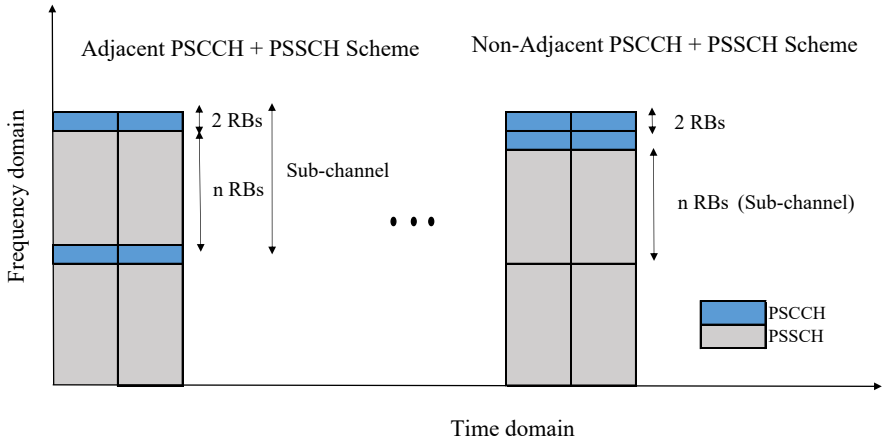

FIGURE 2.5: Physical sub-channel structure in LTE V2X communication.

The NR V2X supports different numerologies from subcarrier spacing (SCS) of 15kHz to 60kHz in FR1 (below 6GHz) and SCS of 120kHz in FR2 (between 6GHz up to 52.6GHz) [19]. Furthermore, in NR V2X, cyclic prefix OFDM (CP-OFDM) is used wherein the control and data information are multiplexed in the time domain, i.e., Time Division Duplex (TDD). Similar to LTE design, PSCCH, and PSSCH are utilized to carry the sidelink control information and data with different that the PSCCH and associated PSSCH are transmitted together in the same subframe. The first symbol of the subframe is utilized for automatic gain control (AGC) to adapt the received signal level at the receiver side accordingly. A new Physical Sidelink feedback Channel (PSFCH) is specified in NR V2X to guarantee reliability for unicast and group cast communication. To this purpose, the last symbol in the subframe is reserved to carry an acknowledgment or negative acknowledgment signal when the feedback is configured for a resource pool. Furthermore, channel quality information (CQI) may carry on the feedback channel for efficient link adaptation. The PFSCH are only (pre-)configured in every 1, 2, or 4 subframes. Figure 2.6 and 2.7 illustrate two examples in which PSCCH and PSSCH are multiplexed in a subframe (slot) in NR V2X communication for the case PFSCH is not configured or is configured in the physical channel structure, respectively.

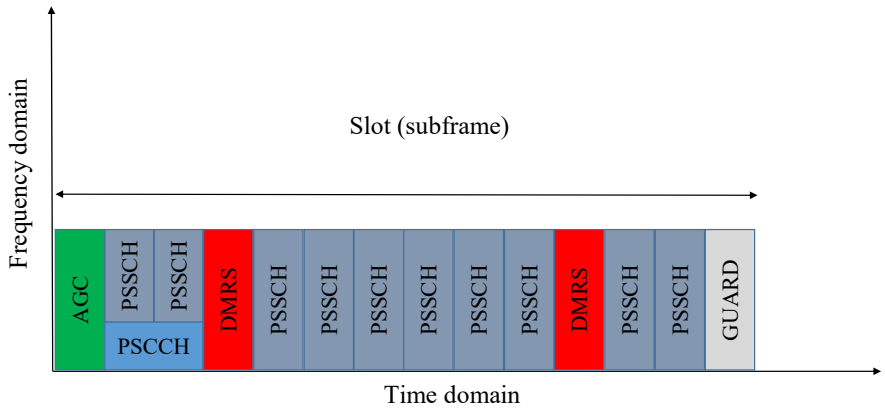

FIGURE 2.6: Physical sub-channel structure in NR V2X communication. An illustrative example of a slot with 2 symbols PSCCH, 2 symbols PSSCH-DMRS, when PSFCH is not configured.

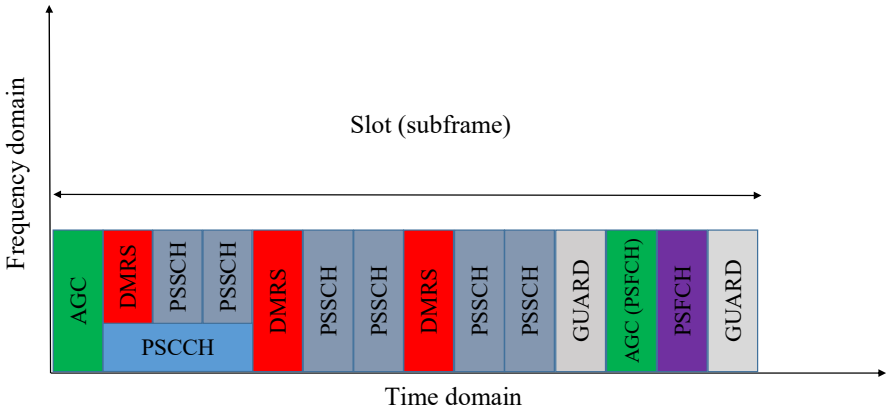

FIGURE 2.7: Physical sub-channel structure in NR V2X communication. An illustrative example of a slot with 3 symbols PSCCH, 3 symbols PSSCH-DMRS, and PSFCH.

2.3.3.2 LTE and NR V2X Resource Allocation

Thanks to the scarcity of valuable radio resources and the essence of vehicular communications, the diversity of radio resource allocation techniques are used to guarantee the reliability and latency required by the safety and non-safety use cases. In LTE, two modes, Mode 3 and Mode 4, have already been standardized for V2X communication with a focus on which entity is involved in the resource allocation mechanism. In Mode 3, the BS allocates the radio resources to the vehicular users. This way, the reliability and latency requirements of the applications are ensured. However, the users should be in a communication range of the network, i.e., in-coverage scenario. Another approach is autonomous resource selection, i.e., Mode 4, wherein all vehicular users perform sensing and select radio resources based on the recent sensing measurement and periodically indicate their selected resources through control information that other nearby users can use for the resource selection procedure. Mode 4 is generally applied when the vehicular users are outside of network coverage, i.e., out-of-coverage, or the resource selection procedure load is offloaded from the network to the users.

The autonomous resource allocation in LTE V2X communication, i.e., Mode 4, is performed based on the energy-sensing, wherein every UE monitors the energy of resource over frequency and time domain. In the frequency domain, the granularity of resource allocation is radio resource block(s) or sub-channel(s), whereas, in the time domain, energy-sensing is undertaken at the slot-basis. A radio resource is considered as a busy channel if Received Signal Strength Indicator (RSSI) of the sub-channel (s) is higher than the RSSI threshold configured by the BS, and thus it is excluded from the candidate resource list to avoid any collision. Afterward, the UE selects radio resource (s) from the candidate resources randomly depends on the size of the arrived packed and transmission parameters. The sensing window in LTE is 1000 subframes [63], in which the recent subframes before the packet arrival time are monitored. Suppose a user has a packet at a time instance of n, the user considers those sensing sample between n and $n - 1000$ with a constant step of 100ms and makes a list of candidate frequency/time resources whose the RSSI average are lower than the configured RSSI threshold. Next, a vehicular selects sub-channel(s) in a time interval between $n + T1$ to $n + T2$, i.e., resource selection window. In the selection window, n and $T1$ are packet arrival time instances and packet processing time that a UE needs to be prepared for the data transmission. Packet delay budget T2 determines an upper bound for time that the UE is allowed to buffer a packet before transmission. Finally, the transmission frequency/time resource(s) is randomly selected from the selection window. When the number of frequency/time radio resources is less than 20% of the entire radio resources, the received signal strength threshold increases by 3 dB, and the radio selection process are repeated. Figure 2.8 shows the autonomous resource selection timings procedure for LTE V2X communication.

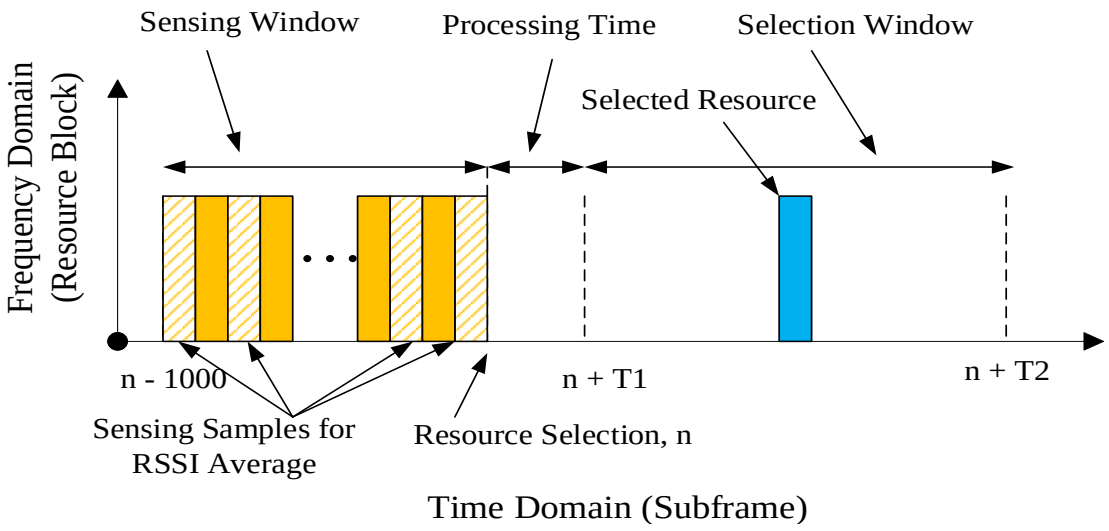

FIGURE 2.8: Mod4 resource selection based on energy-sensing in LTE V2X communication.

Similar to LTE V2X communication, two modes of resource allocation, i.e., Mode 1 and Mode 2, are specified for NR V2X. In Mode 1, gNodeB (gNB) grants the radio resources to every vehicular user who is in its communication range. For this purpose, the gNB signals the granted radio resources to a specific vehicular user either through a higher layer signaling, i.e., radio resource control (RRC), or a physical layer signaling, i.e., downlink control information (DCI).

In Mode 2 resource selection of NR V2X, every user performs sensing on the configured radio resources without involving a gNB. A vehicular user uses the recent sensing information to select the radio resources and then indicates the reserved resources and transmission parameters by a two-stage sidelink control information (SCI) [64]. This information helps other nearby users to avoid selecting the already reserved resources. In the two-stage SCI, the time-frequency of the reserved resources is indicated by the first stage SCI. All vehicular users performing sensing are mandated to decode the first stage SCI to maintain the reserved radio resources record in the recent past. Besides, some specific information, namely, the second stage SCI format, is indicated by the first stage SCI to reduce processing time due to blind decoding [64]. Note that the second stage of two-stage SCI is sent together with the data channel, i.e., physical sidelink shared channel (PSSCH), on which some additional information like source and destination addresses are conveyed [64].

Figure 2.9 depicts the timeline of sensing and resource selection in Mode 2 with respect to resource selection triggering time instance, τ_a. The vehicular user considers an interval containing N_s samples, i.e., sensing window, $\tau_a - \tau_s$ from the recent past measurements. The sensing window is configured differently, i.e. 1100ms and 100ms for periodic and aperiodic traffic, respectively.

The vehicular user decodes the first stage SCI received during the sensing measurement and excludes all reserved sub-channels that are indicated in the first stage SCI. Note that, due to half-duplex communication, a vehicular user can not transmit and receive simultaneously; thus, the vehicular user also excludes those time-frequency resources that can not be monitored during its transmission. Then, the vehicular user selects resources for its transmission from the selection window that starts immediately after $\tau_a + \tau_{proc}$ and cannot be longer than the maximum packet delay, τ_{MAX}. The number of the radio resources in the selection window should be equal to or greater than 20 % of total available resources N_{Total}; otherwise, the received signal threshold is incremented by 3dB, and the procedure is repeated.

Note that for periodic traffic, a set of time-radio resources are selected for a specific time duration, i.e., semi-persistent scheduling. In contrast, for aperiodic traffic, a maximum of four time-radio resources, including re-transmissions, are allowed to be selected [65].

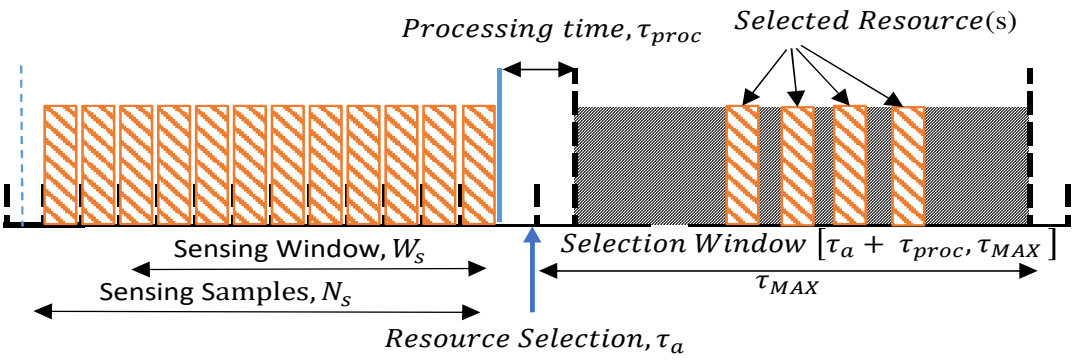

FIGURE 2.9: Time-line of sensing-based resource selection in NR-V2X communication, when re-evaluation feature is not configured [19].

Many researches have been undertaken with a focus on the network-centric resource allocation approach that in what follows, we discuss the few of them.

Authors in [66] cast the radio resource allocation and power control problem as an optimization problem considering reliability and latency required by V2X communications. A Separate resOurce bLock and powEr allocatioN (SOLEN), say SOLEN, is proposed applying the Hungarian and interior point method or Newton's method to solve it optimally. In this way, even though the proposed SOLEN method is heuristic by dividing the whole process into two stages, the optimal solution for each stage could be achieved, which to some extent, promises good performance of the SOLEN algorithm. The numerical results show the superiority of the SOLEN algorithm over other algorithms in terms of the total sum rate.

A stringent resource allocation algorithm is required to assign radio resources to the platoon members who are asking for radio resources such that fulfill the QoS required by the car platooning use case. To this aim, authors in [67] proposed two radio resource scheduling algorithms through which radio resources are dynamically allocated to the platoon members taking into consideration reliability and latency requirements. In particular, the proposed algorithms consider cooperative awareness messages within platoon members, where all platoon members are in a coverage area. However, the proposed algorithms seem dysfunction when the platoon members are in an area that is delimited by the network infrastructure, e.g., in Tunnel. In [68], it is proposed to divide the radio resources based on the service priority. To this aim, part of the radio resources is reserved for the services that can not be pre-scheduled, e.g., emergency brake. The authors considered the number of vehicles and the size of the out-of-coverage area as two parameters that assist the network controller to predict the number of radio resources required for the emergency.

The current sensing-based autonomous resource selection specified in 3GPP is a promising approach that assists in mitigating the message collisions in LTE and NR V2X communication and accommodate latency and reliability required by the applications mentioned earlier. To show the efficacy of sensing-based radio resource allocation, some state of the art are outlined in the following:

Authors in [69] proposed to enhance the radio resource selection by embedding piggyback messages on the periodic safety message. The piggyback message indicates the next starting resource location in time-frequency domain. This way, the nearby users avoid transmitting on the same time-frequency resources, which results in collisions reduction. Although the proposed scheme incurs some overhead due to the inclusion of the piggyback information, the achieved reliability outweighs the bandwidth cost, especially for the future vertical applications with stringent reliability requirements [1].

In [70], Yang et al. proposed a new resource selection algorithm for the urban V2V communications scenario. More specifically, a Vehicular User Equipment (VUE) performs radio resource selection in two stages. At the first stage, the VUEs are classified based on the heading direction of the vehicles. Then, the sensing-based collision avoidance mechanism is applied. The proposed two-stage autonomous resource selection scheme shows a significant performance gain compared with the existing algorithms.

Transmission power also plays a prominent role in vehicular communications. Authors in [71] proposed an adaptive power control mechanism though which each vehicle exploits the sensing information to control the power transmission. The vehicle has an energy-sensing result larger than a specified received signal threshold, chooses the smallest transmit power. Simulation results show the superiority of the proposed algorithm in terms of packet reception ratio compared with the other studied algorithms.

In [72], the authors proposed a radio resource allocation algorithm for V2V communications in case of out-of-coverage areas that are delimited by the network infrastructure. A MAP-RP scheme is proposed wherein the map of resources is embedded in the radio resource selection procedure. Results show up to 20% better packet reception ratio in the proposed algorithm compared with two sensing-based benchmark algorithms.

Authors in [73] proposed a cluster-based resource allocation scheme wherein a cluster head performs sensing on a resource set and reserves the resource set. To be more specific, the cluster head is able to assign its selected resources to its cluster members. Although the proposed algorithm incurs some signaling overhead, it shows a better performance compared with the resource selection algorithm in LTE for both in-coverage and out-of-coverage scenarios.

In [74], authors presented multi-dimensional discrete-time Markov chain (DTMC) based model to address autonomous resource selection problem in cooperative awareness message in LTE based V2V communication and IEEE 802.11P standard. The DTMC model consists of a dependent node model, a queuing model, and traffic generators, wherein closed-form solutions can be obtained on a limited number of iterations. The two technologies are compared in terms of the average delay, the collision probability, and the channel utilization. The results show that IEEE 802.11p is superior in terms of average delay, whereas V2V Mode 4 outperforms in collision resolution.

Resource allocation and power control have been the main research topics in V2X communications, where the goal is to optimize spectral efficiency, reliability, latency, and energy efficiency. Authors in [75] propose a joint resource allocation and power control method to optimize energy efficiency for electric cars. The results show the proposed method can be effective in certain scenarios, e.g., when every vehicle satisfies a minimum rate requirement. Authors in [76] propose a new resource allocation method for delay-tolerant applications with energy efficiency and latency constraints. The method is implemented in a two-step algorithm, where in the first step, optimal power is allocated while relaxing the latency constraint. Then, the radio resources are allocated when both latency and energy consumption constraints are satisfied.

2.4 Optimization Methods for Radio Resource Allocation

This section discusses some optimization methods to address the resource allocation problems in D2D communications. Specifically, we discuss the bipartite graph in graph theory by which the relation between two different classes of objects can conveniently be described and modeled. To this aim, we first explain the basic concept of graph theory and briefly discuss the basic approaches and some applications. Applying the graph theory to resource allocation is not a strange idea. However, this concept is scattered in the literature that mostly done in Adhoc manner and cognitive radios. We discuss the state of the art that is associated with the radio resource allocation problem in D2D communications, particularly by leveraging bipartite graphs in Section 2.4.1.

The auction theory consists of a set of well-defined mathematical tools wherein enable to resolves of interaction among independent players and predict the strategy that is taken by every individual player. Those features put the auction in a prominent place within microeconomics and game theory. In D2D communications, all users can compete and cooperate in selecting of the radio resources. Therefore, resource allocation and access to

the radio resources in D2D communications can be considered an auction in the market. The auction theory provides useful mechanisms for resource allocation problems in D2D communication. Notably, in a distributed resource allocation, auctions can minimize messages exchange among the different D2D users. Thus, the auction theory seems to be a viable solution, especially for cooperative D2D communication. In Section 2.4.2, we first introduce the scope and detail of the auction theory, and then some related state of the art is discussed.

2.4.1 Bipartite Graph in Graph Theory

This section lays the foundation of resource allocation study in D2D communication by defining the graph theory. The fundamental terminologies of graph theory that are described here are also used as a base for the algorithm developed in Section 3.6.3.

A graph consists of three finite sets, U, V, and E. Element U and V are called vertices. The edge E represents a connection between a pair of vertices. For instance, the U and V might be { a, b, c, d }, and $\{e, f, g, h\}$ respectively. The element E might be $\{\{a,f\}, \{b,g\}, \{d,h\}\}$. The elements U, V, and E, are a graph G.

There is no unique drawing a graph; the graphical presentation is used to define different concepts in graph theory. Figure 2.10 illustrates an exemplary representation of the graph G.

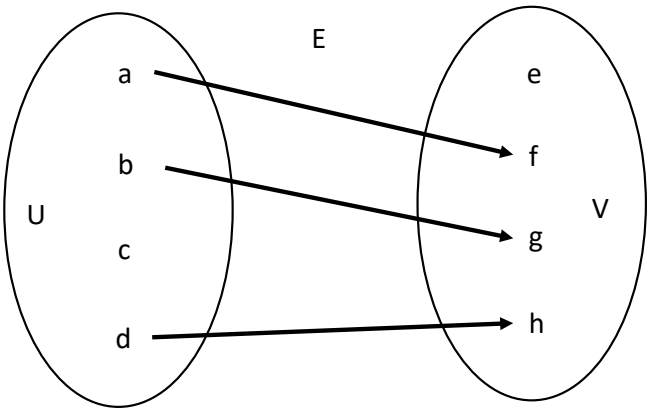

FIGURE 2.10: An illustration of graph theory.

Some of the definitions in the graph theory are described as follows:

Definition 2.4.1.1. A graph has a loop when two vertices of an edge are identical, i.e., $E = (U, U)$ or E=(n, V). An edge of graph G is multiple edges if it appears numerous times in the edge family of the graph. If a graph does not form loops or multiple edges, it is a simple graph.

Definition 2.4.1.2. Two vertices U and V of a graph G are adjacent when there exists at least one edge joining them together, and the vertices are incident with that edge. Similarly, two distinct edges are adjacent when there is a common vertex for both edges.

The Figure 2.11 represents the illustration of adjacent vertices and adjacent edges.

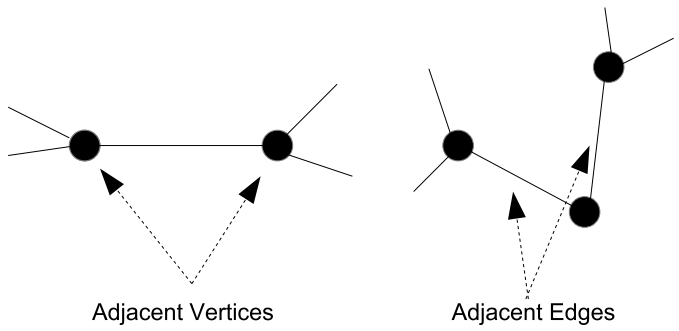

FIGURE 2.11: Illustration of adjacent vertices and edges.

It is worthy of mentioning that a simple graph is a complete graph when each pair of distinct vertices are adjacent. The complete graph on n vertices by $\frac{n(n-1)}{2}$ edges. Figure 2.12 exemplifies the complete graph with 5 vertices.

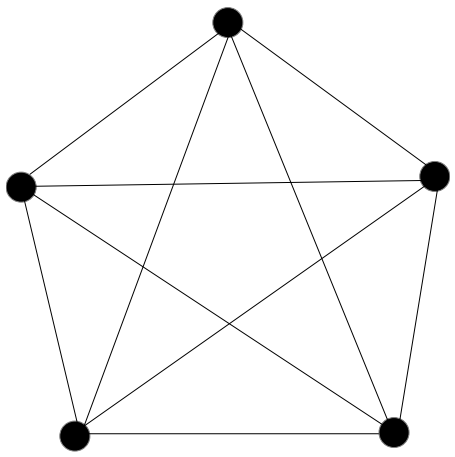

FIGURE 2.12: Illustration of complete graph.

Definition 2.4.1.3. The graph family G is a bipartite graph, if the vertices of a graph G is divided into two disjoint vertices, U and V, wherein an edge connects a vertex in set U to a vertex in set V.

Alternatively, Bipartite graph vertices can be shown with black, and white color wherein every white vertex in U is joined the black vertex in V by an edge indicated in E. A Bipartite graph is a complete graph when all vertices in U are fully connected to all vertices in V by edges. Figure 2.13 denotes a complete bipartite graph with 3 black vertices and 4 white vertices.

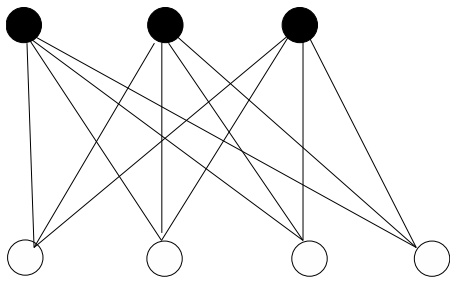

FIGURE 2.13: Illustration of complete Bipartite graph with three and four vertices.

The bipartite graph can be used to model many problems, e.g., assignment problems. Such problems aim to maximize the number of edges whose not share the same endpoint, i.e., matching. The matching concept in the Bipartite graph is defined as follows:

Definition 2.4.1.4. Two edges of a bipartite graph are said to be independent when they have no common end vertex and loop. A matching is a set of separate pair edges of a graph. A matching with maximum cardinality is called maximum matching.

It is worth mentioning that a graph with maximal matching is different from a maximum matching. The maximal matching in the Bipartite graph is matching with the property that if any edge is added, it would not be a matching anymore. In contrast, a maximum matching contains the most significant possible number of edges. The Edges with red color in Figure 2.14 exemplifies the difference between the maximum and maximal matching in the graph theory.

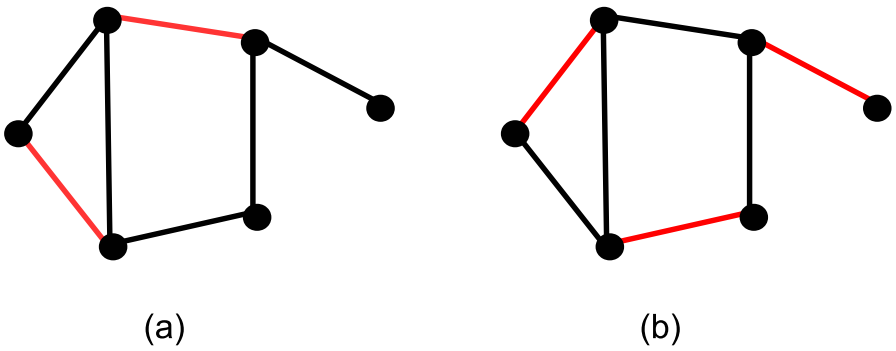

FIGURE 2.14: An illustrative example of (a) Maximal matching (b) Maximum matching in Bipartite.

In continuation of the Bipartite graph definition, the alternating and augmenting path in the matching are explained as follows: The alternating path is a path that starts at an unmatched vertex and then continues, alternately, edges from not matching and matching. The alternating path that ends in an unmatched vertex is an augmenting path. Note that in a practical search, we start with matching and keep applying augmenting paths until an optimal matching is achieved. This way, algorithmic complexity of finding such a matching is reduced to an augmenting path exploration.

Another version of matching is weighted matching wherein every edge in the graph is weighted by a specific value, e.g., utilization rate. The objective of unweighted and weighted matching are different. The unweighted matching aims to find the largest

number of edges, while in the weighted matching, the aim is to find a matching with the largest total weight. In a weighted bipartite graph, the matching problem is cast as a maximum weighted bipartite matching or assignment problem, wherein the Hungarian method is envisioned as a canonical solution to address the assignment problem [77].

The section continues to review state of the art in the context of graph theory with a focus on radio resource allocation in the V2X communications.

Authors in [78] proposed a two stages algorithm wherein radio resources and power are allocated to both vehicular and cellular users. Firstly, they applied a water-falling method to assign power equally to both vehicular and cellular users. The orthogonal radio resources are shared between the cellular users and vehicular users, which can increase interference among the users. Then, the radio resource allocation problem is transformed into a maximum weight matching problem in a bipartite graph. In the bipartite graph, the users are sharing resources place in one disjoint vertex of the graph, and the radio resources are considered as another vertex. They use the Hungarian method to address the problem. Secondly, the transmit power is converted into a convex problem and then is adjusted for both vehicular and cellular users through an interior point method. The results reveal a slightly better performance of the proposed scheme compared to the other studied algorithms.

Authors in [79] proposed a graph-based resource allocation algorithm for broadcast V2V communications aiming to maximize the sum-rate of the network. The vehicles and radio resources form vertices and the edges of the bipartite graph. Besides, the edges of the graph are weighted with the achievable throughput associated with the perceived SINR of every vehicle. Then, the vehicular users are divided into different clusters wherein the orthogonal radio resources are allocated within the cluster. Moreover, the radio resource between the two clusters can be reused. In this way, the resource allocation conflict among the vehicular users is reduced, and an optimum solution through maximum matching in bipartite graph yields. Analytical analyses show the optimality of the proposed algorithm in terms of the sum-rate.

In [80], a radio resource allocation algorithm is proposed, wherein QoS requirements for both V2I and V2V users considering QoS are taken into consideration. The resource allocation problem is cast mathematically as a sum ergodic capacity maximization for cellular users while ensuring the reliability for all V2V users. The authors first model the problem with a Bipartite graph and apply the bisection search and the Hungarian methods to achieve the maximum ergodic capacity.

Authors in [81] proposed a geography-based resource allocation algorithm in which the impact of boundary interference and vehicle density are taken into consideration. Firstly, a geographical area is divided into different groups, and all vehicle members are decided based on a set of defined rules. Then, the geographical area selection is transformed into a matching maximization problem in a bipartite graph, which can be addressed by the classical Kuhn-Munkres algorithm, as mentioned earlier.

2.4.2 Auction Theory

This section first explains the basic concept and elements of auction theory, whose principle is used for the algorithm, developed in Section 3.6.4. The auction theory in a Bipartite graph theoretic-model is then described. Besides, the optimization methods

and some applications are discussed. Finally, the state of the art with a focus on auction-based radio resource allocation is represented.

An auction has different forms that are mainly characterized by universality and anonymity. In other words, the auction may be used to sell every good no matter who is the bidders. An auction is generally characterized by a set of rules that govern the sale and buy of an object. For example, in a standard auction, the participant with the highest bid would win the auction. On the contrary, in a non-standard auction, regulations are ruled differently, and not nearly the regulations in a conventional auction should be followed [82]. In the following, four types of conventional auctions are defined.

Definition 2.4.2.1. **First-price auction:** It is an auction wherein the object is sold to those who paid the highest bid. Alternately, in a procurement auction, a bidder who submits the lowest bid is considered as a winner. In first-price auctions, bidders submit bids simultaneously, i.e., sealed-bid. Also, bidders show a bid value more moderate than their actual value.

Definition 2.4.2.2. **Second-price auction:** An auction where the bidder who presented the most noteworthy bid is granted the item being sold and follows through on a cost equivalent to the second most elevated sum bid. On the other hand, in an acquirement sell-off, the winner is the bidder who presents the most reduced bid and is paid a sum equivalent to the next least submitted bid. Practically speaking, second-price auctions are either sealed-bid, in which bidders submit offers concurrently or English auction, in which bidders keep on raising each other's proposals until just a single bidder remains. The casual comfort of second-value auctions first called attention to by William Vickrey, is that offering one's actual value is a prevailing procedure. Then again, first-value auctions likewise grant the item to the most elevated bidder; however, the payment is equivalent to the sum bid.

Definition 2.4.2.3. **English auction:** English auction is a kind of consecutive second-price auction in which an auctioneer guides contributors to beat the present standing bid. New bids must expand the current offer by a predefined increase. The auction closes when no contributors are eager to outbid the present standing offer. At that point, the contributors who put the current offer is the winner and pays the sum offer. An English auction, where the most noteworthy bidder pays the sum offer, is named a second-value sell-off since the triumphant bidder needs just outbid the following most elevated bidder by the base addition. Hence, the victor adequately pays a sum equivalent to (marginally higher than) the second most elevated offer.

Definition 2.4.2.4. **Dutch auction:** A sort of the first-price auction in which a "clock" at first demonstrates a cost for the article available to be purchased generously higher than any bidder is probably going to pay. Afterward, the clock step by step diminishes the cost until a bidder "Hum in" or shows their readiness to pay. The auction is then finished up, and the triumphant bidder pays the sum thought about the clock at the time the individual in question halted the procedure by "Humming in". These auctions are named after a typical market instrument for selling blooms in Holland; however, they likewise reflect stores progressively decreasing costs on particular things.

Most auction hypothesis spins around these four "standard" auctions sorts mentioned previously. Be that as it may, other auction types have likewise gotten some scholarly investigation as the following.

Definition 2.4.2.5. **Japanese auction:** A kind of consecutive second-value auction, like an English auction in which an auctioneer routinely raises the present price. The

participants must show a signal at each price level their readiness to stay on the auction and pay off the current cost. Hence, in contrast to an English auction, every participant must offer at each level to remain in the auction. The sale closes when just a single bidder demonstrates her ability to remain inside the auction. This auction design is otherwise called the button auction.

Definition 2.4.2.6. **All-pay auction:** Bidders place their offers in sealed envelopes and, at the same time, hand them to the auctioneer. The envelopes are opened, and the person with the most elevated offer successes, following through on a cost equivalent to the certain sum that the individual in question offers. All losing bidders are additionally required to pay to the auctioneer comparable to their offer in an all-pay auction. This auction design is non-standard, but it may be utilized to comprehend things, for example, political competitions or queuing for rare items. The most direct type of an all-pay auction is a Tullock auction, in some cases called a Tullock lottery, wherein everybody presents an offer that both the defeated persons and the victors pay their submitted offers. The auction is instrumental in portraying specific thoughts in open decision financial aspects. The dollar auction is a two-player Tullock auction, or a multiplayer game, in which just the two most remarkable bidders pay their offers. Different types of all-pay auction exist, for example, the war of attrition, where the most noteworthy bidder wins, yet all (or both, all the more commonly) bidders pay just the lower offer.

Definition 2.4.2.7. **Unique-bid auction:** A kind of technique game identified with customary auction in which the victor usually is the person with the most reduced exceptional offer, albeit less regularly the auction standards, may indicate that the unique outstanding offer is the victor. One of a kind offer auction is typically utilized as a type of rivalry or lottery.

Definition 2.4.2.8. **Generalized second-price auction (GSP):** A non-honest auction technique for various things, the first idea of as a natural extension of the Vickrey auction, it does not preserve some significant properties of the Vickrey auction. It is utilized predominantly with regards to keyword auctions, in which guaranteed search slots are sold on an auction basis.

In all the above auction mechanisms, a bidding strategy has an important rule to achieve equilibrium among all bidders. In a game with private information, the bidding strategy is a mapping from a player's private information to his action. For example, in a sealed bid auction, the secret information is the player's value, and the action is the bid submitted. In other words, the bidders with the higher costs are tending to pay more to win; thus, mapping from value to bid is ascending. This mapping for a bidder can be written as follows.

$$b = B\left(v\right), \tag{2.1}$$

where b is a biding value and B_i and v_i are mapping function and value respectively. We will think about games in which there is no known discrimination among the bidders. Most of the time, we will assume that the strategies of the various bidders are the equivalent.

A list of the strategies of the n bidders is defined as a strategy profile. Given complete information, a strategy profile $\{B_i\left(v_i\right), ..., B_n\left(v_n\right)\}$ is an equilibrium of the game if every bidder's strategy increases his benefit when the others are playing as indicated by the strategy profile. Each strategy is a "best reaction" to the others' strategies.

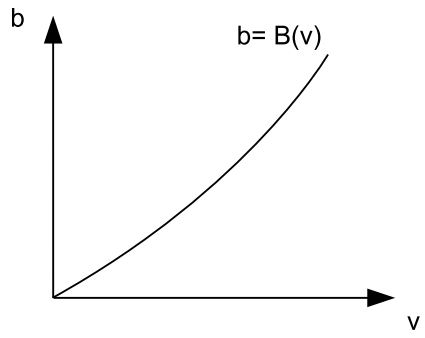

FIGURE 2.15: An illustrative example of equilibrium bid strategy function.

Figure 2.15 shows a illustrative example of equilibrium bid strategy function. We will show that there is a unique symmetric equilibrium bid function. Given than $w(v)$ to be equilibrium probability for a buyer having value v. The buyer loses the auction when other buyers propose a higher equilibrium bid than others. Given that the probability of a tie situation is negligible, the probability of buyer winner i is equal to the probability of all other buyers that have lower values. Note that, the probability that buyer j has a lower value is $Pr\{v_j \leq v_i\} = F(v_i)$. As a result, the equilibrium probability for two players are equal to $w(v_i) = F(v_i)^2$. In the auction, payoffs are defined as an expected profit of a player based on the bidding strategy function. Let $U(v)$ be a buyer's equilibrium expected payoff and is the win probability times the gain $v - b(v)$ when the buyer wins. As a result, the payoff can be formulated as follow.

$$U(v) = w(v)(v - b(v)). \tag{2.2}$$

Where the first term denotes the equilibrium payoff of a buyer on the value v, and the second term represents the buyer pays the price. Note that the cost is paid by the buyer is the expected revenue of the seller.

We close this section by reviewing of the radio resource allocation as a prospect application in the auction theory. To this aim, we look into some state of the art in the context of the radio resource allocation employing the auction theory [83], [84], [85], [86], [87].

In [83], the authors proposed an optimal spectrum assignment mechanism that is characterized by incentive compatibility, fairness, efficiency, benefits maximization, and computational manageability. To that aim, an auction-based approach is proposed wherein ever user equipment UE submits its demanded bandwidth by the BS. The BS duty is to design the allocation strategy through auction theory, e.g., pricing rule, to maximize the accrued benefit.

Authors in [84] investigated in the amenability of Game theory in radio resource allocation for D2D communications. The non-cooperative and cooperative behavior of mobile users in the context of D2D communication underlaying cellular networks is analyzed. The authors outlined that a non-cooperative game and auction game models are suitable to address the resource allocation problem in direct D2D communications. Also, they propose a cooperative game among mobiles to solve the radio resource allocation problem for a group of D2D users that forms a local area network.

In [85], the authors proposed an auction-based distributed approach by which the radio resources are allocated for D2D communications. The complexity and optimality of the proposed solution are discussed, and the applicability of the proposed scheme in a practical system is examined. The auction-based resource allocation depends on the offering procedure whereby the agents (i.e., underlay transmitters) make their offer on the resources (e.g., RB and power level). Every transmitter offers a price for the resources depending on the costs (e.g., the interference caused to the cellular users) of the desired resources. The ideal task depends on the suitable determination of the offers - the unassigned transmitters raise the cost of the desired resources and increase the price accordingly. At the point when the offers of all transmitters are accessible, the resources are allotted to the most elevated bidder. The results showed that the proposed solution has enough tightness to the achievable data rate while having less complexity and minimum involvement of the central controller node.

Xu et al [86] discussed a radio resource allocation approach for D2D communication underlying LTE downlink network. The authors introduced a new radio resource allocation employing a reverse iterative combinatorial auction wherein all radio resources are considered as a commodity. In the proposed algorithm, the bidders first contend for the radio resources while excluding the D2D users from the auction. This way, the valuation of each radio resource is obtained. Next, a non-uniform descending price auction algorithm is applied considering the channel gain of the D2D communication and the imposed cost on the cellular network. Also, the proposed algorithm is examined in terms of time-complexity and cheat-proof. Simulation results demonstrated the efficacy of the auction-based resource allocation algorithm in terms of the sum-rate.

In [87], Huang et al. proposed a cooperative radio resource allocation scheme based on the auction theory. The authors consider the Signal to Noise Ratio (SNR) and the transmission power of every user as a commodity in an auction mechanism wherein the relay power allocation among users is coordinated in a distributed manner. The uniqueness of Nash equilibrium in both auctions is examined through the non-negative matrix theory. Besides, it has been appeared to accomplish the power auction efficiently. Furthermore, the SNR auction has been believed to be adaptable in accomplishing different trade-offs among faintness and efficiency, relying upon the priority weight. Moreover, it has been demonstrated that users can accomplish one of a kind Nash equilibrium in a distributed and asynchronous style. It has been additionally indicated that the primary properties of the two auctions are relevant for networks with various relays in different areas.

2.5 Summary

As preparation for the detailed discussion of the thesis contributions, this chapter has outlined the fundamental literature that relates to the rest of the thesis. The shortening TTI and D2D communication are introduced by which the uRLLC application requirements can be fulfilled. In D2D communication, *Overlay* and *Underlay* resource allocation are described. Specifically, in the *Overlay* D2D communications, autonomous radio resource allocation in V2X communications is explained, and the related state-of-the-art are described. Finally, Graph and Auction theory are explained, and the literature to date considering the Bipartite Graph- and Auction-based resource allocation are explained.

CHAPTER 3

Sub-granting Radio Resource Scheme

Contents

This chapter introduces the framework of the sub-granting radio resource approach in overlay D2D communication. The structure forms the basis for the performance evaluation presented in the subsequent Chapters. Starting with an introduction to motivation for proposing the sub-granting scheme, we continue in the second and third sections to discuss the pros and cons of different scenarios and explain the system model considered for the sub-granting scheme study. Section 3.4 explains the design aspect of the sub-granting scheme, wherein the necessity of modifications in the physical layer and developing new algorithms in Media Access Control (MAC) layer for transmitter and receiver are discussed. The shortening TTI advantages in latency reduction inspire us

to enhance the algorithms at the transmitter and the receiver aiming to reduce the data transmission time and overhead between two communicating devices while utilizing the sub-grant scheme. Further information corresponding to the proposed enhancement inspiring from the shortening TTI is explained in Section 3.5. Section 3.6.1 describes the principle of operation of the sub-granting scheme. In the sub-granting scheme, the beneficiary user selection problem is formulated as an uplink cell throughput maximization problem. Section 3.6.2 discusses the beneficiary user selection problem and proposes a dedicated and an open sub-granting algorithms employing the maximum matching in the Bipartite graph and the Auction theory to address the problem mentioned earlier.

3.1 Introduction

The LTE sidelink is an adaptation of the core LTE standard that allows direct communication between two LTE devices without going through a BS. The LTE sidelink was defined by 3GPP in Release 12 as a standard that can be used for public safety communications. Figure 3.1 illustrates an access stratum protocol stack for user plane in the sidelink interface, i.e., PC5 interface, consisting of Packet Data Convergence Protocol (PDCP), Radio Link Control (RLC), MAC, and Physical (PHY) in the LTE technology. Further detialed about functionalities of different layer are decribed in [88]. In the previous chapter, a comprehensive literature survey on D2D focusing on the overlay radio resource allocation algorithms was undertaken, and the pros and cons in this regard were discussed. Considering semi-persistent scheduling in the overlay D2D communication, we endeavor to investigate the radio resource allocation avenues to increase spectral efficiency in the LTE network.

The M2M is envisioned as one of the widespread applications in LTE and future wireless communication whose generated data is relatively small, i.e., the payload length of a single transmission ranging between 10 to 50 Bytes (See Table 3.1) [89]. However, LTE currently fails to efficiently utilize the available communication resources as the granularity of the allocation is too coarse. Therefore, with any possible MCS, a typical transmission of a M2M application may not fully occupy the minimum radio resource block size that needs to be allocated to a single user. As a consequence, valuable radio resources would be wasted in the current radio networks, in case of multiple deployed M2M applications.

Just recently, the idea to allocate resources below subframe basis, i.e., shortening the length of a TTI to 0.5ms or even a single OFDM symbol, was introduced in [90] and [91]. We follow up with this idea and propose a novel resource reuse scheme on a sub-grant basis. For instance, partially or fully unutilized grants that were initially reserved

Table 3.1: Example of M2M closed-loop control application requirements [89].

Application Type	Packet size [Byte]	Cycle time [ms]
Printing Machines	30	2
Machine Tools	50	0.5
Packaging Machines	15	5
Sensor actuator	20	not specified

for a D2D communications, i.e., sub-grant provider user, are granted to D2I-UEs, i.e., the beneficiary user. This way, we increase the D2I-UE throughput with unused D2D resources, which would otherwise be wasted.

Our scheme is based on the assumption that in each transmission interval, the sub-grant provider user is aware of the unoccupied-scheduled resources. Besides, the sub-grant provider user utilizes a small portion of the allocated radio resources to indicate the free symbols to a nearby beneficiary user in order to use the remaining portion of the scheduling grant. This way, we increase the overall cell throughput in the cellular network. Also, in this chapter, we overview the requirements, problems, and procedures to realize the sub-granting scheme in LTE technology. To this aim, we first take a short look into the current sidelink communication in LTE technology to identify the requirements and changes needed for the realization of the sub-granting scheme in the sidelink protocol layers.

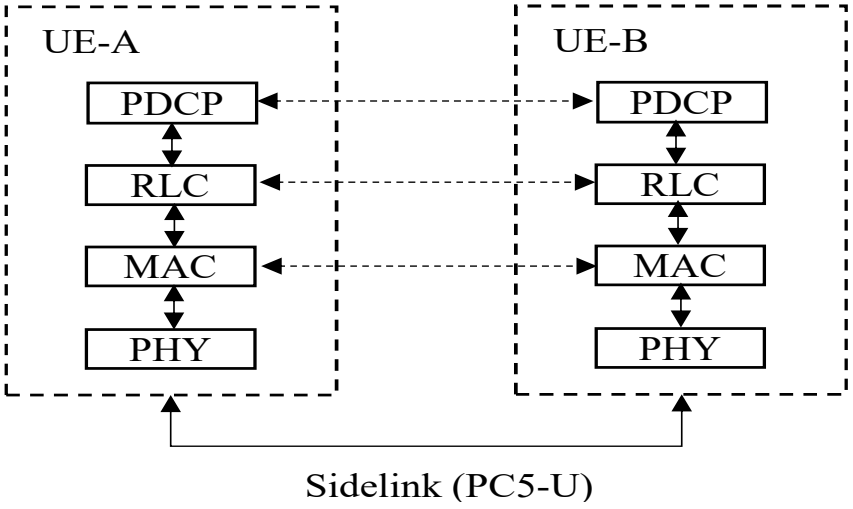

FIGURE 3.1: Visualization of user plane sidelink protocol layer in LTE technology.

3.2 Possible Scenarios in Sub-granting Scheme

We analyze different sub-granting scenarios considering the communication type for beneficiary users and sub-grant provider users. The sub-grant provider user and the beneficiary user could be either D2D or D2I communication, whereby four types of sub-granting scenarios are defined. Figures 3.2 - 3.5 illustrate the sub-granting scenarios and use cases. Generally, in a D2I communication, the eNB has global knowledge of the location, signal level, and buffer status of the user based on the measurements received from the cellular users in every measurement interval. In contrast, in D2D communication, the eNB is not aware of some information, namely user buffer status report and channel measurement between two communicating, or this information can be achieved at the cost of high measurement and signaling overheads on the eNB. In a centralized approach, e.g., DSGRR algorithm, the eNB selects a beneficiary user based on the available measurement information to increase the overall uplink throughput. Note that although the eNB has initially scheduled radio resources for the D2D users, the radio link condition and traffic buffer status of the D2D communication may change, and thus

the D2D communication information becomes outdated quickly. This reason makes the D2D user an inappropriate candidate for the beneficiary user in a centralized scenario. In contrast, the D2D user can independently decide and grant un-utilized resources to the beneficiary user selected by the eNB, whereby the D2D user becomes a suitable candidate as the sub-grant provider in a centralized scenario. In a decentralized approach, e.g., OSGRR, the eNB is not involved in the beneficiary user selection procedure. Thus the sub-grant provider user and the beneficiary user can be either a D2D or a D2I user, and thus four different scenarios can be defined.

Different use cases can apply the sub-granting scheme. One example is sub-granting radio resources from V2V user to Pedestrian to Infrastructure (P2I), M2M, V2I user, and vice versa.

In the following sections, the centralized and decentralized approaches are described, and the corresponding performance metrics, e.g., the uplink cell throughput, overhead, and the average number of the selected beneficiary user, in stationary and dynamic scenarios are formulated. Here, we consider the D2D and the D2I UE as the sub-grant provider and the beneficiary users, respectively, in order to have a fair comparison between the proposed algorithms.

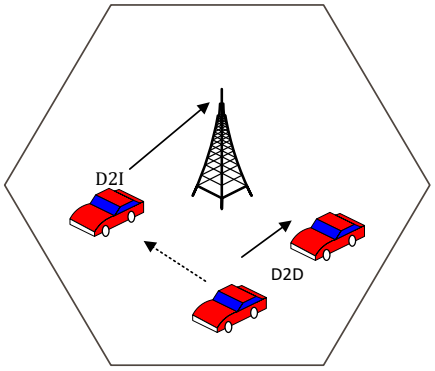

FIGURE 3.2: Sub-granting from D2D user to D2I user

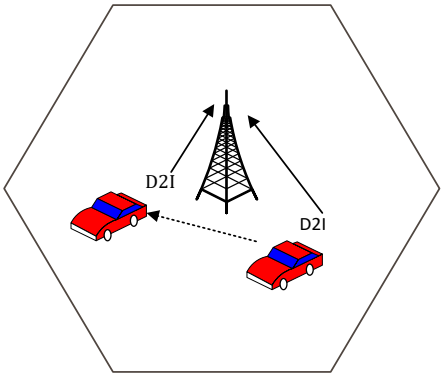

FIGURE 3.3: Sub-granting from D2I user to D2I user

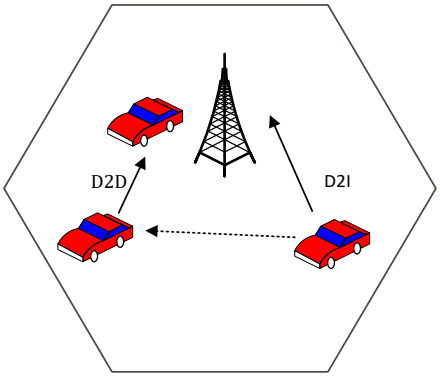

FIGURE 3.4: Sub-granting from D2I user to D2D user

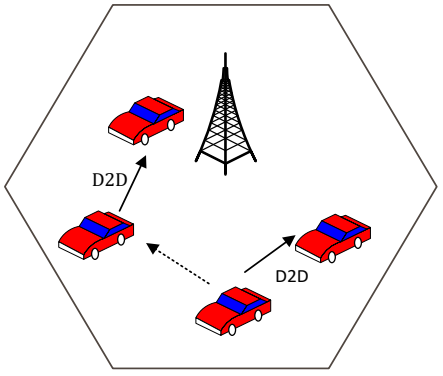

FIGURE 3.5: Sub-granting from D2D user to D2D user

3.3 System Model

We consider a single-cell environment with M D2I users (D2I-UEs) and N D2D users (D2D-UEs) denoted by sets $C = \{1, ..., M\}$ and $D = \{1, ..., N\}$, respectively. All users are uniformly distributed over the cell. We assume users also randomly move through the cell. Figure 3.6 graphically shows an example of the network. Let us assume there are F Resource Blocks (RBs) in the uplink direction for both D2D and D2I users. The eNB coordinates L RBs for D2D pairs and the remaining $(F - L)$ RBs for D2I-UEs. The eNB orthogonally schedules uplink radio resources for D2I users at every scheduling time by any reasonable scheduling scheme. To avoid scheduling delays, the eNB assigns one Resource Block (RB) to every D2D-UEs for a specific time (see Label (1) in Figure 3.6). We assume that the D2D-UEs can disseminate the signaling information indicating the allocated but unused resources, i.e., sub-granting (see Label (2) in Figure 3.6), to the all nearby D2I-UEs, i.e., beneficiary user (see Label (3) in Figure 3.6). Also, the D2I-UEs are a side-link capable user who can communicate with other users in proximity through the side-link communication [48].

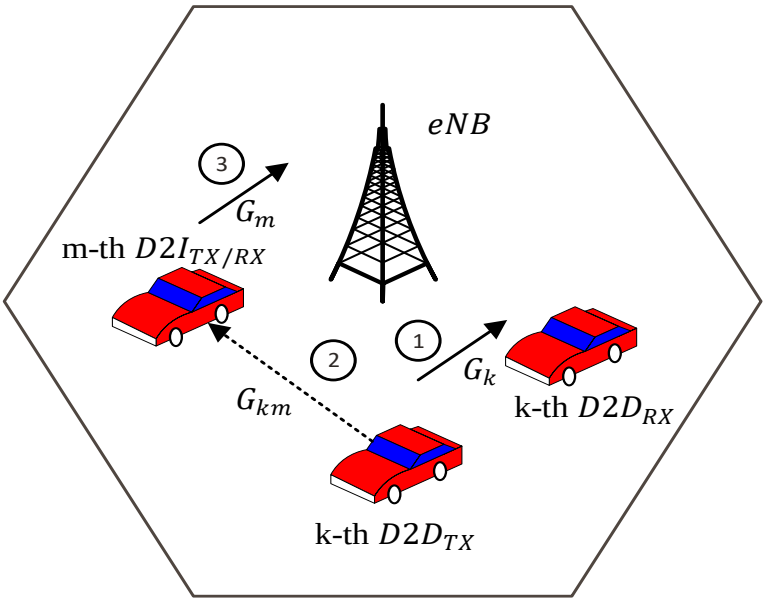

FIGURE 3.6: A typical network is consisting of one eNB, one D2D-UE, and one D2I-UE. The $k - th$ D2D user sub-grants the un-used radio resources to the $m - th$ D2I user, when channel gain G_{km} between $k - th$ D2D user and $m - th$ D2I user is above a certain threshold.

The further assumptions in this study are made as follows:

- All D2I-UEs are full buffer users with best-effort traffic payload.
- D2D-UEs have small traffic payload with the same reliability and latency requirements, e.g., ultra-reliable and low-latency applications.
- All D2D and D2I users are synchronized in time and frequency from the BS.
- All users' velocities are assumed to be constant during movement. At the initiating position and the cell border, the users choose an arbitrary route on a random basis.

- The processing time for decoding sub-granting signaling message and encoding data S_{Min} is assumed to be less than the time of two symbols for the beneficiary user.
- We assume the channel condition remains unchanged during the beneficiary user selection process. Besides, the amplitude of the received signal with distance is assumed to follow an exponential decay as follows:

$$G = \mathrm{c} \times r^{-\alpha}|\mu|, \tag{3.1}$$

  where r is the distance between two entities, c is a constant value, and α capture path-loss exponents, and μ represents the large- and small-scale fading phenomena.
- We assume an open-loop power control mechanism that the transmission power of every communicating entities is controlled by the path-loss [92].
- We assume that the BS is aware of the Channel State Information (CSI) and buffer status report of D2I users. Besides, all users are equipped with a global positioning system (GPS), and thus be able to send the positioning information to the central network in every (pre-) configured time interval.
- To reduce the processing time due to blind decoding during the sensing procedure, it is assumed that the sensing procedure is only performed on the (pre-)configured radio resources by the BS.
- The notations used in the dissertation are summarized in Table 7.1.

3.4 Sub-granting in PHY/MAC Layers

This section describes the modifications required to realize the sub-granting scheme in the physical and MAC layers. To this aim, additional fields in the physical layer devised through which a flexible subframe for the sub-granting scheme is constructed. Besides, some algorithms are required to be developed in the MAC layer to delegate the unutilized radio resources from the sub-gran provider to the selected beneficiary user. Further, in the physical layee, an algorithm is developed to react immediately to the sub-granting signaling such that to make receiving sub-frame size flexible depending on the number of sub-granted symbols at the beneficiary user.

3.4.1 General Modifications in Physical Layer

In the sub-granting scheme, in order to achieve the required responsiveness of the D2I-UE, we assume several modifications in the physical layer that can be summarized as follows:

- Recalling turbo coding shows better performance compared with convolution coding, and thus is adopted for data communication in LTE [63]. However, the turbo coding can not fulfill the latency required by the uRLLC applications, since the receiver starts decoding after the complete transport block is received. On the contrary, the convolution coding enables the receiver to decode the data per OFDM

Table 3.2: List of Notations

Notation	Interpretation
D	The set of D2D users where $d_k \in D$ for $k = 1, ..., N$
C	The set of D2I users where $c_m \in C$ for $m = 1, ..., M$
L	The set of allocated RBs to D2D
F	The set of available RBs on BS
B_w	Allocated bandwidth
b	Allocated RBs to every entities where $b = 1, ..., F$
$\mathbb{X}$	Allocation indicator for sub-granting
α_c	Path loss component for D2I
α_d	Path loss component for D2D
μ_c	Fading component for D2I
μ_d	Fading component for D2D
σ_0	White Gaussian noise
σ	Shadowing term
P_m	Transmission power of D2I transmitter, $m = 1, ..., M$
P^C_{max}	Power threshold limit for D2I transmitter
P_k	Transmission power of D2D transmitter, $k = 1, ..., N$
q	Modulation and coding scheme of every entities
ϵ^D_{th}	Minimum Block Errors Rate (BER) threshold for D2D
ϵ^{sg}_{th}	Minimum BER threshold for sub-granting
ϵ_{mk}	Measured BER between D2D and D2I
ϵ	General term for BER
T	Subframe transmission time
τ	Transmission duration
T_{me}	Channel state information measurement interval
T_{pos}	Positioning measurement interval
T_{br}	Bids transmission interval
S_{Min}	Processing time of sub-granting signaling
$\mathcal{Z}$	Unique number of a cellular user in network

symbol.
Therefore, to reduce delay for decoding, convolution codes instead of turbo codes are applied. The convolution coding allows starting processing symbols while they are being received [93].

- Flexible framing mechanism that can be used to carry additional signaling information, i.e., the number of the first free OFDM symbol in our case.

Figure 3.7 depicts an illustrative example of the LTE subframe and the proposed customized subframe employed by the sub-granting.

3.4.1.1 Contextual Information in Sub-granting Signaling

The proposed resource reuse scheme requires a signaling mechanism that is used by the original owner of a scheduling grant to inform a beneficiary user, i.e., D2I-UE in its vicinity about the number of resources that can be reused.

In principle, multiple ways to convey the details about this sub-grant are conceivable. One possibility would be to send the sub-grant over a dedicated channel, e.g., the Physical Sidelink Control Channel (PSCCH) [48]. However, using an out-of-band scheme for signaling also occupies resources in that channel and may soon become a bottleneck as the number of UEs increases.

In order to not increase the load of any other channel, in-band signaling could be used as an alternative. Within an in-band scheme, the required control information is embedded in the actual data transmission. For example, one possibility is to insert a *marker* at the end of the D2D-UE's transmission that is used to pass the sub-grant to the D2I-UE. This way, the sub-grant would be valid starting from the time at which the marker has been received until the end of the subframe. However, putting a marker at the end of the D2D-UE's subframe imposes a considerable burden on the processing capabilities of the D2I-UE because it is required to react immediately in order to utilize the sub-grant fully. Therefore, we propose to let the D2D-UE embed the sub-granting signaling information, i.e., the marker, at the beginning of transmission inside the first symbol of a subframe. This marker contains the offset relative to the beginning of the subframe from which the sub-grant is valid. As each subframe may contain an individual sub-grant, the exact number of symbols available for the D2I-UEs can be determined by D2D-UEs, given that both UEs are time-synchronized. After receiving and decoding the first symbol of a nearby D2D-UE, this provides the D2I-UE enough time to prepare and schedule its transmission. Figure 3.7 illustrates the structure of the modified subframe and legacy subframe for D2D-UE and D2I-UE. Note that we assume that the D2I-UE requires a minimum number of symbols for decoding the sub-grant and preparing its transmission, denoted as S_{min} in Figure 3.7.

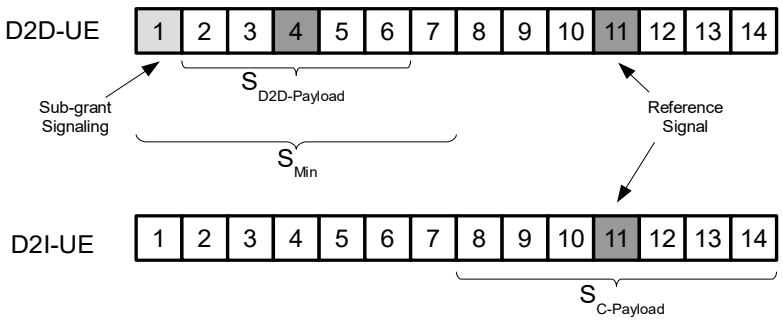

FIGURE 3.7: Illustration of the modified subframe structure and symbol allocation, assuming that the D2D-UE transmits 6 symbols (of which 4 are for data) and the D2I-UE 7 (of which 6 are for data).

The additional overhead for signaling includes the S_{FT} by which the marker indicates an unused sub-grant within the subframe. If set, the RB pair further includes the ID of the selected UE as well as the starting symbol of the sub-grant. The marker requires a single bit. Assuming zero processing time, the maximum number of symbols that a sub-grant can be valid for, is 12, i.e., $12 = 2 \cdot 7 - 2$. Note that in every uplink Physical Resource Block (PRB), one symbol is used for transmitting the DMRS. Therefore, encoding the symbol offset requires at most 4 bits, i.e., $2^4 = 16$. Assuming that eight symbols would be the maximum number of symbols for reuse, even 3 bits would be sufficient. Further assuming that the maximum number of UEs to address is 8, we need an additional 3

bits for encoding the beneficiary user identity. Altogether, this sums up to 8 additional bits for signaling that can be modulated on a robust modulation scheme, e.g., BPSK or QPSK modulation symbols that are not used for data transmission. In order to further improve the probability of being able to decode successfully them, they could be further spread across multiple sub-carriers within the PRB.

3.4.2 Sub-granting Provider

As early mentioned, the BS schedules a set of radio resources for every D2D users in a semi-persistent manner. Then, the sub-grant provider is able to grant the unutilized radio resource to that the nearby users to utilize the allocated radio resources efficiently. The sub-grant provider informs the nearby beneficiary users about the unused resources and plays no role in the beneficiary user selection process.

Algorithm 3.4.1 Sub-grant provider

```
1:  procedure SUBFRAME TRANSMISSION
2:      Discovery ← (D2I- IDs and CQIs)
3:      while (HaveSchedulingGrant) do
4:          S_FT := 0                                   ▷ normal subframe
5:          if (HaveFreeSymbols) then
6:              S_FT := 1                               ▷ customized subframe
7:              S_D2I_ID ← Selected D2I-UE
8:              S_FFS ← First Free Symbol
9:          end if
10:         TransmitSubFrame()
11:     end while
```

Algorithm 3.4.1 describes the sub-grant delegation of the D2D-UE for the D2I-UE resource reuse, where

- S_{FT} denotes the subframe type. The first bit is set to 0 for normal subframe, and set to 1 for a customized subframe, indicating a free sub-grant.
- S_{D2I_ID} denotes the ID of the selected D2I-UE, i.e. the receiver of the sub-grant.
- S_{FFS} indicates the starting symbol of the subframe, i.e., the symbol from which the D2I-UE can start to insert its data.

During the discovery procedure (line 2 in Algorithm 3.4.1), the serving cell will provide the D2D-UEs with a list of D2I candidates in their vicinity that may require additional resources. Along with the ID of each D2I-UE, this list also contains the channel quality indication (CQI) between the D2I-UE and the eNB. For each subframe that the D2D-UE transmits, the subframe type is initially set to "normal", indicating that no free resources are available. In a case that the D2D-UE does not use all symbols of the subframe, the subframe type is set to "customized", i.e., S_{FT} is set to 1. In addition, the selected D2I-UE ID as well as the number of the symbol from where to start inserting D2I-UE data (S_{FFS}) is included in the subframe.

3.4.3 Sub-granting Beneficiary User

As previously explained, every beneficiary user can monitor other D2D users in the proximity to decode the sub-granting signaling and re-utilize the sub-granting radio resources indicated in the sub-granting signaling. To this aim, it is necessary to devise an algorithm that enables the beneficiary user to receive the sub-grant. This algorithm is executed on any UE that is assigned to another UE, i.e., beneficiary user selection, for PRB reuse and, thus, is expecting to receive a sub-grant (see line 2 of Algorithm 3.4.2). Note that we assume that the eNB assists in the beneficiary user selection procedure. Thus, a D2I-UE that is not assigned to any D2D-UE or is not the sub-granting receiving capable is not required to monitor the traffic of other UEs.

The purpose of this algorithm is to receive and decode the sub-grant and to allocate its data transmission. Therefore, the D2I-UE overhears any D2D-UE transmissions in order detect a subframe containing a sub-grant destined to itself. Every incoming subframe is checked by the D2D-UE in order to detect a subframe including a sub-grant. For any customized subframe, the D2I-UE also checks the D2I-UE ID included in the customized subframe. If it is equal to its ID, the D2I-UE inserts its own data, starting at the position of the first free symbol, indicated by S_{FFS}.

Algorithm 3.4.2 Sub-grant Beneficiary User

```
1:  procedure SUB-GRANT REUSE
2:      Discovery ← (D2D-UE resource grant)
3:                                  ▷ assign potential D2D-UE's resource to D2I-UE
4:      while (NewSubFrame & AssginedForResue) do
5:          if (S_FT == 1) then                                  ▷ customized subframe
6:              if (S_D2I-ID == myID) then
7:                  TransmitSubFrame(offset=S_FFS)
8:              end if
9:          end if
10:     end while
```

3.5 Flexible Subframe in Sub-granting

Transport Block (TB) is nothing but the payload, which is passed between MAC and the physical layers. The TB size is provided in Tables [63] which is a function of MCS and the resource block allocation configured by scheduler [92]. In the case of data transmission, when traffic payload arrived from the application layer in MAC is smaller than a determined TB size, the packet needs to be transmitted immediately due to the low latency requirements, some dummy bits, i.e., padding information, are added to the packet to make it fitted to the TB sizes that are specified in [48]. This incurs overhead on the MAC. This overhead can be reduced, applying the shortening TTI [91]. However, even the shortening TTI subframe with the smallest granularity might be too coarse for those applications with a small payload. Besides, in D2D, the transmission parameters between the transmitter D2D and the receiver D2D are configured in a specific time interval [63]. This way, the overhead increases, since the transmission parameters, e.g., subframe size, are not configured flexibly, especially when the instantaneous traffic payloads are smaller than the configured resources. To address this problem, we develop

algorithms for the transmitter D2D, i.e., sub-gran provider, and its intended D2D receiver aiming at the overhead and latency reduction. For this purpose, the transmitter D2D adopts a subframe size such that to be tailored to the traffic payload and then the size of the transmitted data is indicated through sub-granting signaling. The intended D2D receiver then exploits this sub-granting signaling to identify the subframe size and instantly transfers the receiving data to the MAC. This results in increasing the maximum responsiveness and flexibility of the subframe size and consequently reducing the transmission time between a transmitter D2D and its intended receiver.

In the following, we explain the algorithm developed at the receiver of the sub-grant provider as explained earlier: First, the side-link interface is established, and the receiver configures the parameters (see step (1) in Algorithm 3.5.1). During sidelink control period, when the subframe type is set to "Customized subframe" or "Flexible subframe," the receiver is mandated to decode the sub-granting signaling information. Then, the data length indicated in the signaling information is determined, and the received data is transmitted to the MAC.

Algorithm 3.5.1 Receiver ($D2D - UE_{RX}$)

```
procedure CUSTOMIZED SUBFRAME RECEIVE
    SidelinkConfiguration ← (N_RB, N_SF, S_TB, I_B)
    while (T_SC > 0) do
        DecodeSignaling
        if S_T := Customized then
            Decode S_FS
            SendDataToUpperLayer
        else
            ReceiveNormalSubframe
        end if
    end while
```

3.6 Sub-Granting Radio Resource Algorithms

Intuitively, the maximum throughput is achieved applying the sub-granting radio resource scheme when a beneficiary user with the highest modulation and coding scheme is selected to exploit un-utilized radio resources of a sub-grant provider. Selecting an appropriate beneficiary user can be formulated as a selection problem in the sub-granting scheme. In this section, two algorithms in a centralized, i.e., DSGRR, and decentralized manner,i.e., OSGRR, are proposed by which the best beneficiary users are selected to maximize the overall cell throughput.

3.6.1 Operational Principle of Sub-granting Radio Resource

This section briefly explains the operational functionality of beneficiary user and the sub-grant provider in the DSGRR and the OSGRR algorithms.Figures 3.8 demonstrates the operational state-machine of a beneficiary user in the centralized algorithm, i.e., dedicated sub-granting. In the dedicated sub-granting algorithm, every UE provides the eNB with their actual position information and CSI towards the eNB in a specific time

interval. Afterward, the algorithm computes a hypothetical geographical area for every sub-grant provider user and seeks for a beneficiary user inside the area who achieves the maximum throughput. Every selected beneficiary user is informed about the paired sub-grant provider users and monitors the sub-granting signaling at every time interval to utilize the sub-granting resources.

In a scenario with mobile users, the position and CSI information need to be updated more frequently, resulting in a high overhead on the cellular network. To reduce the overhead arising from the position and CSI information transmission, a distributed sub-granting algorithm, i.e., open sub-granting, is proposed. Figure 3.9 shows the state-machine of the beneficiary user functionality for the open sub-granting algorithm. In this algorithm, the beneficiary user measures the received signal strength of the nearby sub-grant provider users and the eNB. Then, a bid value associated with every sub-grant provider user is computed based on these measurements. The bid value and the sub-grant provider identity are exchanged between nearby beneficiary users. The beneficiary user with the highest bid value can transmit on the sub-granting resource for a time interval.

In both algorithms, the sub-grant provider only informs the nearby beneficiary users about the unused resources and has not an impact in the beneficiary user selection process. Figure 3.10 depicts the functionality of the sub-grant provider in the dedicated and open sub-granting algorithms. In the dedicated sub-granting algorithm, the selected beneficiary user identity and the number of free symbols are indicated by the sub-granting signaling. In contrast, in the open sub-granting algorithm, only the number of free symbols and the sub-grant provider identity is transmitted.

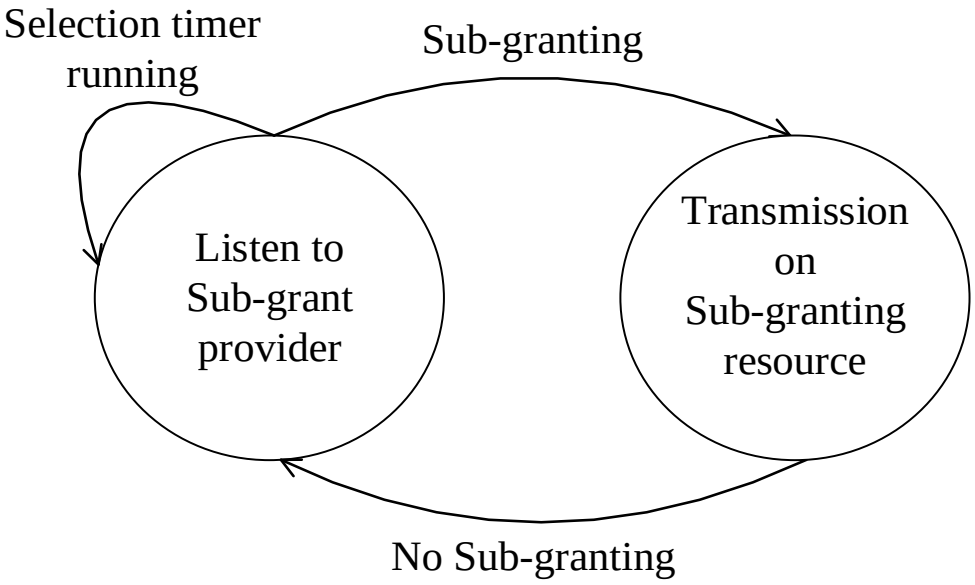

FIGURE 3.8: State-machine diagram of a beneficiary user functionality on the dedicated sub-granting algorithm.

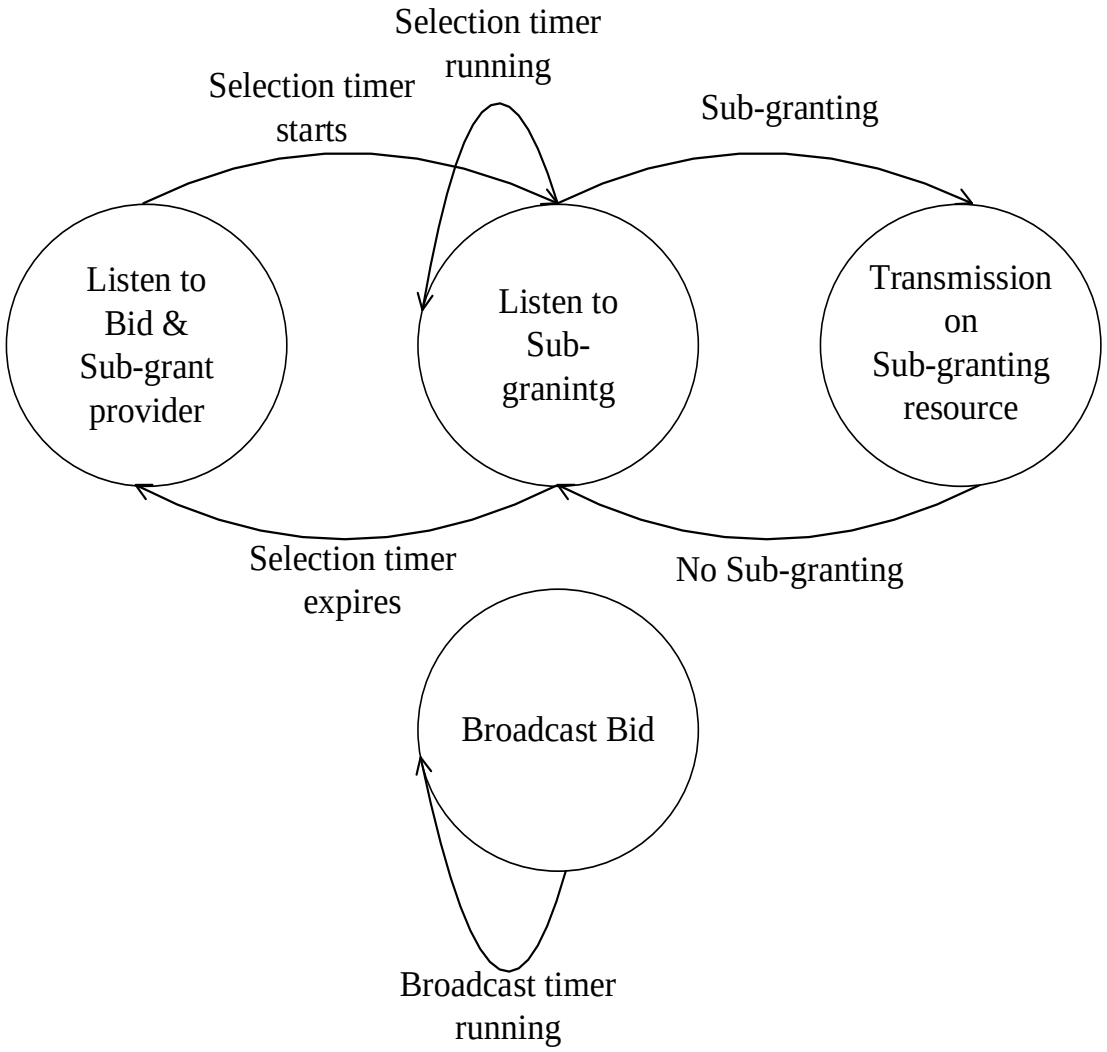

FIGURE 3.9: State-machine diagram of a beneficiary user functionality on the open sub-granting algorithm.

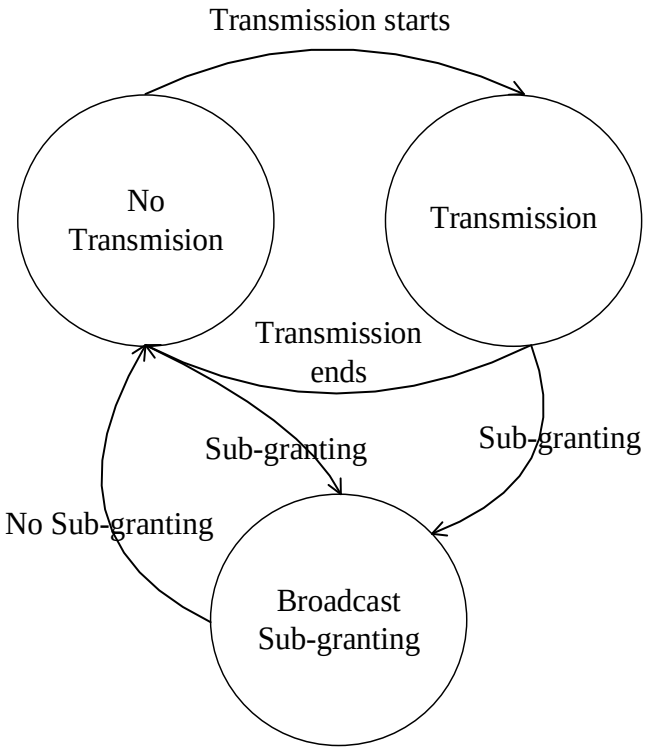

FIGURE 3.10: State-machine diagram of sub-grant provider functionality.

3.6.2 Beneficiary User Selection Problem Formulation

The uplink cell throughput is decomposed into the aggregated throughput of the D2I and D2D users within the cell. The radio link condition and the positioning information of all users need to be transmitted to the cellular network. This measurement transmission incurs a significant overhead on the cellular network, which results in cell throughput degradation. Considering the measurement and positioning information overhead, the uplink cell throughput can be reformulated as:

$$\begin{aligned} R_{cell}\left(\epsilon,\tau\right) = & \sum_{m=1}^{M}\left(R_m\left(\epsilon,\tau\right) - \hbar_m\left(\tau\right)\right) \\ & + \sum_{k=1}^{N}\left(R_k\left(\epsilon,\tau\right) - \hbar_k\left(\tau\right)\right), \end{aligned} \tag{3.2}$$

where R_m is the achievable data rate of D2I user at every scheduling time τ for a specific bit errors rate ϵ and yields as follows [94]:

$$R_m\left(\epsilon,\tau\right) = B_w \log_2\left(1 + \frac{GP_m}{\sigma_0 B_w \Gamma}\right), \tag{3.3}$$

where G is the radio channel gain that is calculated from (3.1), P_m is the transmission power of every D2I users, B_w and σ_0 stand for the allocated bandwidth in Hz and white Gaussian noise, respectively. And, $\Gamma = \frac{-ln(\epsilon)}{1.5}$ [94]. In case of D2D user with small traffic payload, (3.3) is not accurate enough, thus the achievable throughput R_k for D2D user

is reformulated as follows [42]:

$$R_k(\epsilon,\tau) = B_w \log_2\left(1+\frac{GP_k}{\sigma_0 B_w}\right) - \sqrt{\frac{B_w V}{\tau}} Q^{-1}(\epsilon)\log_2(e), \tag{3.4}$$

where $Q^{-1}(.)$ is the inverse Gaussian Q-function, and V reflects stochastic variability of the channel given by:

$$V = 1 - \frac{1}{1+\left(\frac{GP_k}{\sigma_0 B_w}\right)^2}. \tag{3.5}$$

In (3.2), $\hbar_k$ and $\hbar_m$ are the overhead due to the sub-granting signaling, the positioning information and radio link measurement reports transmitted by the D2I and D2D users. Authors in [26] manifested the user throughput is proportional to qb over the transmission time, τ. Where q is the MCS and captures the bit error rate ϵ. Moreover, b stands for the number of allocated resource blocks (RB). Consequently, the sub-granting throughput R_{mk} yields from $q_m b_k$ over the transmission duration $(T-\tau_k)$, where b_k is the sub-granted RBs from the k-th D2D user and q_m is MCS of the m-th D2I beneficiary user. Additionally, a binary variable of $\mathbb{X}_{mk}$ for resource allocation from k-th D2D user to the m-th D2I beneficiary user is defined:

$$\mathbb{X}_{mk} = \begin{cases} 0, & \text{if } T-\tau_k < S_{Min}, \\ 1, & \text{otherwise.} \end{cases} \tag{3.6}$$

Where S_{Min} is a processing time of a UE that depends on hardware and the number of allocated resources in time and frequency domain [91]. We now rewrite (3.2) for the dedicating and open sub-granting considering the D2I and D2D overhead as follows:

$$\begin{aligned} R_{cell}(\epsilon,\tau) = &\sum_{m=1}^{M}\left(R_m(\epsilon,\tau) - \hbar_m(\tau)\right) \\ &+ \sum_{m=1}^{M}\sum_{k=1}^{N}\mathbb{X}_{mk} R_{mk}(\epsilon, T-\tau_k) \\ &+ \sum_{k=1}^{N}\left(R_k(\epsilon,\tau) - \hbar_k(\tau)\right). \end{aligned} \tag{3.7}$$

Equation (3.7) considers the case where the D2D users are ultra-reliable and low-latency communications with absolute reliability and latency requirements, while D2I users have the best-effort traffic. More precisely, we assume that the reliability requirements for D2D users are satisfied if the bit error rate of D2D communication ϵ_k is lower than the configured threshold ϵ_{th}^{D}. Then, D2D users can grant $T-\tau$ of the allocated but unused resources in symbols basis to the D2I users. However, in the case of the erroneous environment, the D2I users may fail to decode the sub-granting signaling message. Therefore, we adopt the general approach initially proposed in [94] to calculate the upper bound bit error rate (ϵ) between D2D and D2I users as follows:

$$\epsilon \leq 0.2 e^{\frac{-1.5\delta}{q-1}}, \tag{3.8}$$

where $\delta = \frac{GP}{\sigma_0 B_w}$. We then proceed to maximize the sum rate of the cell by selecting the best beneficiary users. To optimize the throughput in (3.7), we only need to maximize the second term since the first and third terms are constant and have no effect on the

solution. The optimization problem can be expressed as follows:

$$\underset{(m,k)\in C\times D}{\text{maximize}} \sum_{m=1}^{M}\sum_{k=1}^{N} \mathbb{X}_{mk} R_m\left(\epsilon, T-\tau_k\right), \tag{3.9a}$$

subject to

$$\epsilon_{mk} < \epsilon_{th}^{sg},\ \forall\ m=1,...,M, k=1,...,N, \tag{3.9b}$$

$$\mathbb{X}_{mk} \in \{0,1\}\ \forall\ m=1,...,M, k=1,...,N, \tag{3.9c}$$

$$\sum_{m=1}^{M} \mathbb{X}_{mk} = 1,\ \forall\ k=1,...N, \tag{3.9d}$$

$$\sum_{k=1}^{N} P_m + \mathbb{X}_{mk} \times \frac{\left(P_{max}^{C} - P_m\right)}{b_m} < P_{max}^{C},\ \forall\ m=1,...,M, \tag{3.9e}$$

where (3.9b) is constraint showing errors limit for the D2D sub-granting signalling. Constraint (3.9c) denotes that the available resources for sub-granting should be greater than the processing time required by the beneficiary users. It is assumed that only one beneficiary user is allowed to use a sub-granted resource (constraint (3.9d)). Note that the power headroom indicates how much transmission power is left for a beneficiary user to use in addition to the transmission power being used by current transmission, i.e., $P_{max}^{C} - P_m$. Generally, the transmission power of every entity is proportional to the number of allocated RBs [92]. Thus, the additional transmission power due to the sub-granted resources to the beneficiary users should not increase the beneficiary user transmission power beyond the power constraint P_{max}^{C} (constraint (3.9e)).

The optimization problem in (3.9) aims to find a list of beneficiary users that maximizes cell throughput. This problem can be defined as a maximum weighted matching (MWM) problem in bipartite graphs with some non-linear constraints [95]. When there exists a large number of D2I and D2D users, an exhaustive search becomes intractable due to its high computational complexity. To avoid drawbacks in using an exhaustive search solution, two algorithms are suggested in centralized and distributed fashions to address the beneficiary user selection problem in the sub-granting scheme.

Specifically, the relation between the sub-grant provider users and the beneficiary users is first modeled by a time-varying bipartite graph. Then, the edge of the graph is weighted differently based on the beneficiary user selection algorithm, i.e., dedicated or open sub-granting algorithm, at every selection time instant. Figure 3.11 is an illustration of the system model in the form of a graph model, where the edge of the graph is being updated in every beneficiary user selection time instant. The sub-grant provider D and beneficiary users C construct two vertices of the graph. Every user in D is connected to the users in C. In the following sections, we propose two heuristic algorithms to achieve the maximum matching through the bipartite graph and auction theory to address the beneficiary user selection problem in the sub-granting scheme.

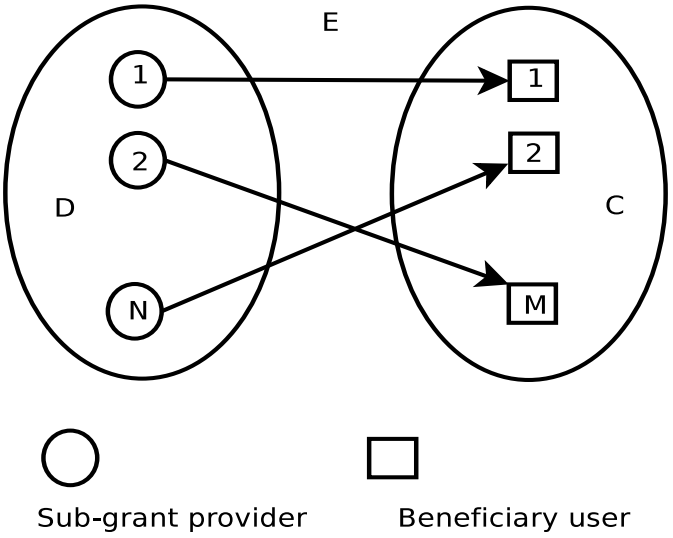

FIGURE 3.11: An Illustrative example of graph model in the sub-granting scheme. The sub-granting provider and the beneficiary users are vertices of the graph model through which edges are connected together. The edges are weighted based differently based on the algorithms.

3.6.3 Dedicated Sub-Granting Radio Resource (DSGRR) Algorithm

In this section, we discuss the centralized dedicated sub-granting radio resource algorithm to address the beneficiary user selection problem of the sub-granting scheme (3.9). The optimization problem is decomposed into two stages. In the first stage, a hypothetical geographical area, an error-limited area, for every sub-grant provider is calculated wherein the sub-granting signaling can be reliably received. In the second stage, the edges of the constructed bipartite graph are weighted by the beneficiary user data rate, updated in every beneficiary user selection-time interval. The proposed algorithm then solves the beneficiary selection problem, and the maximum number of the beneficiary users to achieve the highest cell throughput is obtained.

3.6.3.1 error-Limited Area (eLA)

As previously discussed, CSI between the sub-grant provider and the beneficiary user is not known or at least can be computed at the cost of additional signaling overhead on the cellular network. To avoid such overhead, a hypothetical circle around every sub-grant users based on the maximum error probability criterion, i.e., ϵ_{th}^{sg} is calculated. To this end, we use (3.8) to calculate the signal to noise level δ_{th}^{sg} related to ϵ_{th}^{sg} on the margin of hypothetical circle. Then, considering (3.1) and the channel model parameters for D2D communication in [44], the eLA (r_{eLA}) is bounded as:

$$| r_{eLA} | \leq \left(\frac{cP_k \mid \mu_d \mid}{\sigma_0 B_w \delta_{th}^{sg}} \right)^{\alpha_d^{-1}}, \; k = 1, ..., N. \tag{3.10}$$

Algorithm (3.6.1) explains the dedicated beneficiary user selection procedure. When the beneficiary user is inside the hypothetical circle of the sub-grant provider, i.e., eLA. An edge $e \in E$ is weighted with $q_m.b_k$, if there exists at least one vertex $c_m \in C$

inside the eLA (see lines (1) to (10)) in Algorithm (3.6.1). Additionally, we take the power constraint (3.9e) into consideration. Next, the algorithm chooses the beneficiary user c_m with maximum weighted edge e_{mk} associated to every sub-grant providers d_k in a greedy manner. Then, it is iteratively run and ended when all beneficiary users c_m are successfully selected. Also, in every iteration in order to find the maximum matching, the allocated edge is removed from all the sub-grant provider vertices, $d_k \in D$. Finally, every sub-grant provider users are informed about the selected beneficiary users $\mathbb{X}$.

Algorithm 3.6.1 Dedicated Sub-Granting Radio Resource

1: **procedure** BENEFICIARY USER SELECTION
Input: $d_k \in D^{1\times N}, c_m \in C^{1\times M}, \epsilon_{th}^{sg}$
Initialization:
2: Calculate error limited area radius for $d_k \in D$, $k = 1, ..., N$ (see (3.10))
3: $E \leftarrow \phi$
4: **for** $d_k \in D$ **do**
5: **for** $c_m \in C$ **do**
6: **if** $(c_m \in eLA_k)$ & (Constraint (3.9e)) **then**
7: $e_{mk} = q_m.b_k$
8: $E \leftarrow (E \cup e_{mk})$
9: **endif**
10: **endfor**
11: **endfor**
Repeat:
12: $\mathbb{X} \leftarrow \phi$
13: **for** $d_k \in D$ **do**
14: Find $c_m \in C$ with Maximum e_{mk}
15: $\mathbb{X}_{mk} = 1$ & $\mathbb{X} \leftarrow \mathbb{X} \cup \mathbb{X}_{mk}$
16: $E \leftarrow E - \cup_{k=1}^{N} e_{mk}$
17: **endfor**
Output: *Transmit* $\mathbb{X}_{mk}$ *to every* d_k

3.6.3.2 Overhead

Due to the mobility of all users, the positioning and measurement information of users should be transmitted in a shorter time interval, which results in the additional overhead. As previously discussed in Section (3.6.2), the beneficiary user overhead is shown by $\hbar_m$ and yields.

$$\hbar_m(\tau) = \frac{\mathbb{X}_{me} \times O_{me} + \mathbb{X}_{pos} \times O_{pos}}{\tau}, \tag{3.11}$$

where O_{me} and O_{pos} are the constant overhead values due to the channel state measurement and positioning information. $\mathbb{X}_{me}$ and $\mathbb{X}_{pos}$ are set when the measurement time interval T_{me} and positioning information time interval T_{pos} are triggered. Similarly, the sub-granting provider transmits the positioning information to the BS and disseminates the unused radio resources, which incurs additional overhead the cellular network. This overhead is shown by $\hbar_k$ and yields:

$$\hbar_k(\tau) = \frac{\sum_{m=1}^{M} \mathbb{X}_{mk} \times O_{sg} + \mathbb{X}_{pos} \times O_{pos}}{\tau}, \tag{3.12}$$

where O_{sg} is the sub-granting signalling overhead in the every sub-granting occurrences $\mathbb{X}_{mk}$ as explained in (3.6) and constraint (3.9d). Also, the denominator term τ stands for the data transmission time.

3.6.3.3 Time complexity

In the proposed algorithm, nested loops are considered where the sub-grant provider and beneficiary users are the outer and inner loops within the algorithm, respectively. Thus, the central controller requires to run the algorithm $\mathcal{O}(N \times M)$ operations to complete the beneficiary users' selection process.

3.6.4 Open Sub-Granting Radio Resource (OSGRR) Algorithm

Recently the auction theory, which initially developed in the economy, has attracted many scholars' attention and has been applied to various problems in engineering. The essence of an auction environment consists of auctioneers or sellers, bidders, commodities to be sold, and a set of rules which give rise to the game among all the bidders. In some auctions, there exists one seller that can perform the role of auctioneer. As a result, auctioneer and seller terms can be used interchangeably. An auction theory, a subfield of economics, is a useful tool to model and optimize radio resource allocation in wireless communication wherein radio resources can be allocated among different users, following some rules regulated in the market. One well-known auction is the Vickrey-Clarke-Groves (VCG) auction [82], which requires gathering global information from all entities and performing centralized computations.

In this study, we consider one-shot open-cry auction in which the bidders advertise their offers at once and openly based on a bidding strategy in a distributed manner. Let D be a set of distinct objects which offer some commodities, say sub-granting resources, for sale. Moreover, C be a set of buyers wherein each buyer, say beneficiary user, is assumed to assign a valuation $\mathbf{s}_{mk}$ to each seller, i.e., sub-grant provider user, where $k \in D$ and $m \in C$. Every beneficiary user monitors other bids and advertises a selected sub-grant provider after the exclusion of the assigned sub-grant provider users indicated in the broadcast bid. Note that every bid contains information that indicates the preferred sub-grant provider user of every beneficiary user. In this study, it is assumed that a sub-grant provider does not ask for any cost from the beneficiary user on the sub-granting radio resources. In other words, the selecting sub-granting radio resources would not impose any form of the cost on the other cellular users or the cellular network. Furthermore, the achieved throughput of every beneficiary user from the sub-granting resources is reflected in a bid generated through the strategy function. Recall that symmetric equilibrium wherein all players use the same bidding strategy function [82], the strategy function in every beneficiary users s_{mk} yields:

$$s_{mk} = \frac{\beta q_m b_k + (1-\beta) q_{mk}}{q_{max}} + \gamma_m, \ \forall m = 1, ..., M, k = 1, ..., N, \tag{3.13}$$

where q_m and q_{mk} are modulation and coding scheme of m-th the beneficiary user towards the BS and the sub-grant provider user, which are normalized to maximum modulation and coding rate q_{max}. The number of sub-granted resources from the sub-grant provider to the beneficiary user is denoted by b. The term β takes a value between

0 and 1 that shows the impact of the multiplied terms in the bidding strategy function and is configured by the BS. In the first term of the equation, we consider two factors, the first factor guarantees the sub-granting gain, and the latter ensures to choose a sub-grant provider with the higher signal strength to reduce the probability of the sub-granting signaling errors.

Note that if two beneficiary users have the same MCS, the first term of the equation may return the same value resulted in a collision between two beneficiary users due to transmission on the same sub-granting resource. To avoid a tie situation in the equation, a small value of γ_m is added to the first term of bidding strategy function, calculated from the reverse of a unique cellular user-specific number $\mathcal{Z}_m$, say, a temporary mobile subscriber identity (TMSI) [96].

Figure 3.12 shows an illustrative example of the equilibrium bidding value of the strategy function, considering a specific TMSI value for every beneficiary user.

Remark 3.1. The highest cell throughput is achieved when the sub-granting resources are granted to the beneficiary users offering the highest bid value.

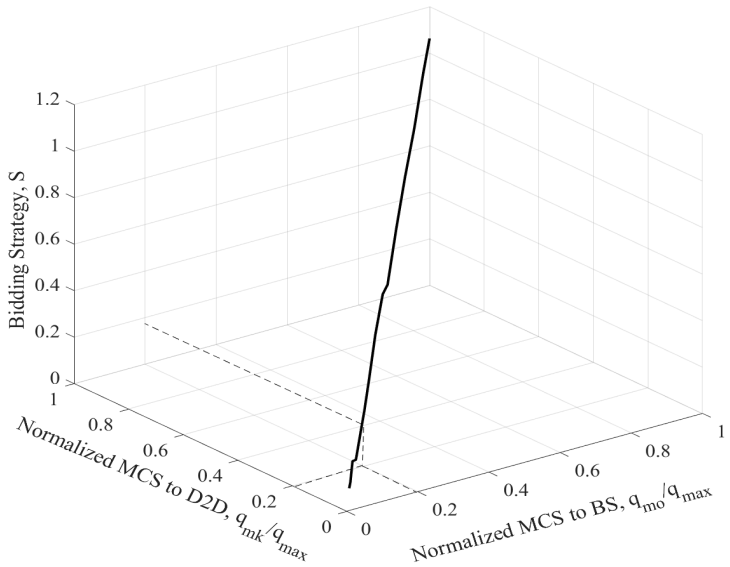

FIGURE 3.12: An Illustrative example of bidding strategy function.

A bipartite graph is used to model the beneficiary user selection problem in the sub-granting radio resource wherein the beneficiary users, bidders, and the sub-grant provider users, sellers, or auctioneers, are two vertices of a graph as illustrated in Figure 3.11. The edges of the graph are weighted by bidding values obtained from the bidding strategy

function. This way, the problem is transformed into the maximum matching in the bipartite graph. Now we propose a closed-form heuristic algorithm, say, open sub-granting radio resource to address the beneficiary user selection problem in the sub-granting radio resource as stated in (3.9).

Algorithm 3.6.2 shows the principle of operation of the open sub-granting radio resource. The beneficiary user's unique value γ_m, β, and bid transmission start time are configured by the BS. Where the bid transmission start time is a time value between two consecutive selection time instances in which every beneficiary user is allowed to transmits the bid value. Also, this value ensures that two beneficiary users do not start transmission at the same time. Thus any possible collision due to a half-duplex communication in the D2D communication is avoided. Then, every beneficiary user calculates a bid value s_{mk} associated to every sub-grant provider users using (3.13) considering the bit errors rate and power head room stated in constraints (3.9b) and (3.9e) in (3.9). Note that every beneficiary user chooses a maximum bid value S_{mk} associated to the sub-grant provider user and disseminates the bid value along with the corresponding sub-grant provider user identity. The beneficiary user informs the nearby users about the bid value s_{mk} through D2D communication on the scheduled uplink radio resource at the configured bid transmission start time. Next, the edges of the graph are updated based on its bid value, and other monitored beneficiary users bid values (see Lines (1) to (15) in the Algorithm 3.6.2). Finally, every beneficiary user constructs a list of maximum bid values corresponding to the monitored beneficiary users and the associated sub-grant provider users, i.e., matching list $\mathbb{X}_{mk}$. Note that, a beneficiary user having the biggest bid value on the matching list is allowed to transmit on the sub-granting radio resources over the beneficiary user- selection time interval configured by the BS (see Lines (16) to (20) in Algorithm 3.6.2).

3.6.4.1 Overhead

The overhead in the open sub-granting algorithm is mainly due to biding messages that are exchanged among the beneficiary users and also sub-granting signaling messages. Therefore, the imposed overhead on the beneficiary users $\hbar_m$ yields:

$$\hbar_m(\tau) = \frac{\mathbb{X}_{br} \times O_{br}}{\tau}, \tag{3.14}$$

where O_{br} stands for the overhead value owing to bidding message exchanged among the beneficiary users, and $\mathbb{X}_{br}$ is a value that is set to 1 at every broadcast time interval T_{obr}. Moreover, in case of the sub-granting scheme overhead on the D2D communication h_k, positioning information is not transmitted to the BS, and thus (3.12) can be rewritten as follows:

$$\hbar_k(\tau) = \frac{\sum_{m=1}^{M} \mathbb{X}_{mk} \times O_{sg}}{\tau}, \tag{3.15}$$

3.6.4.2 Time complexity

This section explains the steps required to execute the algorithm. The OSGRR algorithm includes two terms, which each runs in $O(N)$ and $O(M)$ time, respectively. Therefore, the algorithm takes about $O(N+M)$ to find a match list. For $N >> M$ or $M >> N$, the complexity is simply $O(N)$ or $O(M)$ respectively.

Algorithm 3.6.2 Open Sub-Granting Radio Resource

```
procedure BENEFICIARY USER SELECTION
Input: Configure β value used in (3.13)
Initialization:
    Calculate γ_m = 1/Z_m,  m = 1, ..., M
    E ← φ
    for d_k ∈ D do
        if Constraints (3.9b) & (3.9e) then
            Calculate bid value s_mk from (3.13)
            Update edge value of graph, E ← (E ∪ s_mk)
        endif
    endfor
    Select maximum bid value s_mk and broadcast
    Update edge value of graph, E ← E − ∪_{j=1}^{N} s_mj, ∀j ≠ k
    for c_{m−1} ∈ C do
        Monitor bid value s_{m−1k} of other beneficiary user
        Update edge value of graph, E ← (E ∪ s_{m−1k})
    endfor
Selection:
    X ← φ
    for d_k ∈ D do
        Select c_m ∈ C with maximum bid value s_mk
        X_mk = 1 and X ← X ∪ X_mk
    endfor
Output: Macthing List X
```

3.7 Summary

In this chapter, we have presented the radio resource allocation strategy, i.e., sub-granting scheme, for the overlay D2D communication, in which the scheduled radio resources that not fully utilized in the D2D users, i.e., sub-grant providers, are granted to D2I users, i.e., the beneficiary users. We described the system model and the possible scenarios used throughout the dissertation. Then, the required modifications in the physical layer were explained, and some algorithms for the sub-grant provider and the beneficiary user were proposed. We inspired by the shortening TTI and introduced a few changes in the D2D transmitter/receiver by which the transmission time and the overhead between D2D transmitter and D2D receiver can be further reduced. This chapter ended by casting the beneficiary user selection problem mathematically as the uplink cell throughput maximization problem. Furthermore, two algorithms in centralized, i.e., DSGRR, and distributed, i.e., OSGRR fashions, are proposed to address the beneficiary user selection problem in the sub-granting scheme mentioned earlier. In the DSGRR algorithm, the eNB assists in selecting beneficiary users for every sub-grant provider. To this aim, a Bipartite graph is used to model the resource assignment from the sub-grant provider to the beneficiary users, wherein the edge of the graph is weighted by the utilization rate of every beneficiary user achieved from the sub-granting resources, when the beneficiary user is inside a hypothetical area, i.e., eLA. The beneficiary user with the highest rate is selected such that the cell throughput is increased. To avoid any complexity in collecting measurement information in a dynamic environment, we

proposed an OSGRR algorithm based on the auction and Bipartite graph theory. In the OSGRR, the sub-grant providers disseminate the unused radio resources information, and then all beneficiary users monitor information disseminated by nearby users through sensing and broadcast their bid computed by symmetric strategy function. The beneficiary users with the highest bid are chosen to exploit the sub-granting resources until the next beneficiary selection interval.

The sub-granting scheme performance evaluation will be discussed in the following chapters.

CHAPTER 4

Sub-granting Radio Resource Scheme Performance Evaluation

Contents

This chapter provides insight into the achievable throughput gain applying the sub-granting radio resource scheme. The sub-granting scheme is evaluated in terms of uplink cell throughput in a scenario with stationary users, numerically and with a simulation study. Also, the impact of the number of sub-grant provider users and the channel conditions of beneficiary users on the sub-granting gain is investigated when the allocated radio resources to the sub-grant provider users are underutilized.

4.1 Numerical Analysis

The sub-granting radio resources scheme aids to increase radio resource utilization for overlay D2D communication in the cellular network [23]. Considering a single scenario with one D2I user and multiple D2D users in the vicinity. The maximum achievable uplink cellular user throughput is examined for partially utilized radio resource scenarios applying the sub-granting scheme. Besides, the D2I users' throughput gain is evaluated, taking into consideration the overhead due to the sub-granting signaling.

Although the LTE uplink cell throughput is theoretically expected to reach 100 Mbps, i.e., using 64-QAM for data modulation, it is limited to approximately 75 Mbps in practice due to control overhead [63]. Understandably, the fewer symbols are used for data, the lower the overall throughput. In order to calculate the exact throughput incorporating the associated overhead and different MCSs, we have relied on the 3GPP technical specification, i.e., Table 8.6.1-1 and 7.1.7.2.1-1 in [63].

Note that we are considering a cellular user to use MCS indexes 10, 20, 28, i.e., using QPSK, 16-QAM, and 64-QAM for data modulation, respectively. Referring to the MCS indexes in Table 8.6.1-1, the Transport Block Size (TBS) index is derived. Intuitively, the peak throughput can be obtained from Table 7.1.7.2.1-1 through the TBS index and the number of PRBs for different MCSs.

Figure 4.1 shows the normalized D2I user throughput as a function of the number of D2D users for different sub-grant sizes. To calculate the resulting D2I user throughput, we assume a mix of different MCSs, i.e., 64-QAM is only used for 40% of the transmission time. 16-QAM and QPSK are equally often used for the remaining transmission time. Each D2D user is initially assigned one pair of PRBs in every subframe.

Apparently, when the number of D2D users is rising, the D2I user throughput would decrease. In the case of not using the sub-grant technique, the D2I throughput declines by more than 40% in the worst case. On the other hand, when the number of unused symbols in one subframe for every D2D user increases, using our technique leads to an improvement in the D2I user throughput. For example, by granting 10 symbols for reuse and assuming 40 D2D users, the D2I user throughput increases by 30%. Note that even a allocation of four symbols can improve D2I user throughput between 10% to 20%, compared with the common resource allocation methods, as the number of D2D users increases.

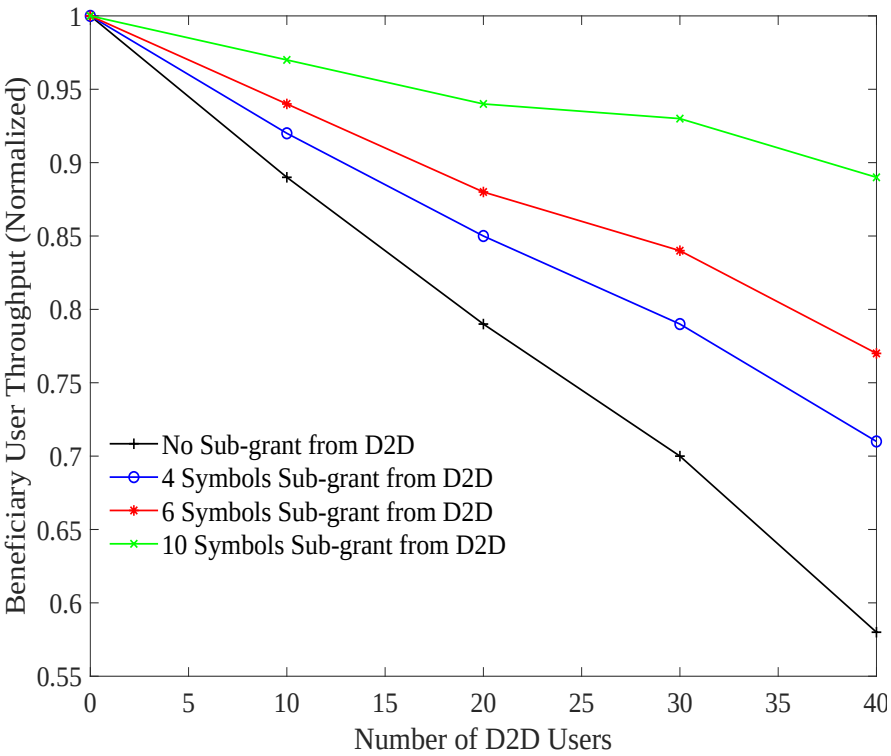

FIGURE 4.1: Normalized D2I user, i.e., beneficiary user, throughput as a function of the unused symbols in a subframe.

4.2 Simulation Study

This section evaluates the uplink throughput applying the sub-granting scheme for different numbers of D2D users [24]. For this purpose, we consider a scenario with one D2I user in the proximity of N D2D-UEs, where N is set to 20 and 40. The D2D users are uniformly distributed within a circular area with a 100 m radius inside the cell. Figure 4.3 shows this scenario. The distance between every D2D pair is set to 20 m, and every D2D-UE$_{TX}$ (i.e., sub-grant provider or transmitter D2D) randomly generates traffic with relatively small payload size ranging between 10 to 300 bytes (cf. MTC applications in [1]). Figure 4.2 illustrates the traffic model of the D2D users.

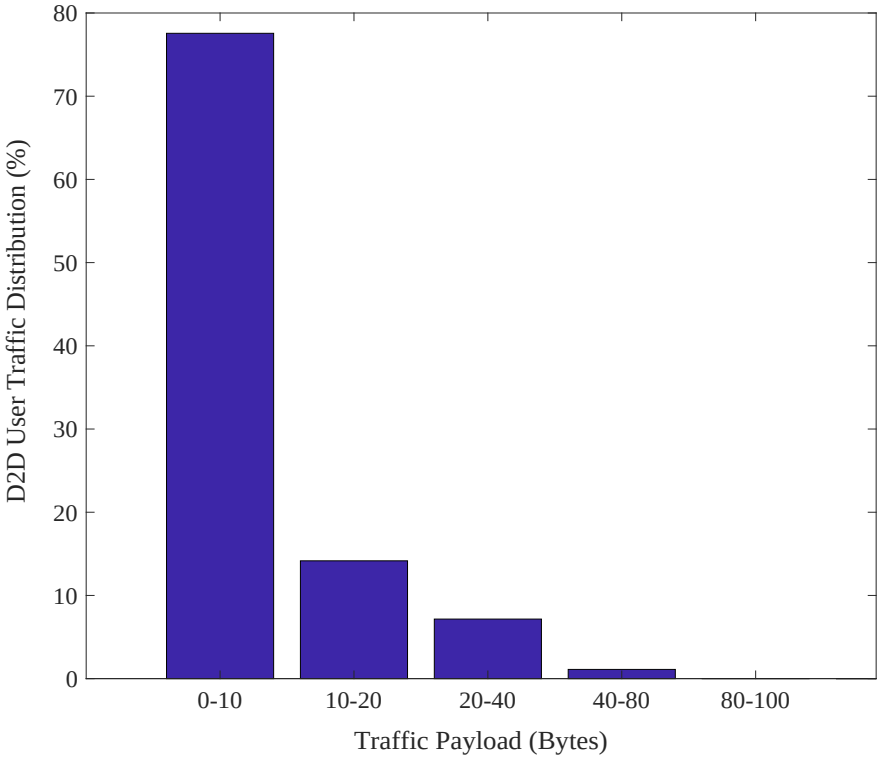

FIGURE 4.2: Traffic model distribution of the D2D user transmitter.

Table 7.2 shows the simulator setup parameters.

TABLE 4.1: Simulation Parameters.

Parameter	**Value**
Frequency, fc and BW	2.6 (GHz), 20 (MHz)
Number of users	1 (D2I), 20 and 40 (D2D)
Cell Radius	250 m
Channel Model [44]	UMi-NLOS α_c: 3.67 $\mu_c : \sigma = 4\ dB$, Rayleigh InH-NLOS α_d: 4.33 $\mu_d : \sigma = 4\ dB$, Rician, K=20 dB
D2D Distribution, Radius	Uniform, 100 (m)
Traffic Model	Packet size=10B, λ=1ms, $\epsilon_{th}^{\mathbb{D}}$=$10^{-5}$ [1]
D2D Distance (d)	20 (m)
Power Control	Open Loop Power Control $D2D$ ($P0$ = -70 dBm/RB) $D2I$ ($P0$ = -107 dBm/RB)
Noise Power	-174 (dBm/Hz)
MAX UE TX Power	23 (dBm)
D2D and D2I Antenna Gain	1 dB
eNB Antenna Gain	10 dB
Simulation Runs	10000

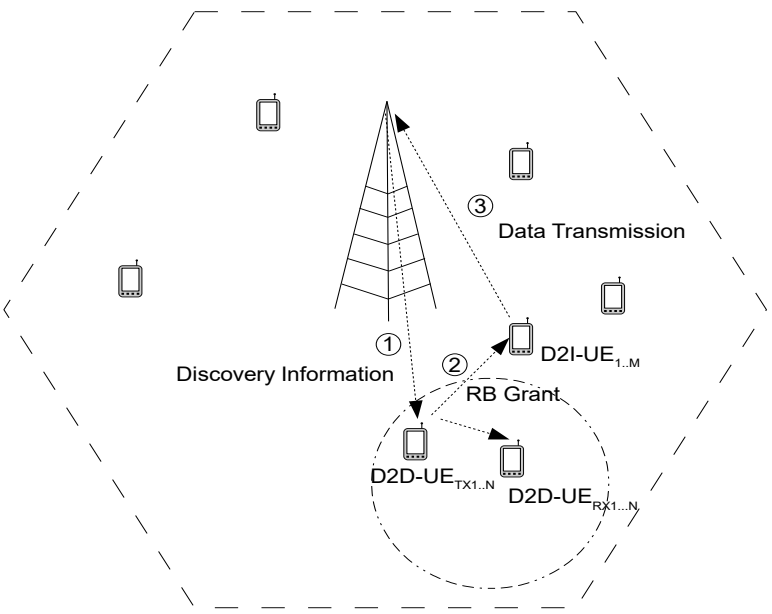

FIGURE 4.3: An Illustrative example of system scenario when multiple D2D users are uniformly distributed in a specific geographical area, and one D2I user, i.e., the beneficiary user, with the highest MCS is in the proximity.

4.2.1 Performance Metric

This section explains a performance metric used to evaluate the sub-granting scheme. The uplink beneficiary user throughput is considered a metric to measure the impact of the sub-granting on the performance of a beneficiary user and the network as a whole.

The number of resource blocks and MCS assigned to every individual beneficiary user is known at the eNB side. Therefore, the eNB can use this information to compute the beneficiary user throughput. Let us consider a scenario with a D2D-UE with 10 OS/RB for sub-granting, and the number of allocated RBs and MCS to the beneficiary users is 10 RBs, 64QAM-5/6, and two symbols are needed for processing time S_{MIN}. When the beneficiary user exploits the sub-granted resources, the uplink throughput for the beneficiary user R_{D2I} yields:

$$\begin{aligned} R_{D2I} &= \left(N_{SYM} + N_{SYM}^{SG} - S_{MIN}\right) N_{CR} \times N_{MCS} \\ &\quad \left(N_{RB} + N_{RB}^{SG}\right) N_{SC} \times T_{SF}^{-1} \\ &= (12+8) \times (5/6) \times 6 \times (10+1) \times 12 \times (0.001)^{-1} \\ &= 12.58\ (Mbps), \end{aligned} \tag{4.1}$$

where N_{SYM} is the number of data symbols in the beneficiary D2I user, and N_{SYM}^{SG} is the number of sub-granted symbols. N_{CR}, N_{MCS}, N_{RB} are coding rate, modulation order, and the number of resource blocks assigned to the D2I user. N_{RB}^{SG} denotes the number of assigned resource blocks to the sub-grant provider (D2D-UE$_{TX}$). N_{SC} and T_{SF} is the number of sub-carrier per RB (i.e., 12 in LTE) and the sub-frame size.

4.2.2 Results and Discussions

Figure 4.4 illustrates the cumulative distribution function of uplink throughput for the beneficiary D2I user in the studied scenarios.The D2I uplink throughput for two scenarios with 20 and 40 D2D users are evaluated. In the scenario with 20 D2D users, the D2I user can only achieve 57 Mbps w/o the sub-granting scheme. On the contrary, the D2I user throughput increases by 17% applying the sub-granting scheme. It is observed that when the number of D2D users increases from 20 to 40, the beneficiary D2I throughput increases by 55% applying the sub-granting scheme. The reason is that in the overlay D2D, a part of resource blocks is dedicated to D2D users. Thus, fewer resources remain for D2I users, resulting in the throughput degradation at the D2I user. Moreover, the applications with a small traffic payload contribute to further wastage of the reserved resources. However, the sub-granting scheme helps to reduce radio resources wastage by delegating the unused resources to the beneficiary user(s).

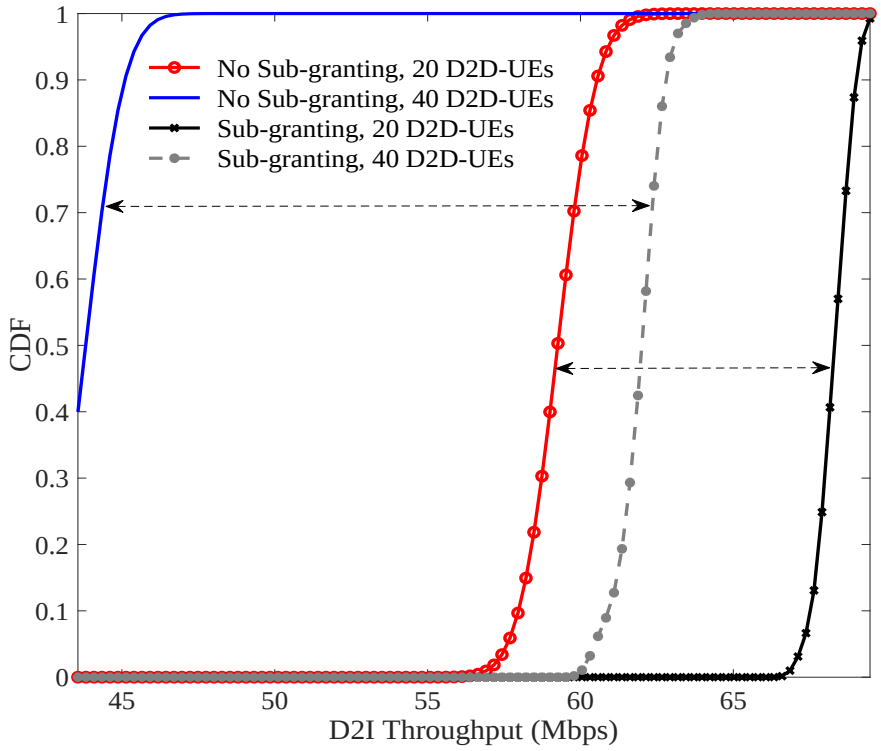

FIGURE 4.4: CDF of D2I user uplink throughput w/ and w/o the sub-granting scheme for two scenarios with 20 and 40 D2D users.

4.3 Summary

In this chapter, we first analyzed the sub-granting scheme in terms of the beneficiary analytically. Then, a further study has been undertaken through a simulation study. Two scenarios with the different number of D2D users, when the D2D users are uniformly distributed within a limited geographical area, are studied, wherein the beneficiary users throughput w/ and w/o sub-granting was evaluated. The results showed that the uplink throughput improves applying the sub-granting scheme. Intuitively, it is because that the allocated but not utilized radio resources can be re-utilized by other nearby users

demanding more radio resources. The next chapter will compare the sub-granting scheme with shortening TTI schemes.

CHAPTER 5

Sub-granting and Shortening TTI Schemes Comparison

Contents

This chapter compares the sub-granting radio resource scheme with the shortening TTI, i.e, s TTI, schemes in terms of transmission delay, overhead, and the uplink cell throughput. First, we analyze both schemes numerically and compare them in terms of D2D throughput and uplink cell throughput. The simulation study is then undertaken considering the flexible sub-frame, and the padding information reduction inspired by the numerical analysis as proposed earlier in the Chapter 3. In the simulation study, the shortening TTI and the sub-granting schemes are compared in terms of overhead and transmission time for a transmitter D2D and its intended receiver D2D.

5.1 Numerical Analysis

Considering the system model discussed in Chapter 3, the uplink cell throughput can be mathematically formulated, when the sub-granting scheme is not utilized, as follows:

$$\eta_{cell} = \eta_c + \sum_{i=1}^{[n\times\lambda]} \eta_{d_i}, \tag{5.1}$$

where η_{cell}, η_c are the uplink cell throughput, D2I-UE throughput. The throughput of ith active D2D-UEs is η_{d_i} and the activity rate of D2D-UE is denoted by λ. Besides, the D2I-UE throughput and i^{th} active D2D-UEs throughput are calculated as follows:

$$\eta_c = \frac{(N_c - n_{rb}) \times n_{sc} \times n_{sb}^c \times \mu}{t_d}, \tag{5.2}$$

$$\eta_{d_i} = \frac{n_{rb} \times n_{sc} \times n_{sb} \times \mu}{t_d}, \tag{5.3}$$

where η_c and η_{d_i} are mainly influenced by the number of resource blocks in the cell N_c, the number of allocated resource blocks to D2D-UEs n_{rb}, the traffic payload in D2D-UEs n_{sb}, and D2I-UE n_{sb}^c. Additionally, n_{sc} and t_d represent the number of sub-carriers per resource block, i.e., 12, and the data transmission duration. The efficiency rate μ is the product of the modulation order and coding rate configured by the cellular network. Recall in the sub-granting the achievable throughput in the equation (5.2) is reformulated as follows:

$$\eta_{c_g} = \eta_c + (\sum_{i=1}^{[n\times\lambda]} \eta_{d_i})^{Act} + (\sum_{i=[n\times\lambda]+1}^{n} \eta_{d_i})^{Non-Act}, \tag{5.4}$$

where η_{c_g} is the uplink throughput for the beneficiary user, taking into account the sub-granting scheme. Besides, $(\ .\ )^{Act}$ and $(\ .\ )^{Non-Act}$ denote the sub-granting throughput achieved by the D2I-UE from the active and the non-active D2D-UEs in which throughput is similar to the equation (5.3) except that a new traffic payload size $n_{sb}^{'}$ yields as follows:

$$n_{sb}^{'} = \begin{cases} N - n_{sb}, & \text{if } n_{sb} > S_{Min} \text{ and active D2D-UE} \\ N - S_{Min}, & \text{otherwise} \end{cases} \tag{5.5}$$

where N is the number of data symbols in the customized, i.e., flexible, sub-frame of D2D-UE (i.e., 12 symbols for data transmission) and S_{Min} is a processing time to decode the sub-granting signaling as mentioned in Chapter 3.

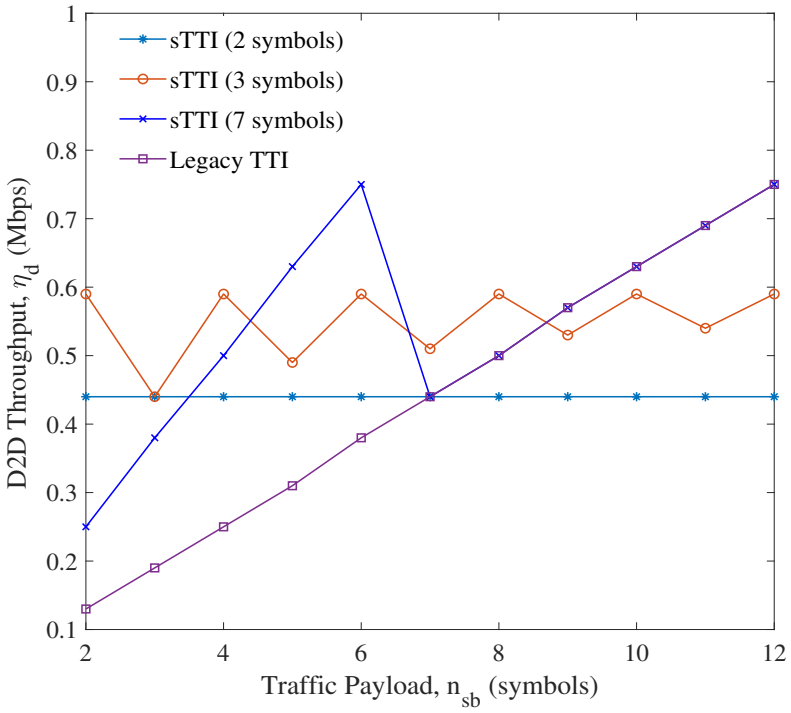

FIGURE 5.1: Illustration of transmitter D2D to intended receiver D2D throughput (η_d), when traffic payload size (n_{sb}) varies for different shortening TTI schemes and legacy LTE subframe.

We evaluate performance of the uplink cell throughput for the sub-granting and sTTI schemes considering different traffic payload sizes [25]. Also, we investigate the impact of the number of users that are transmitting, i.e., utilization rate λ, on the cell throughput for a specific traffic payload size. Two utilization rates of 50% and 100% on cell throughput are examined.

All D2I users are full buffer, i.e., a sub-frame with 12 symbols for data transmission, wherein 8 bits of the subframe is used to indicate the sub-grant signaling [23]. Further, every D2I user 's efficiency rate μ is set to 5.22, which is obtained from the product of modulation order and the coding rate, indicated by $I_{MCS} = 28$, according to Tables 8.6.1-1 and 7.1.7.2.1-1 in [63].

Figure 5.1 shows the D2D-UE throughput η_d for the sTTI and LTE subframe schemes considering different traffic payload sizes n_{sb}. As previously discussed, a receiver needs at least one DMRS in every slot for channel estimation purposes, thus in the sTTI with two symbols, only one symbol can be free for data transmission. This way, a D2D user can achieve 0.44 $Mbps$ throughput when sTTI with two symbols is applied. Similarly, in the sTTI with three and seven symbols, two and six symbols remain free for data transmission, respectively. Hence, when the traffic payload size n_{sb} varies, the achievable throughput for both schemes forms a saw-tooth curve. In case sTTI with three symbols, the throughput varies between 0.44 $Mbps/s$ and 0.6 $Mbps/s$, while the throughput for sTTI with seven symbols varies between 0.25 $Mbps$ and 0.76 $Mbps$. The reason is that the subframe is still coarse for such small traffic payload, and thus a small throughput can be achieved. Besides, the throughput increases proportionally with the traffic payload size, as shown in the figure.

Figure 5.2 compares the sub-granting and sTTI schemes in terms of cell throughput in scenarios with 10 and 40 reserved resource blocks n_{rb}. Further, it is assumed that all D2D users are active, i.e., λ=100%, and one resource block to every D2D user is assigned.

The sub-granting scheme shows better results in terms of throughput compared with the sTTI schemes. The reason is that the unused symbols are re-utilized by the nearby beneficiary user in the sub-granting scheme. Note that the beneficiary D2I needs some time to decodes the sub-granted resources and encodes its own data, i.e., S_{Min}. Therefore, the beneficiary D2I-UE is expected to increase the throughput after the processing time S_{Min}. Figures 5.2(a) and 5.2(b) show the impact of the processing time S_{Min} on the cell throughput. It can be seen that the achievable cell throughput for the sub-granting scheme increases, inversely related to the values of S_{Min}.

Figure 5.2(a) shows that the cell throughput increases between 2% to 4% for the sub-granting scheme compared with the sTTI schemesThe sTTI scheme with seven symbols shows slightly better results for a traffic payload with six symbols compared with the sub-granting scheme. The reason is that when the radio resources are fully utilized, the sub-granting scheme achieves no gain, and only imposes some signaling overhead. In contrast, the cell throughput for the other sTTI schemes (2 and 3 symbols) declines between 2% to 4% depending on the payload size. The reason is that the overhead in sTTI is higher than the sub-granting scheme.

Figure 5.2(b) shows the cell throughput for all schemes when the number of reserved resource blocks is 40. The achievable cell throughput for all the schemes decreases by 10% to 15% except the sub-granting scheme and sTTI with seven symbols in which all allocated resources are fully utilized.

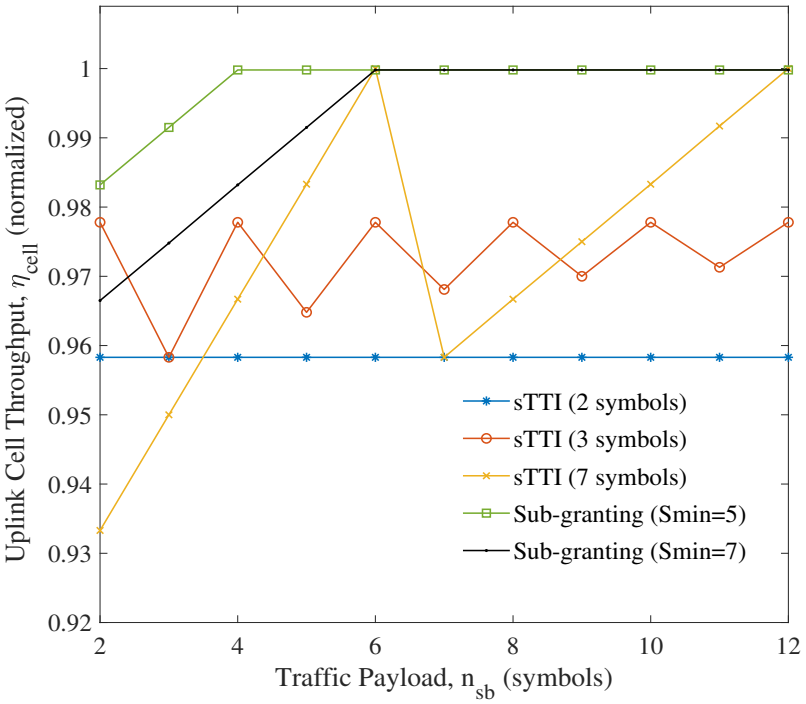

(a)

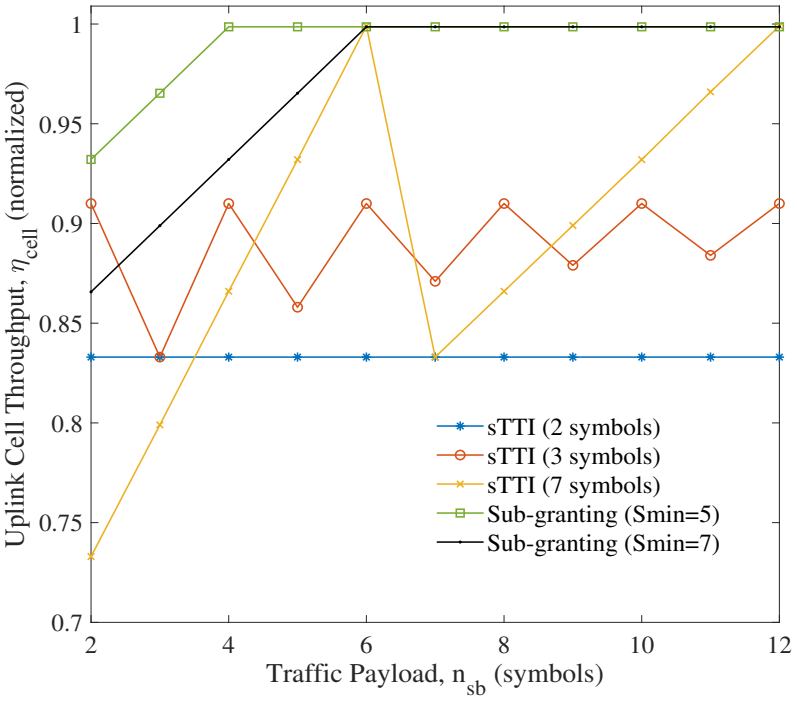

(b)

FIGURE 5.2: Illustration of normalized cell throughput (η_{cell}) for different subframe schemes considering different payload size (n_{sb}) and same utilization rate (λ=100%) for two different scenarios: (a) n_{rb}=10; (b) n_{rb}=40.

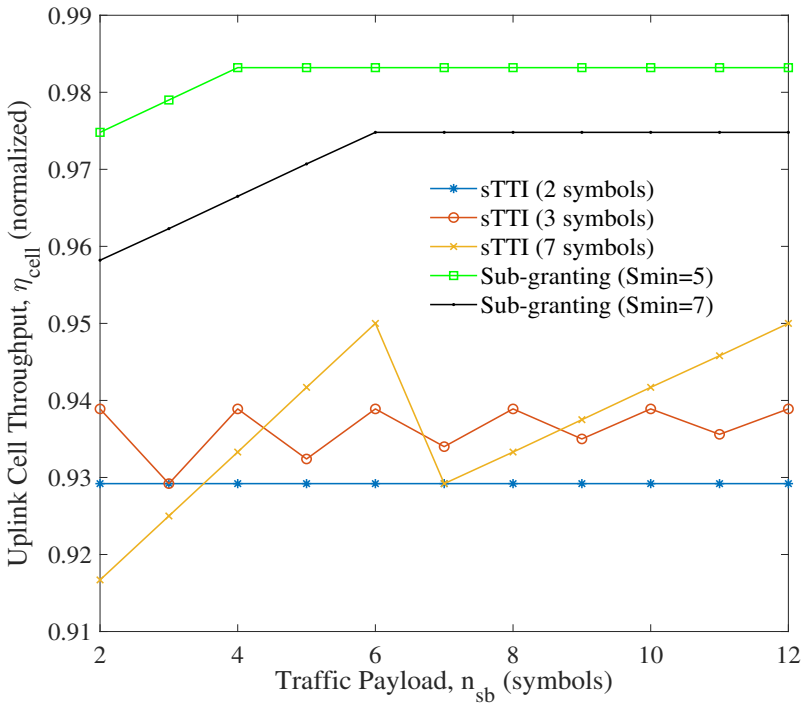

(a)

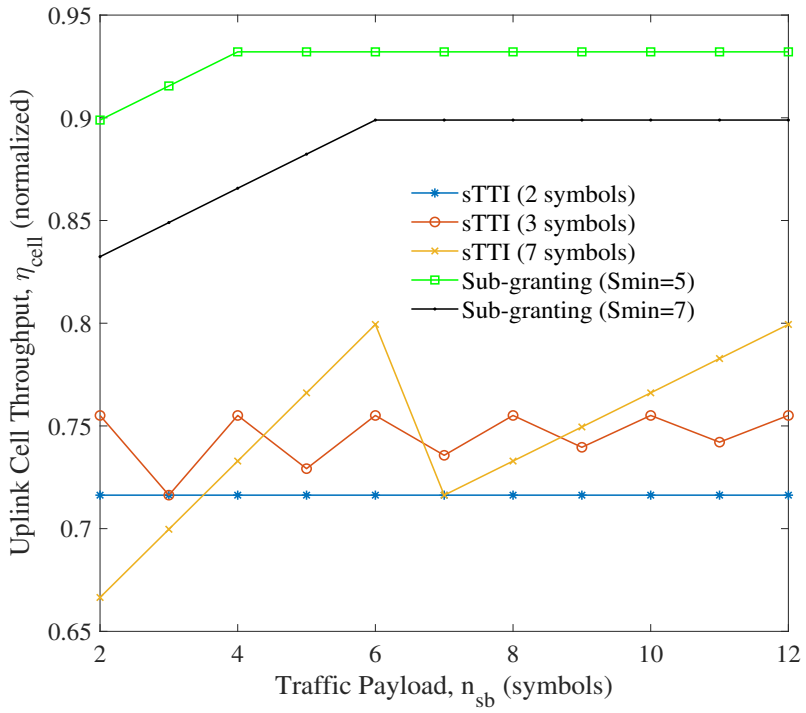

(b)

FIGURE 5.3: Illustration of normalized cell throughput (η_{cell}) for different subframe schemes considering different payload size (n_{sb}) and same utilization rate (λ=50%) for two different scenarios: (a) n_{rb}=10; (b) n_{rb}=40.

The utilization rate λ impact on the cell throughput η_{cell} is shown in the figure 5.3. When n_{rb} is 10 and only 50% of the D2D users are active, the cell throughput decreases between 2% to 7% for all the schemes (see Figure 5.3(a)). Moreover, the cell throughput further decreases between 10% to 20% when the n_{rb} increases to 40 (Figure 5.3(b)). However, the cell throughput for the sub-granting scheme increases by 4% and 20% compared to the other schemes in the studied scenarios. (Figure 5.3(b)). The reason is mainly that the unused resource can be re-utilized by the nearby D2I users, applying the sub-granting scheme.

Figure 5.4 illustrates the impact of utilization rate λ and number of reserved resource block n_{rb} on the uplink cell throughput η_{cell}. For this analysis, the specific payload size, i.e. $n_{sb} = 4$, is considered. The cell throughput is seen to be linearly proportional to the utilization rate. In general, the cell throughput for the sub-granting scheme outperforms the other schemes due to granting the otherwise unused resources to the beneficiary D2I-UE. With 10 reserved resource blocks, the cell throughput for all shortening TTI schemes decreases between 2% and 4% compared with the sub-granting scheme (Figure 5.4(a)). When 40 resource blocks are assigned to the D2D users, the achievable cell throughput for all shortening TTI schemes decreases by between 20% and 40% depending on the utilization rate (Figure 5.4(b)). The reason is the part of allocated radio resources are wasted due to the DMRS overhead, and the traffic payload is smaller than the allocated radio resources. In contrast, the sub-granting scheme shows a less cell throughput reduction, i.e., between 4% to 10%. The reason is that in the sub-granting scheme, the un-utilized radio resources are reused by the nearby users (Figure 5.4(b)).

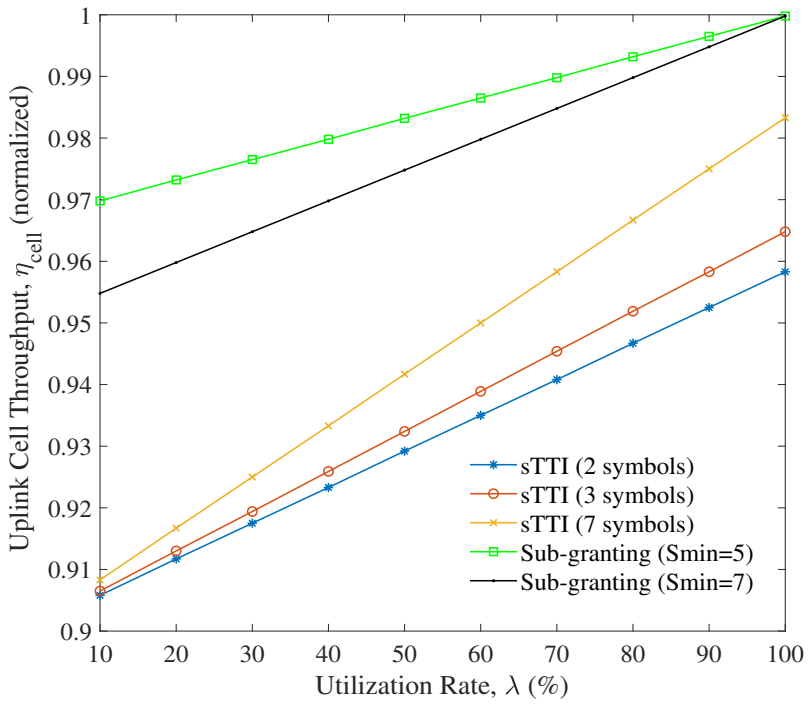

(a)

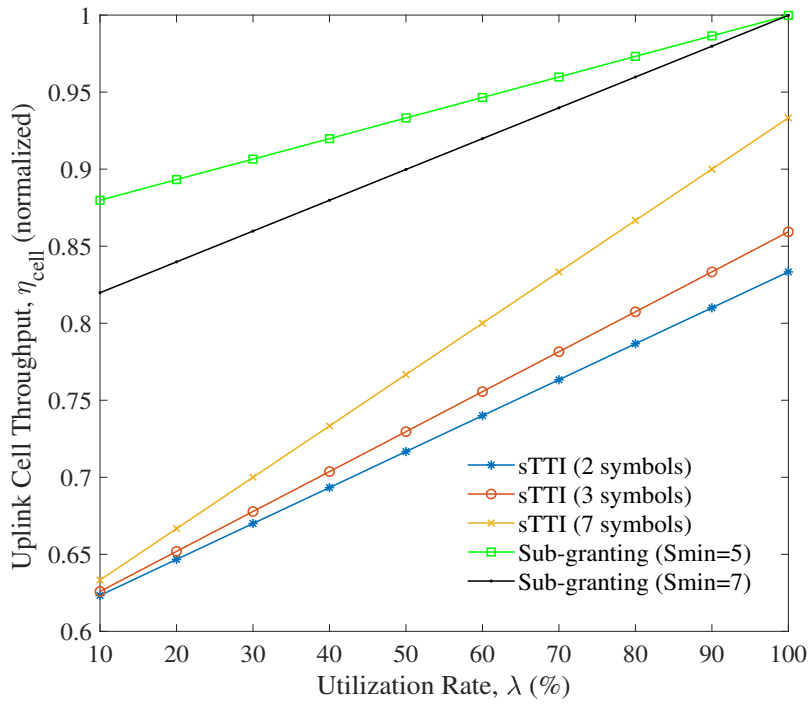

(b)

FIGURE 5.4: The Illustration of normalized cell throughput as a function of utilization rate for different subframe schemes considering the scenarios: (a) n_{rb}=10, n_{sb}=4 (symbols); (b) n_{rb}=40, n_{sb}=4 (symbols).

5.2 Simulation Study

In Chapter 3, we have described the impact of the flexible subframe design of the sub-granting scheme, i.e., customized subframe, on the overhead and transmission time between a transmitter and receiver D2D. Recall the flexible subframe, the padding information in D2D transmitter is reduced, and a D2D receiver algorithm is enhanced such that to decode the data while it is received. Here, we use a simulation study to compare the shortening TTI schemes and the sub-granting scheme applying the flexible subframe in terms of the transmission time and overhead. For this study, we consider the scenarios and simulation parameters explained in the previous chapter. In remaining part of this section, we explain the performance metrics and discuss the results.

5.2.1 Performance Metric

The data transmission time and the overhead between a D2D transmitter and receiver are considered as metrics to compare the shortening TTI and the sub-granting scheme with flexible subframe design as explained earlier.

5.2.1.1 D2D Transmission Time

The data transmission time between D2D-UE$_{TX}$ and D2D-UE$_{RX}$ is mainly influenced by the traffic payload and the data transmission rate. Recalling that for MTC applications with small / finite block length payload, authors in [42] justify that Shannon capacity, can not be an accurate way to calculate the spectral efficiency for applications with small traffic payload, and needs to be reformulated in accord with the new application characteristics, thus the data rate R ($\frac{bits}{s}$) yields:

$$\frac{R\left(\epsilon, \tau B_w\right)}{B_w} = log_2\left(1 + \frac{\delta p_{tx}\mu}{\sigma_0 B_w}\right) - \sqrt{\frac{V}{\tau B_w}}\, Q^{-1}\left(\epsilon\right) \log_2 e \ , \tag{5.6}$$

where ϵ and B_w are bit error rate and the allocated bandwidth. The data transmission is denoted by τ, and δ, and μ capture path-loss and shadowing. The value p_{tx} is transmitting power, and σ_0 is the additive white Gaussian noise. Besides, $Q^{-1}\left(.\right)$ is the inverse of the Gaussian Q-function, and the dispersion factor V captures the stochastic variability of the channel that yields:

$$V = 1 - \frac{1}{1 + \left(\frac{\delta p_{tx}\mu}{\sigma_0 B_w}\right)^2}. \tag{5.7}$$

Table 7.2.3-2 in [63] is applied to derive the modulation and coding scheme pertaining to the upper bound of the achievable spectral efficiency as denoted in (5.6). Considering the above description, the achievable data rate is obtained by multiplying modulation, and coding scheme, allocated RBs, and subframe size. Consequently, the data transmission time is computed by dividing the traffic payload to the data transmission rate. For example, when the payload size is 100 bits and a PRB is assigned to every D2D-UEs, the maximum achievable rate is 4.8 bits/sub-carrier*OFDMA symbol(OS) (6*0.8) for the highest modulation and coding scheme, i.e., 64QAM-4/5, through which the

transmission time lasts two subframes (4 OS) taking into consideration a subframe with 2OS.

5.2.1.2 Overhead

This section discusses the average overhead as a metric for each D2D user when applying the shortening TTI, and flexible subframe in the sub-granting scheme. Recalling to LTE, the padding information is appended to the transport block when the number of arrived bits in the MAC is smaller than the size of the transport block. Besides, in the physical layer, at least one DMRS in every slot is required for channel estimation at the receiver. In our study, the padding information and DMRS are considered as an overhead, which is computed as follows.

First, the D2D-UE$_{TX}$, i.e., sub-grant provider, computes the number of padding bits considering the difference between the traffic payload and the size of the transport block corresponding to the maximum spectral efficiency of D2D communication. Then, the number of bits used to convey the DMRS is calculated considering configured modulation and coding scheme and resource blocks for every D2D communication. It is a worthy note that in the flexible subframe in the sub-granting scheme, the number of configured DMRS can vary depending on the length of the subframe. This way, the number of DMRS in the flexible subframe is expected to be less than or equal to that of other schemes, e.g., sTTI schemes. For example, when there exist a 100 bits, traffic payload and spectral efficiency of D2D communication are 64 bits/OS/RB. In the case of a subframe with 2OS, two subframes are required to carry such a traffic payload. This way, considering the conventional definition of overhead, it is approximately 170 bits in this example. In contrast, in the flexible subframe in the sub-granting scheme, it amounts to 90, which is by far less than the sTTI subframe with 2OS.

5.2.2 Results and Discussions

This section evaluates the average transmission time and overhead in D2D communication for the flexible subframe in the sub-granting scheme and compares it with the shortening TTI schemes [24].

Figure 5.5 illustrates the average transmission time between D2D transmitter and receiver users. Generally, a subframe with a finer granularity is expected to shorten the data transmission time. For example, the subframe with 14OS, i.e., LTE subframe, displays the highest transmission time ranging from 1 to 1.4 milisecond (ms). The average transmission time for the subframe with the finest granularity, i.e., 2OS, is higher than the flexible subframe in the sub-granting scheme. The reason is that the traffic payload size generated by D2D transmitter is bigger than the transport block size needed for the transmission, and thus multiple subframes with 2OS are needed to dump the available traffic at the transmitter. For example, even for the smallest traffic payload, e.g., 80 bits, with the highest modulation scheme, at least two subframes with 2OS are required. In contrast, in the flexible subframe, i.e., customized subframe, the subframe size is chosen based on the actual traffic payload at the transmitter. Besides, the receiver starts decoding the data while it is received by which the transmission time between D2D user is further reduced. The average transmission time in the flexible subframe is about o.2ms in the studied scenario, as shown in Figure 5.5.

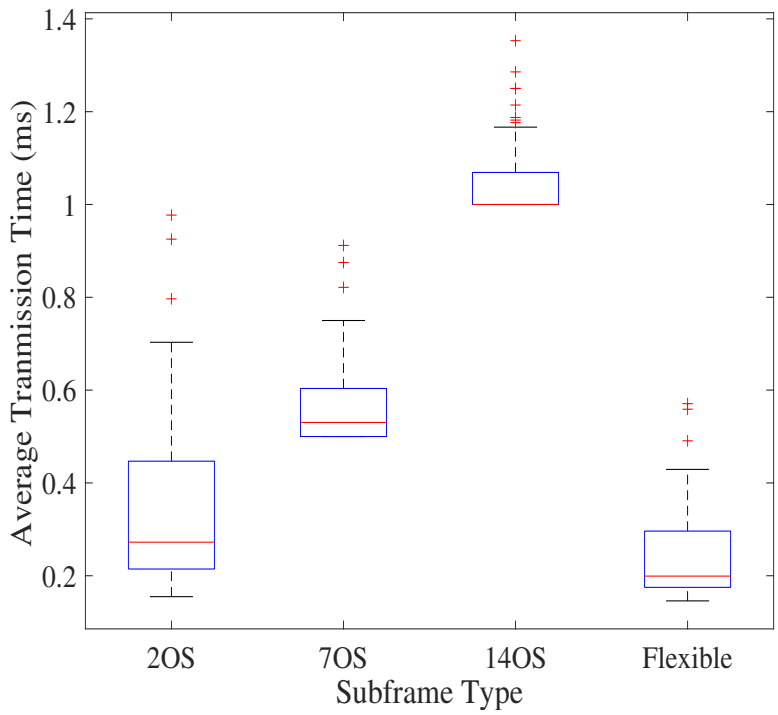

FIGURE 5.5: Average transmission time for D2D-UE for the different subframe schemes in the sub-granting and sTTI schemes.

Recall that the DMRS and padding information are taken into consideration as overhead in D2D communication. Figure 5.6 compares the overhead for the different subframe schemes in the studied scenarios. The flexible subframe, i.e., customized subframe, in the sub-granting scheme shows at least 30% less overhead compared with the other shortening TTI and legacy LTE subframes. The overhead reduction is because, in the customized subframe, the D2D transmitter appends less padding information to the TB, and besides, the fewer number of the DMRS is adopted in the flexible subframe as mentioned earlier. The subframe with 7OS shows a slightly higher overhead than the subframe with 2OS. The reason is that the traffic payload is small, and thus more padding information needs to be added on the subframe with 7OS, whereby the overhead on the subframe with 7OS is increased compared with the subframe with 2OS. The results show almost 82% overhead for the subframe with 7OS. Moreover, the subframes with 14OS hold coarse granularity whereby increases the overhead, especially for the applications with small traffic payload. Consequently, even though the sub-granting scheme imposes the sub-granting signaling as explained earlier, it is observed that the imposed overhead is less than that of other subframe schemes due to the flexibility of the subframe size and padding information reduction.

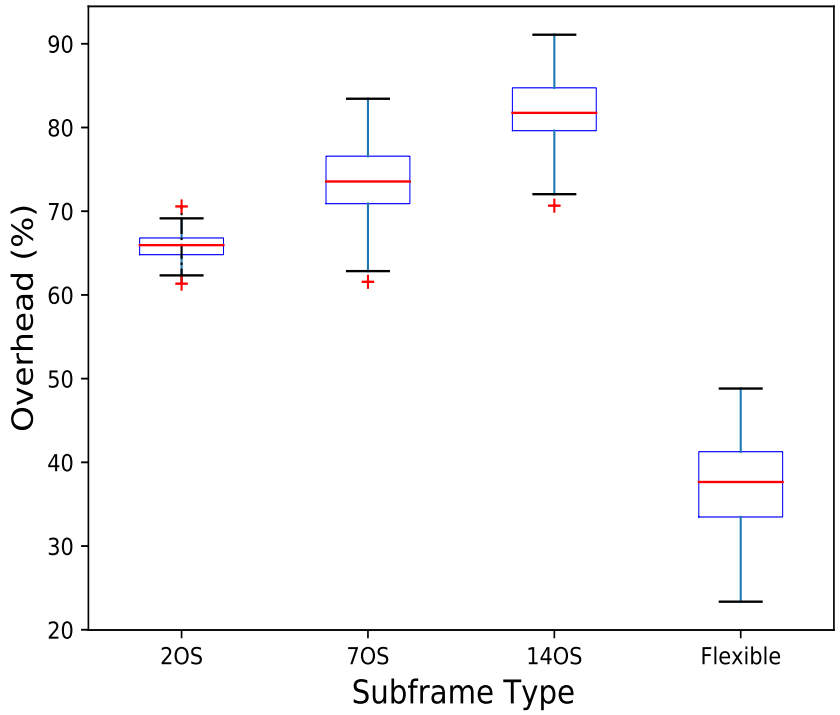

FIGURE 5.6: Average overhead for D2D-UE for the different subframe schemes in the sub-granting and sTTI schemes.

5.3 Summary

In this section, we first numerically evaluated the flexible subframe in the sub-granting scheme and compared it with different sTTI in terms of the cell and D2D throughput. Also, the impact of traffic size on cell throughput was investigated. Recalling the sub-granting scheme, a receiver capable of the sub-granting scheme needs some time to decode the received sub-granting signaling and encode its data into the sub-granted resources, denoted by the processing time. Here, the processing time impact on the cell throughput was studied, and the impact of the D2D user activity rate on the cell throughput in the sub-granting scheme was investigated. Inspiring from this analysis, we introduce a flexible sub-frame, in which the padding information in the D2D transmitter is reduced, and the D2D receiver is mandated to exploit the piggyback signaling in the flexible subframe to be able to decode the data while it is received. The chapter continues by comparing the overhead and data transmission time of the flexible subframe in the sub-granting scheme with the shortening TTI schemes and the legacy LTE subframe. Although in the flexible subframe in the sub-granting, a part of the subframe is dedicated to the sub-granting signaling, the data transmission time and the overhead are significantly reduced in favor of the flexible subframe in the subframe sub-granting scheme.

Finally, it is observed that even the shortest subframes will impose some overhead, especially for the applications with small-payload traffic, which results in increasing transmission time. With insight into the done analysis, the flexible subframe design in the sub-granting scheme seems a viable solution to efficiently exploiting the allocated radio resources when the radio resources are allocated to the users in a semi-persistent

manner. The next chapter will discuss how a beneficiary user is selected in the sub-granting scheme to maximize the cell throughput.

CHAPTER 6

Beneficiary User Selection Algorithms Performance Evaluation in Sub-granting Scheme

Contents

In Chapter 3, we cast the beneficiary user selection problem mathematically as an optimization problem to maximize the cell throughput. A centralized algorithm, i.e., a Dedicated sub-granting, and distributed algorithm, i.e., open sub-granting, were proposed by which the maximum number of beneficiary users are selected that resulted in the cell throughput maximization. In this chapter, we first endeavor to evaluate the dedicated sub-granting algorithm performance by comparing it with a random selection algorithm. Then, a comparison between dedicated and open sub-granting algorithm is conducted wherein the performance of both algorithms in a dynamic scenario is evaluated.

6.1 Dedicated Sub-granting and Random Selection Comparison

The beneficiary user selection problem in the sub-granting scheme was addressed by a centralized algorithm, say DSGRR, as early discussed in the chapter 3 and in [26]. This section compares a dedicated sub-granting and random selection algorithms in terms of cell throughput, the number of selected beneficiary users, and the beneficiary user throughput. In the following sections, the simulation parameters and performance metrics are first explained. Then, the observations and results are discussed.

6.1.1 Simulation Parameters

We assume a single cell system with a carrier frequency centered at 2.6 GHz. There are 100 RBs available, and 20 RBs are allocated to 20 D2D users in a semi-persistent manner. The remaining RBs are scheduled among 50 D2I users based on their Channel Quality Index (CQI) with each D2I user getting at least one RB. In this topology, the cell radius is 600 meters. The channel models in [44] are used for path loss and log-normal fading effects. Besides, we consider Rayleigh and Rician fading models for the fast fading effects on D2I and D2D communications, respectively. Finally, the beneficiary user selection process is performed at every time interval of 100 ms. Simulation parameters are summarized in Table 6.1.

Table 6.1: Simulator setup parameters.

Parameter	**Value**
Frequency, fc and BW	2.6 GHz, 20 MHz
Number of users	50 D2I, 20 D2D
Cell Radius	600 m
D2D Distance (d)	20 m
Channel Model [44]	UMi-NLOS α_c: 3.67 $\mu_c : \sigma = 4\ dB$, Rayleigh InH-NLOS α_d: 4.33 $\mu_d : \sigma = 4\ dB$, Rician, K=20 dB
Traffic Model	Packet size=10B, λ=1ms, $\epsilon_{th}^{\mathbb{D}}$=$10^{-5}$ [1]
Power Control	Open Loop Power Control $D2D$ ($P0$ = -70 dBm/RB) $D2I$ ($P0$ = -115 dBm/RB)
Noise Power Density (σ_0)	-174 dBm/Hz
MAX UE TX Power	23 dBm
D2D and D2I Antenna Gain	1 dB
eNB Antenna Gain	10 dB
ϵ_{th}^{sg}	10^{-3}
Simulation Runs (i)	10000

6.1.2 Performance Metrics

We base our evaluation on the following metrics:

- Cumulative distribution function (CDF) of the cell throughput in case of considering/relaxing constraint (3.9e).
- Beneficiary user average throughput.
- The number of selected beneficiary users and the sub-granting signaling errors.

We evaluate the proposed algorithm in terms of the criteria mentioned earlier and compare the proposed algorithm with no sub-granting (No SGRR) and random sub-granting radio resource (Random SGRR) which are considered as baseline methods in our study. In No SGRR, the allocated radio resources are being wasted when the D2D user has not utilized the allocated resources. However, in the Random SGRR, a beneficiary user is randomly being chosen in every sub-granting scheduling scale.

6.1.3 Results and Discussions

Taking into account the traffic requirements given in [1], we use same traffic model as in Chapter 3 considering the parameters in Table 7.2. Besides, we assume that the indoor hotspot non-line-of-sight (InH-NLOS) model for channel gains for all D2D communications while the urban micro hexagonal cell layout non-line-of-sight (UMi-NLOS) model is considered for channel gains for the D2I communications. For both D2D and D2I communications, LTE open loop power control is assumed [92]. The transmission power distribution of D2I users is shown in Figure 6.2. As previously discussed, a geographical area for every D2D users, eLA, is determined, wherein the sub-granting signaling message can reliably decoded. Figure 6.1 shows the relationship between the eLA and desired received power, $P0$, in the open loop power control equation. Intuitively, for a specified signaling error value (i.e., ϵ_{th}^{sg}), a bigger eLA area is achieved at the cost of higher D2D transmission power (higher $P0$).

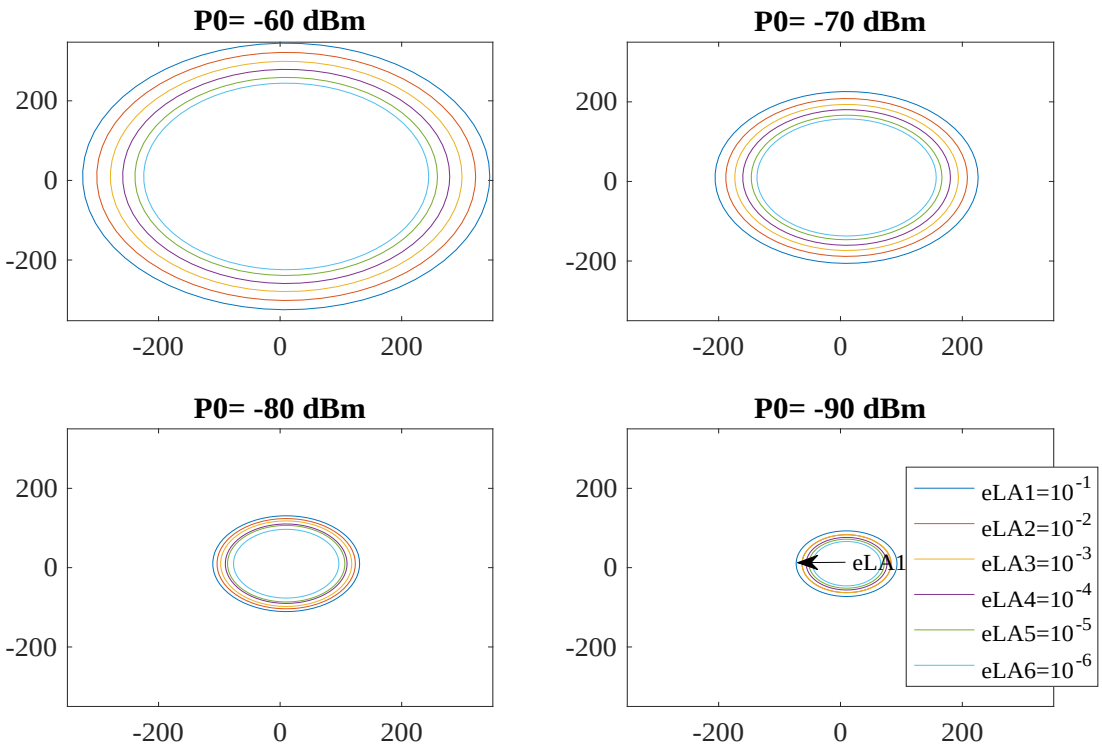

FIGURE 6.1: An illustrative example of eLA for different desired received power ($P0$).

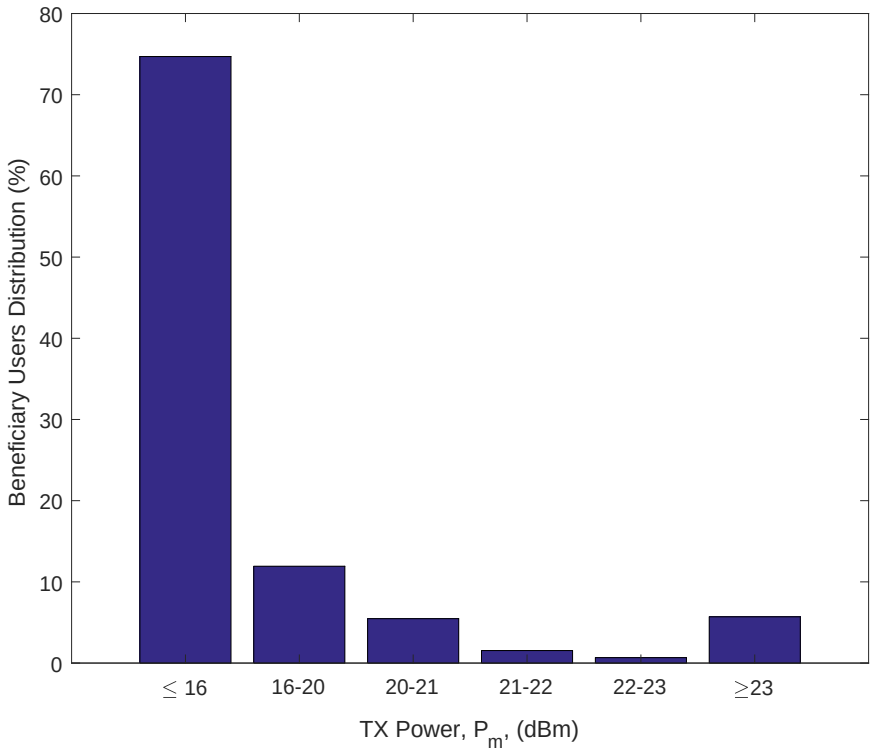

FIGURE 6.2: Illustration of beneficiary users transmission power distribution.

In Figure 6.3, the cell throughput is evaluated w/ and w/o power constraint (3.9e). Compared to the proposed SGRR and Random SGRR, the No SGRR has significantly

degraded performance, which is mainly due to radio resource wastage. In Figure 6.3(a), when the power constraint is relaxed, the Random SGRR increases the cell throughput by 10.5% compared with the No SGRR. Additionally, it is observed that the proposed DSGRR increases the cell throughput by 25% compared with the Random SGRR. This main reason is attributed to the selection of beneficiary users with the highest CQI. Figure 6.3(b) illustrates the cell throughput that can be achieved considering the power constraints. The cell throughput decreases by 2% for the proposed algorithm when the power constraint is applied. The main reason is attributed to the transmission power distribution in the studied scenario, as it is shown in Figure 6.2.

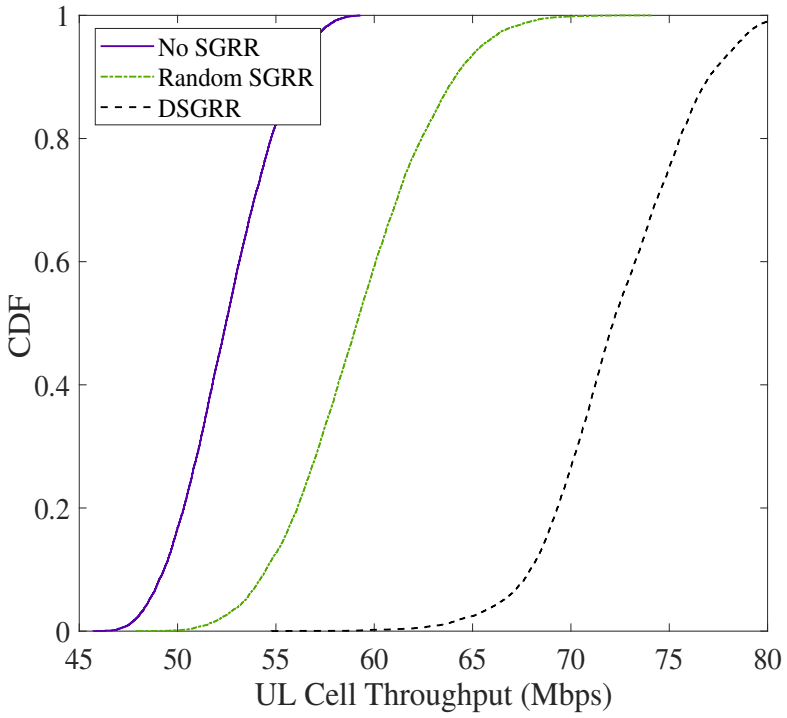

(a)

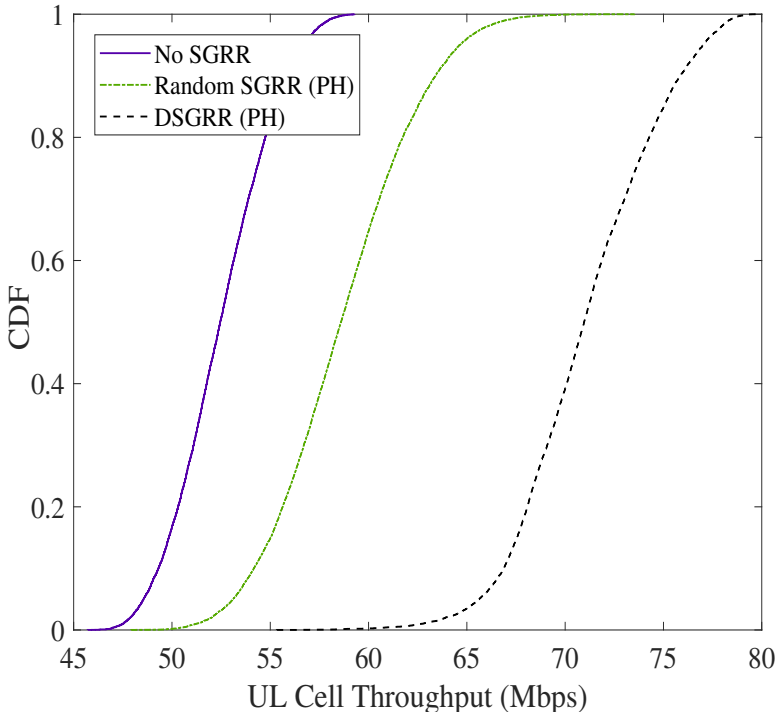

(b)

FIGURE 6.3: Illustration of UL cell throughput in the different schemes: (a) w/ power constraint (b) w/o power constraint.

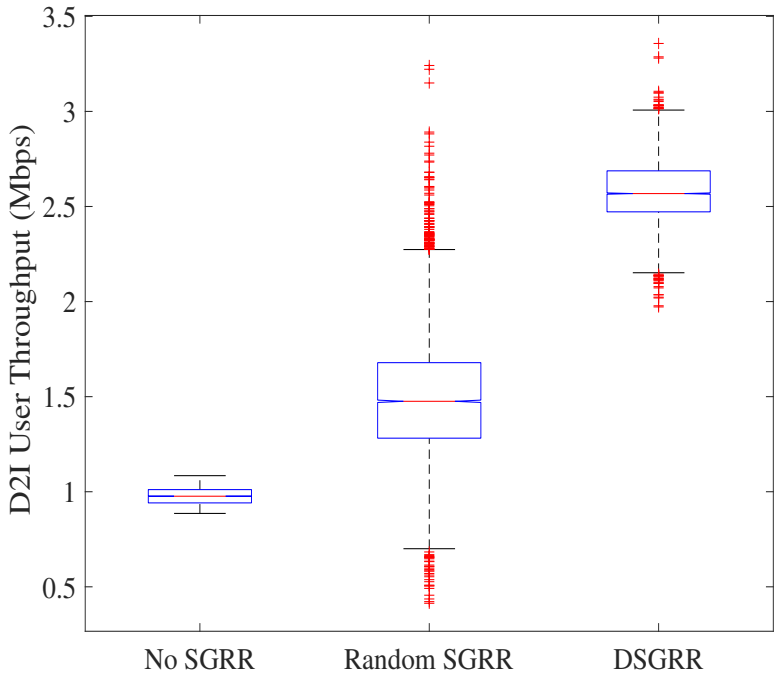

FIGURE 6.4: Illustration of beneficiary D2I user throughput for different algorithms.

Figure 6.4 represents the achieved throughput by beneficiary D2I user applying the different algorithms when no power constraint is taken into consideration. The average throughput achieved by the beneficiary user increases by 73% for the proposed DSGRR compared with the Random SGRR. This reason is due to the fact that in the random selection, the farther beneficiary users are chosen, which reducing the sub-granting signaling decoding probability. Besides, in the random selection algorithm, no criteria, e.g., CQI, in the selection process, are taken into consideration. Although the Random SGRR shows a degraded performance compared with the SGRR, it can still achieve a better performance than the No SGRR. We observe that the average beneficiary D2I user throughput increases by 50% for the Random SGRR compared with the No SGRR. The reason is that even in the Random SGRR selection, a part of the unused resources can still be re-utilized by the selected beneficiary users.

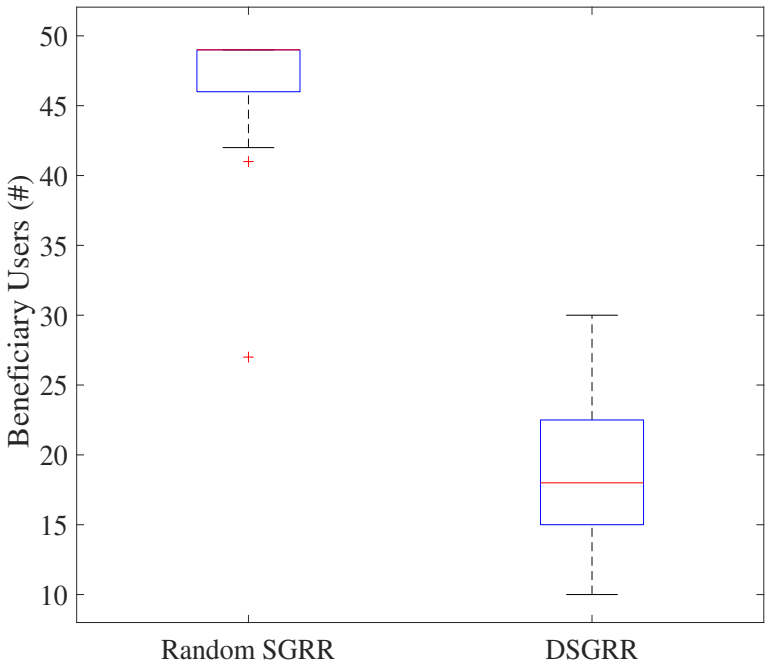

FIGURE 6.5: Number of selected beneficiary users.

Figure 6.5 and Figure 6.6 represent the number of selected beneficiary users and sub-granting signaling errors for the Random SGRR and the proposed DSGRR algorithms. Although the higher number of beneficiary users is selected in the Random SGRR than the proposed DSGRR (see. Figure 6.5), the Random SGRR increases the sub-granting signaling error by 40% (see. Figure 6.6). This is because, in the Random SGRR, no constraints on the selection process are taken into consideration, and thus farther beneficiary users are selected, which might increase the likelihood of not decoding the sub-granting signaling.

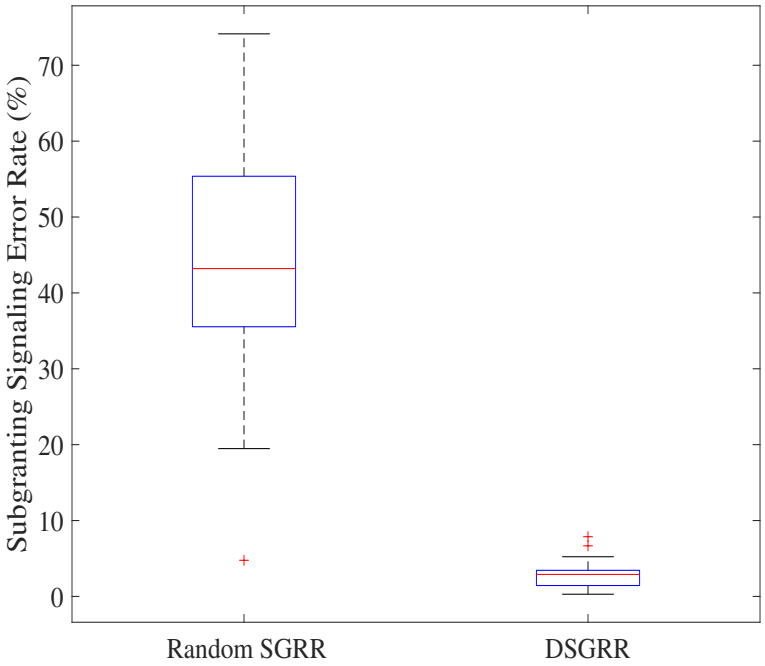

FIGURE 6.6: Sub-granting signaling errors for Random SGRR and DSGRR algorithms.

6.2 Dedicated and Open Sub-granting Comparison

A centralized approach might incur significant overhead on the network due to the necessity of measurements in a dynamic environment. The measurement burden can be offloaded to the D2D and D2I users through a distributed approach. In Chapter 3 a distributed approach was decribed wherein all D2I users as a bidder contributes to an auction to identify a beneficiary user for every sub-grant provider [27]. Here, in this section, we compare a distributed method, say OSGRR, with a DSGRR in terms of some performance criteria. To this aim, first, the simulation setup parameters and performance metrics are described, and then the results and observations are discussed.

6.2.1 Simulation Parameters

We assume a single cell system with a carrier frequency centered at 2.6 GHz. There are 100 RBs available, and 40 RBs are allocated to 40 D2D users so that each D2D user is assigned an RB in a semi-persistent manner. The remaining RBs are scheduled among 60 D2I users equally. In this topology, the cell radius is 300 meters, and all users are uniformly distributed within the cell and move in random directions with constant speeds. At the cell border, the UEs select a random direction towards inside the cell and continue moving inside the cell. The channel models in [44] are used for the path-loss and large-scale fading, i.e., shadowing effects. More specifically, the indoor hot-spot non-line-of-sight (InH-NLOS) and the urban micro hexagonal cell layout non-line-of-sight (UMi-NLOS) models are regarded as channel gains for the D2D and

D2I communications, respectively [44]. Besides, we consider the Rayleigh and Rician fading models to capture the small-scale fading effects, but without loss of generality, we assume that the channel conditions do not vary during the sub-granting signaling and bid information transmission. For both D2D and D2I communications, LTE open loop power control is assumed [92]. The transmission power distribution of D2I users is shown in Figure 6.7. In this study, we apply same traffic model as explained in the Chapter 3 based on the requirements given in [1] (See Table 6.1).

To avoid any non-uniformity in user distribution due to mobility inside the cell and have more realistic outcomes, the simulator is run ten times in which the simulation duration is 4000ms, and then the results are averaged over every simulation run. Most of the simulation parameters are the same as the previous study, summarized in Table 6.1. In addition, those simulation parameters that are new or modified for this study are summarized in Table 6.2.

TABLE 6.2: Network parameters used in the simulator.

Parameter	**Value**
Number of users	60 D2I, 40 D2D
Cell Radius	300 m
User Velocity	30Kmph
Power Control	Open Loop Power Control $D2D$ ($P0$ = -90 dBm/RB) $D2I$ ($P0$ = -107 dBm/RB)
Simulation Runs (i)	4000
T_{me}, T_{pos}, T_{br}	480ms
β	0.9

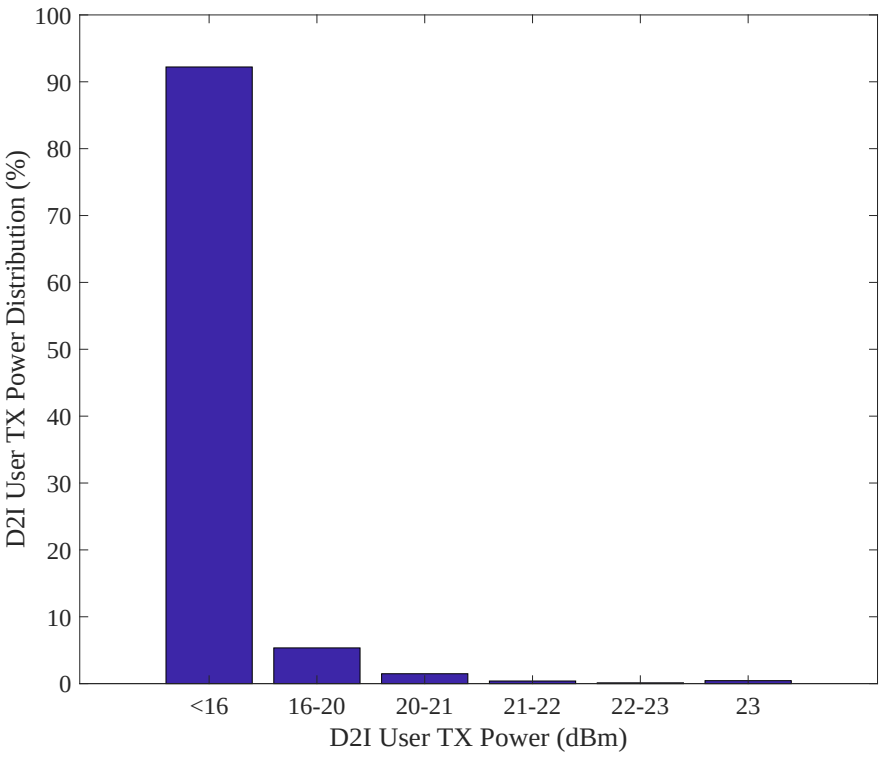

FIGURE 6.7: D2I Transmission Power Distribution.

6.2.2 Performance Metrics

The following metrics are studied in our study:

- Uplink cell throughput.
- Average throughput of beneficiary user.
- Number of selected beneficiary users.
- Sub-granting signalling errors rate.
- Overhead rate.

6.2.3 Results and Discussions

As indicated in the DSGRR algorithm, for every sub-grant provider, a geographical area eLA is specified, wherein the sub-granting signaling message can be reliably decoded. This way, the measurement transmission to eNB, which is needed for the beneficiary resource selection, is avoided. Recalling that the relationship between the eLA and desired received power, $P0$, in the open-loop power control equation is shown in Figure 6.1 in Section 6.1.3. Considering a specified signaling error value (i.e., ϵ_{th}^{sg}), a bigger eLA area is achieved at the cost of higher D2D transmission power (higher $P0$). Despite the circular eLA shape shown in Figure 6.1, the actual geometry eLA is irregular and thus far from being circular. The reason is because of large-scale fading phenomena, i.e., shadowing, employed in (3.10), different signal power around the sub-grant provider is received. Thus, the spatial geometry of the eLA area is distorted. In our analysis, we assume an identical shadowing around a sub-grant provider in every eLA estimation interval whereby a circular eLA is formed.

As discussed in Algorithm (3.6.2), the value β should be set in a way to achieve the maximum gain from the sub-granting resources. Figure 6.8 illustrates the impact of β value on the uplink cell throughput. When β value is set to 0.1, the achieved throughput is 3.5% less compared with the β value of 0.9. It is because, in the latter one, the beneficiary users with better CQI value towards the BS are selected. Although the difference between the achieved throughput with β values of 0.9 and 0.5 is marginal in the studied scenario, the results show the slightly higher uplink throughput when β value is set at 0.9.

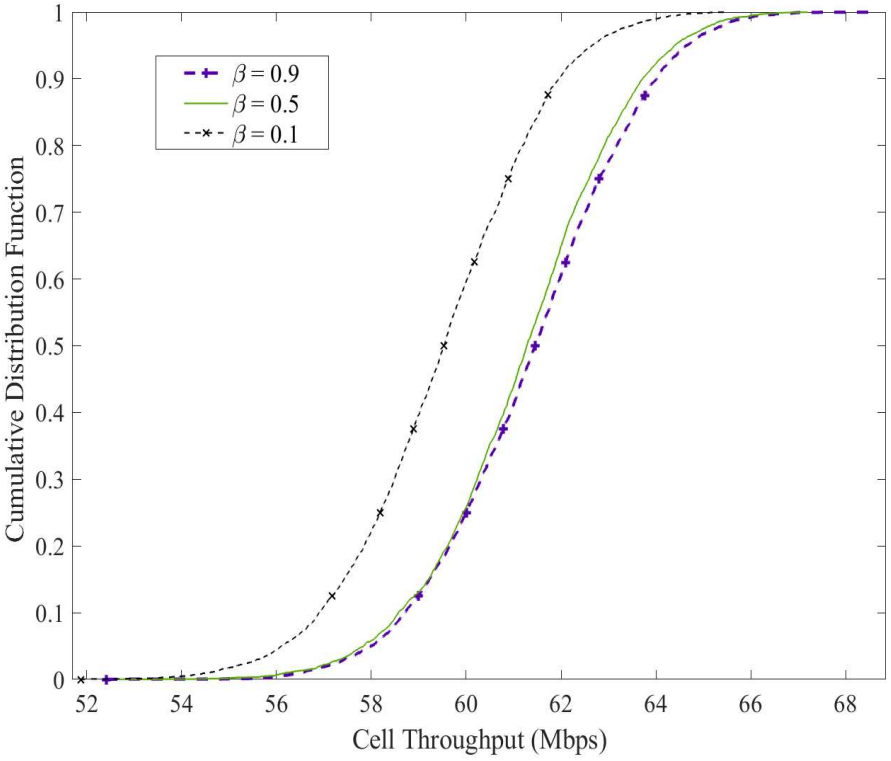

FIGURE 6.8: Impact of beta value on cell throughput for the OSGRR. The highest cell throughput is achieved at a value of β 0.9.

Although using a centralized approach could achieve an optimal solution for the beneficiary users' selection problem, it will increase the burden of overhead arising from the measurement. Therefore, an eLA based beneficiary selection algorithm, i.e., DSGRR, was proposed in [26] where the overhead is reduced. However, in the DSGRR algorithm, a large-scale fading can only be estimated, whereas, in the OSGRR algorithm, both large- and small-scale are captured in the measured received strength signal from the sub-grant provider users. Due to the small-scale fading in the OSGRR, the probability of receiving a signal from the sub-grant provider is higher. As a result, the average coverage radius of a sub-grant provider becomes bigger in the OSGRR than the eLA area, estimated in the DSGRR. Figure 6.9 shows an illustrative example of a coverage area for the OSGRR and DSGRR algorithms.

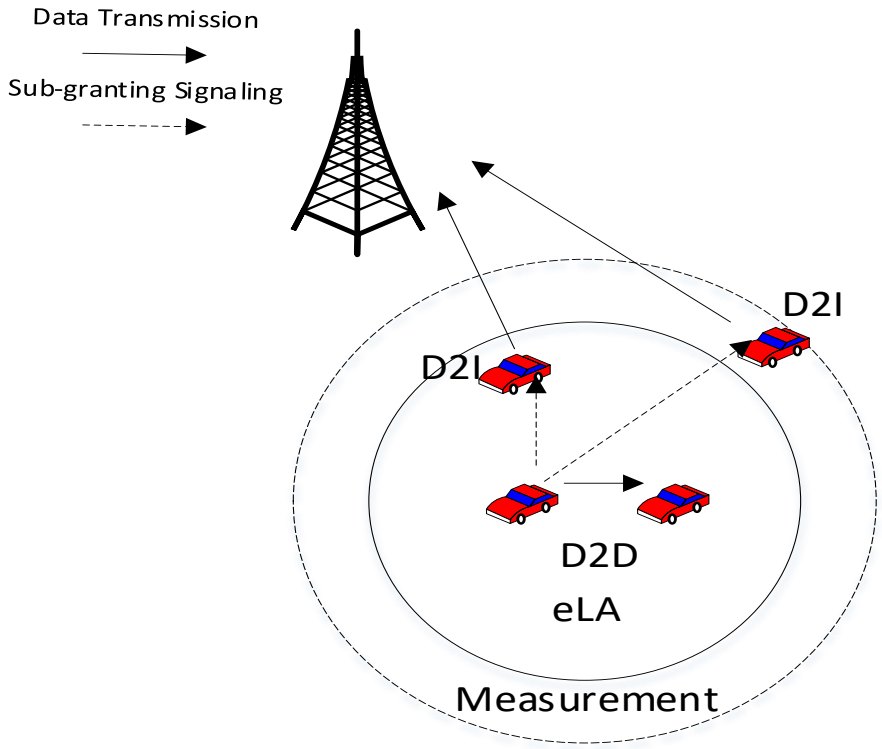

FIGURE 6.9: An illustrative example of the sub-grant provider coverage area for measurement-based and eLA-based approaches.

Considering the above explanation, more beneficiary users receive the sub-granting signaling in the OSGRR, which the chance of the sub-granting resources being used by the beneficiary users increases.

To prove this, the number of the candidate beneficiary users of every sub-grant provider for both algorithms is investigated. As shown in Figure 6.10, the number of the candidate beneficiary users is higher in the OSGRR compared with the DSGRR. The reason is that the measurement-based method, i.e., OSGRR, will increase the probability of receiving the sub-granting signaling. It is worth noting that the uniform large-scale fading assumption in the eLA computation causes to have a lower number of the candidate beneficiary users of ever sub-grant provider in the DSGRR, resulted in further performance degradation in the DSGRR algorithm.

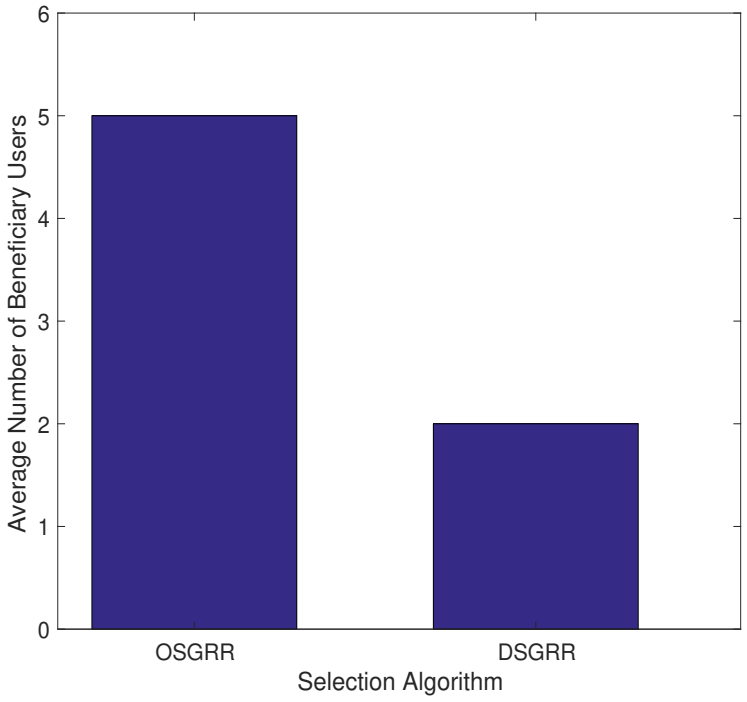

FIGURE 6.10: An illustrative example of the average number of candidate beneficiary users of every sub-grant provider.

Further observation is conducted to show the impact of sub-granting signaling measurement on the beneficiary selection process. For this, the small-scale fading effect and overhead are not considered for both algorithms. It is observed that both algorithms achieve almost the same uplink cell throughput (see Figure 6.11). Note that the marginal difference is due to the stochastic essence of the large-scale fading in both algorithms, whereby the different number of beneficiary users may be selected.

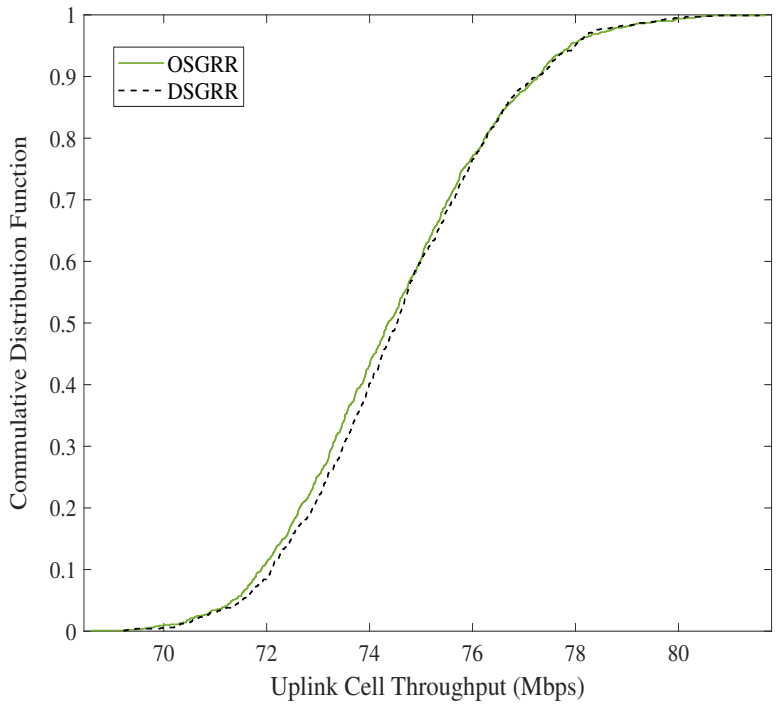

FIGURE 6.11: An illustrative example of comparison of the uplink cell throughput for both algorithms in a scenario with stationary users where the overhead and small-scale fading are not considered.

In the dedicated sub-granting algorithm, i.e., DSGRR, every entity transmits CSI measurement and position information to the eNB at a time interval of 480 ms. Then, the eNB informs the sub-grant provider user about the beneficiary user identity through control information. These measurements and control information is conveyed by the uplink/downlink LTE physical layer control channels. This study assumes the bandwidth of one resource block and modulation coding scheme of QPSK-1/2 to carry the control information and measurement information in both downlink and uplink, respectively. The overhead due to the uplink measurement is calculated by (sub-carrier) $\times$ (OFDMA symbols) $\times$ (modulation order) $\times$ (code rate) $= \frac{12\times14\times2\times1/2}{8} = 21$ bytes and considering 3 bytes for Cyclic Redundancy Check (CRC), total overhead has amounted to 24 bytes [92].

In the downlink, the overhead is $\frac{12\times3\times2\times(1/2)}{8} = 5$ bytes, and 3 bytes is added as CRC resulted in 8 bytes overhead for the beneficiary user selection indication.

Also, given that every cellular user is equipped with a global positioning system (GPS), every user caters for the cellular network location information (e.g., location estimate, pseudo-range, velocity). Considering the uplink user-assisted information in [97], the overhead due to position information, the MAC layer information, and physical layer information, is about 40 bytes. In this study, it is assumed that the network can obtain a sufficiently accurate position of every user employing user-assisted information.

In the open sub-granting algorithm, i.e., OSGRR, every beneficiary user offers a bid value on the sub-granting resources, and a beneficiary user offering the highest value can utilize the sub-granting resource for a specific transmission interval time, e.g. 480

ms. In (3.13), one byte is required to indicate the CQI values, and 4 bytes are used to show the beneficiary user's unique number γ_m. Considering overhead of MAC and physical layers, i.e., 6 bytes, [92], the OSGRR imposes 11 bytes overhead to indicate the bid value. Note that the sub-granting signaling imposes 1 byte overhead on both algorithms [23]. Table 6.3 illustrates components and size of the overhead for both algorithms.

TABLE 6.3: An illustration of overhead components and size in the OSGRR and DSGRR.

Selection Algorithm	**Overhead Components**	**Size(Byte)**
DSGRR	Position information Measurement information (e.g., buffer status, power head room) Beneficiary user selection signaling Sub-grant signaling	40 24 8 1
OSGRR	Bidding information Sub-grant signaling	11 1

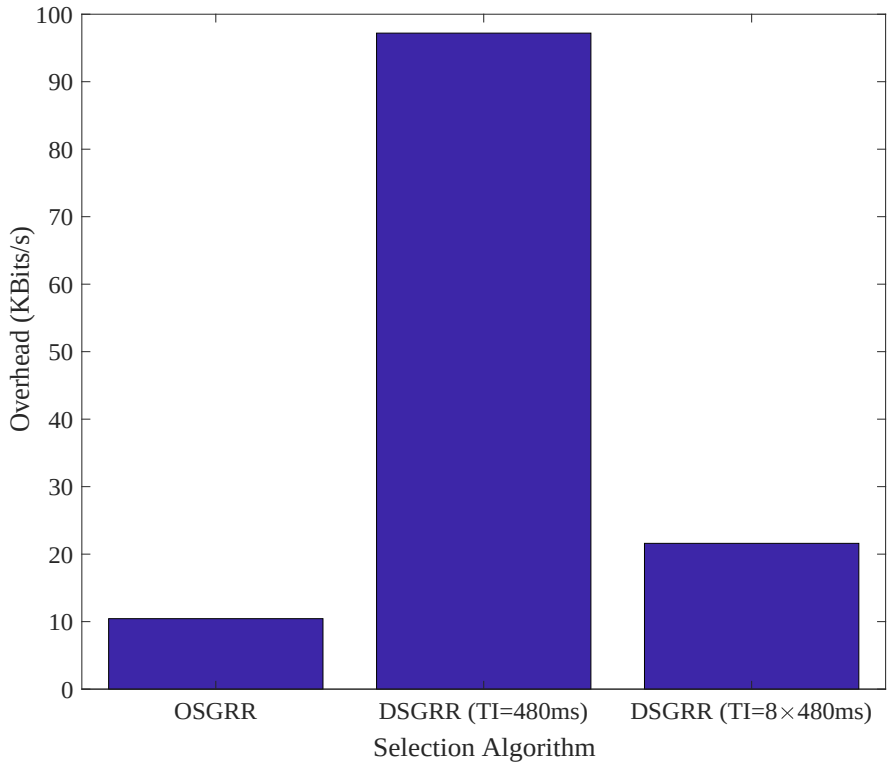

FIGURE 6.12: Overhead comparison between open sub-granting and dedicated sub-granting algorithms. The impact of different position information and measurement transmission interval for the dedicated sub-granting algorithm is shown.

Figure 6.12 compares the overall overhead between the OSGRR and the DSGRR algorithms when the biding transmission interval and position and measurement information transmission interval are the same for both algorithms. Also, the impact of CSI measurement and position transmission interval on the DSGRR algorithm is examined. It can be seen that the overhead on the DSGRR algorithm is higher than the OSGRR

algorithm. The reason is that in the beneficiary user selection process, the volume of measurement and position information that are transmitted to the eNB in the DSGRR algorithm is higher than the biding information exchanged between users in the OSGRR algorithm.

The overhead on the DSGRR is reduced when the measurement transmission interval increases from 480 ms to 8 × 480 ms; however, the result still shows less overhead in favour of the OSGRR algorithm. The reason is that the OSGRR needs a few bytes to broadcast the bids and does not impose any CSI and position information transmission overhead on the eNB. Although in the DSGRR, the overhead can be further reduced by the increment of the measurement transmission interval, the performance will deteriorate as the outdated measurement information is used for the beneficiary user selection.

Figure 6.13 demonstrates the number of selected beneficiary users for both algorithms. The results show that the average number of selected beneficiary users in the OSGRR algorithm is about 10% higher than that of the DSGRR algorithm. As previously discussed, in the OSGRR, a beneficiary user has a higher chance of receiving the sub-granting signalling than the DSGRR due to a measurement-based selection. For example, in the DSGRR, if a beneficiary user is the only candidate at the border of the overlap eLA area of two sub-grant providers, the beneficiary user can be only selected by one of the sub-grant provider users. In contrast, in the OSGRR, farther beneficiary users may receive sub-grating signaling from a sub-grant provider user not assigned to any beneficiary user, resulted in increasing the number of selected beneficiary users. Also, the results confirm that the OSGRR algorithm can serve a higher number of beneficiary users than the DSGRR algorithm.

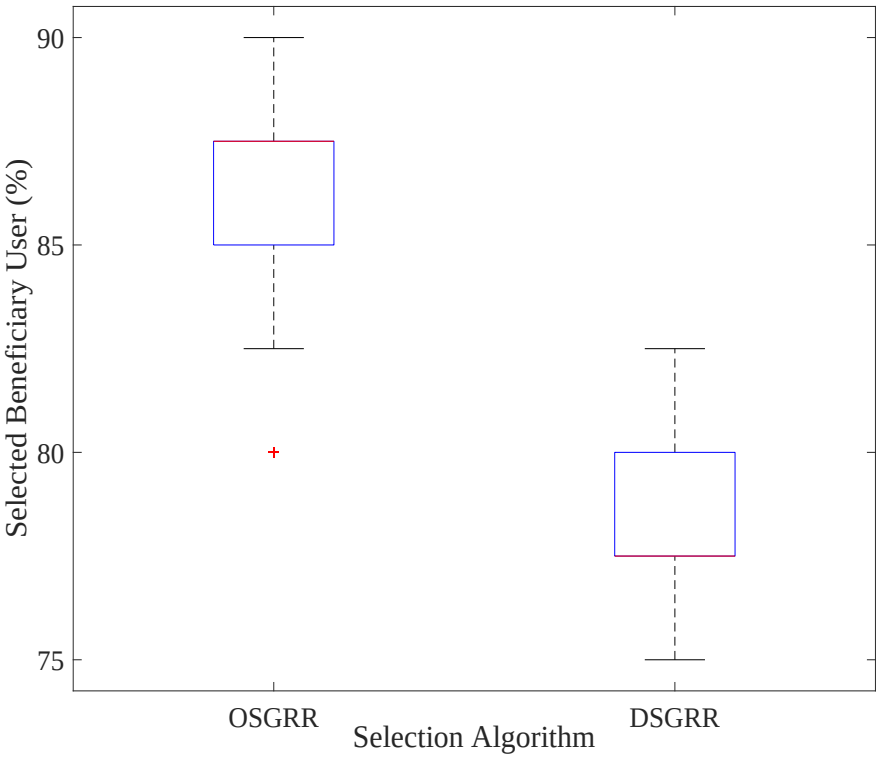

FIGURE 6.13: Comparison of the average number of selected beneficiary users between the DSGRR and OSGRR algorithms.

Figure 6.14 compares the sub-granting errors for the OSGRR and DSGRR algorithms for different position information and measurement transmission interval. The DSGRR shows a lower error rate compared with the OSGRR considering the same transmission interval for position information, CSI, and bid information. The reason is that in the OSGRR, farther beneficiary users are selected, which increases the probability of not decoding the sub-granting signaling owing to the fading between the sub-grant provider and the beneficiary user. In the DSGRR, when CSI and position information transmission interval increases by eight times, the sub-granting signaling errors increase by more than two times due to using the outdated eLA information during the beneficiary selection process.

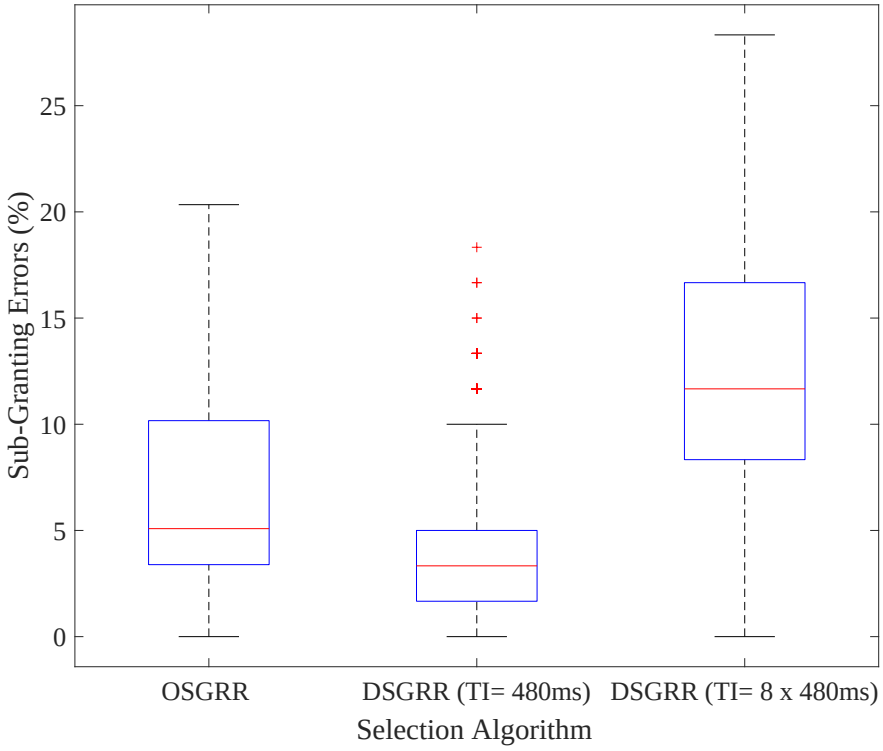

FIGURE 6.14: Sub-granting errors comparison between the DSGRR and OSGRR algorithms.

Figure 6.15 shows the impact of the CSI and position information transmission interval on the DSGRR throughput and compares both DSGRR and OSGRR algorithms in terms of cell throughput. Also, the closeness of both algorithms to the maximum achievable cell throughput is evaluated. To this end, the cell throughput of the DSGRR and OSGRR algorithms are compared with the case w/o any sub-granting algorithm and the maximum achievable cell throughput when all the allocated radio resources are fully utilized. Considering the same transmission interval and speed, as shown in Table 7.2 for both algorithms, the OSGRR shows slightly better results than the DSGRR. The overhead and the number of selected beneficiary users are two factors that mainly contribute to the cell throughput degradation in the DSGRR compared with the OSGRR. As indicated in Figure 6.12, the overhead contributes only to about 5% of the cell throughput reduction in the DSGRR. Another factor in the cell throughput reduction is that having a lower number of selected beneficiary users in the DSGRR, resulted in a higher throughput in favor of the OSGRR.

When the transmission interval increases by eight times, the cell throughput in the DSGRR gradually decreases during simulation runs. The results show about a 10% reduction in the cell throughput than the cell throughput with a shorter transmission interval. In contrast, the cell throughput remains almost constant in the OSGRR over the simulation runs. The results show that the OSGRR could achieve around 85% of the maximum cell throughput. The remaining 15% reduction is mainly due to the sub-granting signaling overhead and lack of a beneficiary user candidate or finding a beneficiary user with the highest MCS. It is noteworthy to mention that 35% of the allocated radio resources are wasted w/o sub-granting scheme (see Figure 6.15).

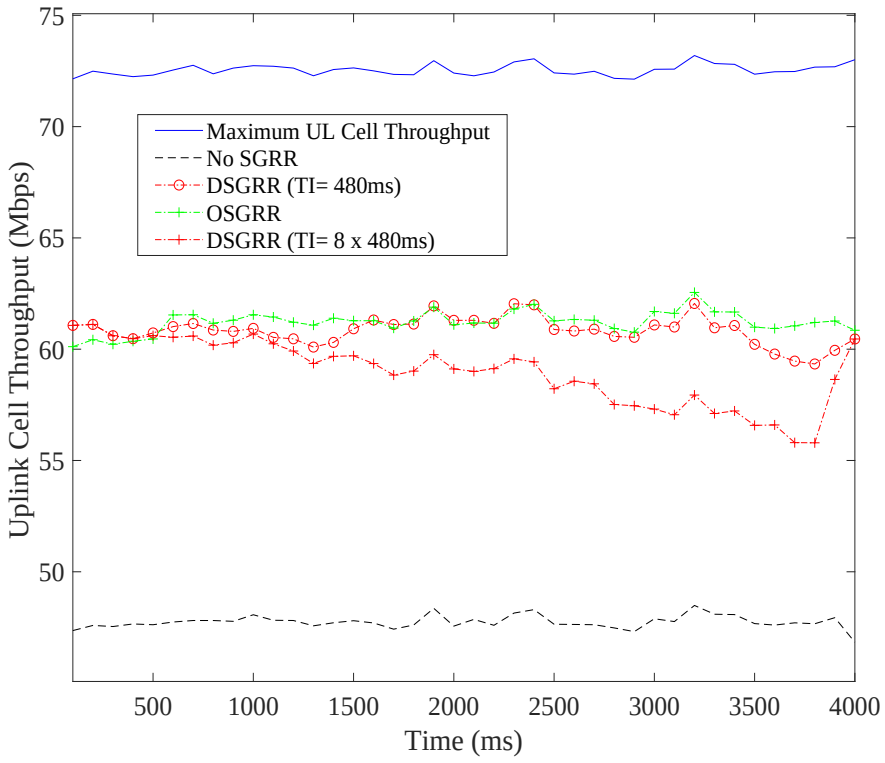

FIGURE 6.15: Performance of different approaches in terms of cell throughput. The impact of measurement and position information transmission interval for the dedicated algorithm is shown.

Figure 6.16 depicts the beneficiary user's average throughput for both algorithms, considering the exact measurement, position, and bidding transmission interval. Also, the figure compares both algorithms with no SGRR being applied. Both algorithms show about a 55% increase compared with no SGRR. This is due to the re-utilization of the unused resources in both algorithms. Although the OSGRR shows higher signaling errors compared with the DSGRR (see Figure 6.14), the average beneficiary user throughput is slightly higher than the one achieved by the DSGRR algorithm. The reason is mainly that more beneficiary users are selected in the OSGRR compared with the DSGRR, and thus the more beneficiary users can re-utilize the sub-granting radio resources resulted in achieving a higher throughput in the OSGRR.

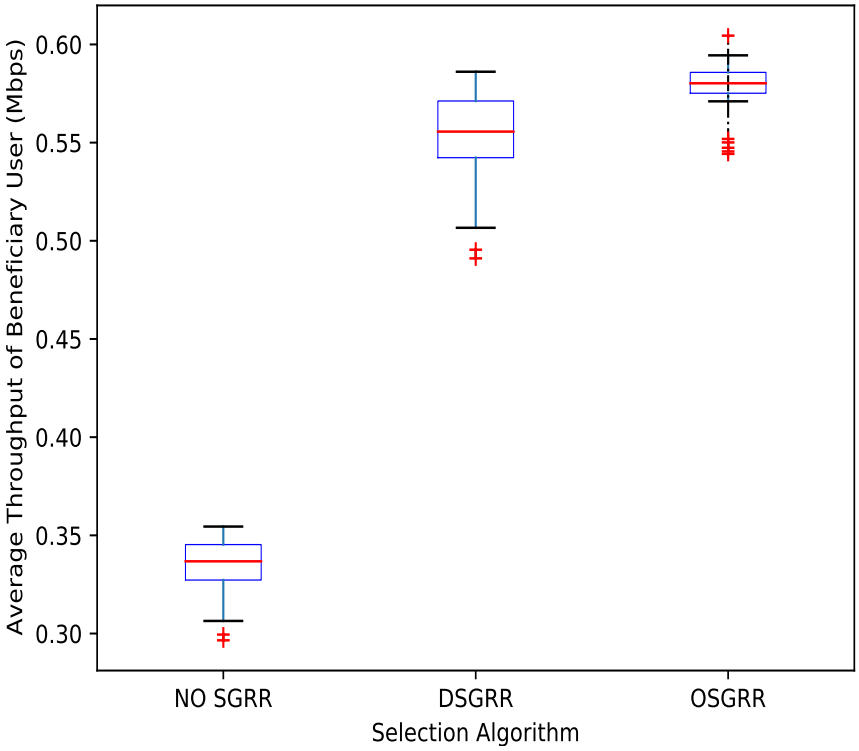

FIGURE 6.16: Comparison of the average uplink throughput of beneficiary user for different approaches.

6.3 Summary

This chapter endeavored to quantify the beneficiary user selection problem in the sub-granting scheme by evaluating the performance of different algorithms in terms of the throughput, overhead, and the number of selected beneficiary users. To this aim, we first evaluate a centralized algorithm, i.e., DSGRR and compare it with a Random SGRR, when all users are stationary. It was observed that the DSGRR algorithm has a better performance in the studied scenario compared with the Random SGRR. The reason is mainly due to considering a selection metric in the beneficiary user selection procedure. However, this technique is not applicable in a scenario with users with high mobility due to the significant overhead incurred by the measurement and positioning information transmission to the network. To avoid such complication, we proposed a distributed approach, i.e., OSGRR, wherein the complexities have been offloaded to the users and users interact with each other cooperatively to select an appropriate beneficiary user for the underutilized radio resources through the sub-granting scheme. The study is followed by comparing the performance of DSGRR with OSGRR algorithm in a fully dynamic scenario.

The overhead of both algorithms is evaluated considering the channel state information, position information, biding information, and sub-granting signaling exchanged among different entities at different transmission intervals. Moreover, both OSGRR and DSGRR algorithms are evaluated in terms of cell throughput, user throughput, and sub-granting signaling errors. Finally, the uplink cell throughput for both algorithms is compared to the maximum achievable uplink cell throughput.

The results show that the overhead imposed by the OSGRR algorithm is less than the DSGRR algorithm. Furthermore, it is observed that the OSGRR algorithm outperforms the DSGRR algorithm in terms of the uplink cell and user throughput, as the OSGRR algorithm can select more number of beneficiary users than the DSGRR algorithm.

The discussion and analysis in this chapter gave us a glimpse into what would be required to generalize the solution of the OSGRR algorithm, especially for autonomous resource selection in V2X communication on the different scenarios. The next chapter discusses the autonomous resource allocation problem for NR V2X network considering reliability and energy efficiency aspects.

CHAPTER 7

Density of Traffic-based Resource Allocation (DeTRA)

Contents

This chapter endeavors to investigates a joint energy efficiency and sum-rate maximization problem in autonomous resource selection in the 5G new radio (NR) vehicular communication while catering for reliability and latency requirements. An autonomous resource allocation problem is formulated as a ratio of sum-rate to energy consumption, where the objective is to maximize the total energy efficiency of power-saving users subject to the reliability and latency requirements. The energy efficiency problem is a mixed-integer programming optimization problem that is computationally complex when the number of users increases. Therefore, a heuristic algorithm, density of traffic-based resource allocation (DeTRA), is proposed to solve the problem. The traffic density per traffic type is considered a metric to split the radio resources and trigger an appropriate resource selection strategy. The simulation results show that the proposed algorithm outperforms the existing schemes in terms of energy efficiency.

7.1 Introduction

Energy efficiency is one of the prominent key performance indicators (KPI) in the 5G networks. The 3rd Generation Partnership Project (3GPP) recently completed a study targeted at the reduction of power consumption on user equipments (UEs) [98]. As previously explained in Section 2.3.3, the V2X communication is one of the use cases in 5G that is recently revolutionized by introducing many different communication types, e.g., from vehicular users to power-saving users [8]. The power-saving users, e.g., pedestrian, e-Bike, electric car, communicating to the nearby vehicles are usually equipped with a battery, and thus energy should be utilized more efficiently.

Resource allocation and power control have been the main research topics in V2X communications, where the goal is to optimize spectral efficiency, reliability, latency, and energy efficiency. Authors in [75] propose a joint resource allocation and power control method to optimize energy efficiency for electric cars. The results show the proposed method can be effective in certain scenarios, e.g., when every vehicle satisfies a minimum rate requirement. Authors in [76] propose a new resource allocation method for delay-tolerant applications with energy efficiency and latency constraints. The method is implemented in a two-step algorithm, where in the first step, optimal power is allocated while relaxing the latency constraint. Then, the radio resources are allocated when both latency and energy consumption constraints are satisfied.

The recent progress in 3GPP specify a promising framework for V2X communication in LTE and NR to ensure the reliability and latency required by different V2X use cases. Authors in [40] overview the latest enhancements concerning standardization in NR V2X communications. NR V2X mainly targets ensuring the reliability, latency, and spectral efficiency for different use cases [8]. However, the vehicular user with an unlimited energy source is assumed, and the power-saving users with a limited energy source, e.g., e-bikes and electric cars, are not considered. In the autonomous resource allocation procedure, i.e., Mode 2, vehicular user equipment (V-UE) performs sensing continuously before each data transmission triggering time interval. This sensing procedure is essential prior to any resource selection triggering time instance at the transmitter V-UE to ensure the reliability of the transmission and avoid any collision. However, this increases the energy consumption of the transmitter users.

In LTE V2X, two resource selection procedures, partial sensing and random resource selection, were introduced to cater for the power-saving users [19]. Random resource selection is the procedure where a power-saving UE does not carry out sensing but randomly selects resources for its intended transmission from the configured radio resource pool. Another power-saving resource selection method specified in the LTE V2X is partial-sensing. It allows power-saving UEs to perform sensing for defined time intervals, resulting in energy saving.

Note that in LTE V2X, periodic traffic is dominant, and the traffic with few periodicities is supported. Thus, a power-saving UE only needs to perform the sensing at specific time intervals. However, traffic with different periodicities in NR V2X poses a significant challenge to the resource selection strategy for the power-saving users. The problem is intensified by the introduction of aperiodic traffic in conjunction with periodic traffic in NR V2X. Therefore, in 3GPP plenary meeting [20], it was decided to leverage the existing resource allocation procedures in NR V2X considering both periodic and aperiodic traffic types for the power-saving users.

This chapter proposes a resource selection algorithm to jointly optimize spectral efficiency and energy consumption for the power-saving V-UEs in NR V2X while considering the reliability and latency requirements. The proposed algorithm exploits the traffic density measurement for each traffic type to split the bandwidth part and chooses the appropriate resource selection strategy within the dedicated bandwidth part [28].

7.2 System Model

We consider an urban area with M V-UEs, uniformly distributed within this area, where some of the V-UEs are with a limited source of energy, i.e., electric cars. The V-UEs, both transmitter and receiver, are represented by the set $M = \{1... M\}$. In our study, both frequency and time domains are considered, where a portion of bandwidth F is scheduled for the V-UEs. The allocated bandwidth is divided equally into K sub-channels in the frequency domain for each transmission unit. Moreover, one sub-channel over a scheduling time unit is defined as one resource block (RB). The V-UE selects a set of contiguous sub-channels proportional to its traffic payload and transmission parameters through a sensing procedure or a random selection procedure. Here, a broadcasting strategy for both periodic or aperiodic traffic types [99] are assumed. In general, the transmitter V-UEs are allowed to transmit on the same resources when the sensing measurement on the sub-channels is below a received signal threshold configured by the higher layers. All receiver V-UEs who are within the communication range of the transmitter V-UEs are able to receive the transmission. Figure 7.1 illustrates the system model where two V-UEs are transmitting on the same RBs within an area controlled by the network. The following assumptions are made in this study:

- The radio channel model between all vehicular users assumed in Section 3.3 is applied. .
- gNB and Global Navigation Satellite System (GNSS) are used as primary synchronization reference for all V-UEs, respectively.
- Open-loop power control is assumed, and the output transmit power of $m - th$ V-UE P_m is expressed as

$$P_m = \min\left(P_{0m}^{TX} G_m, P_{MAX}\right), \forall\ m = 1, ..., M, \tag{7.1}$$

  where P_{0m}^{TX} is a transmitted power corresponding to the desired received power for $m-th$ V-UE user related to the reliability requirements of the application and the higher layer configures it. The value P_{MAX} is the maximum power that the m-th V-UE is allowed to transmit, configured by the network. And, G_m stands for channel gain computed by (3.1).

7.3 Energy Efficiency and Resource Allocation Problem

The V-UEs usually have different reliability and latency requirements. Considering a finite number of available RBs, the reliability is depending on the instantaneous signal

to noise plus interference (SINR) ratio on the RBs. The SINR of an intended receiver V-UE in a communication range of $m-th$ transmitter V-UE is given:

$$\gamma_m = \frac{P_m|g_m|^2}{N_0 + \sum_{l=1,\ l \neq m}^{M} P_l|g_{lm}|^2}, \tag{7.2}$$

where N_0 is an additive white Gaussian Noise (AWGN) and P_m, and P_l are transmission and interference power. Moreover, g_m, i.e., $|g| = G$, and g_{lm} stand for the channel coefficients of $m-th$ transmitter and interfering transmitters to the intended receiver, respectively. In this study, we use the effective exponential SINR mapping method through which the effective SINR value is derived [100]. The receiver V-UE measures instantaneous SINR γ_{mk} on the allocated sub-channels k and then exponential effective SINR γ_m^{eff} for each receiver V-UE towards $m-th$ transmitter V-UE yields as follows:

$$\gamma_m^{eff} = -\beta \ln\left(\frac{1}{K_m B_m}\sum_{k=1}^{K}\exp\left(-\frac{\gamma_{mk}}{\beta}\right)\right), \tag{7.3}$$

where K_m and B_m are the total numbers of sub-channels and corresponding allocated RBs. The parameter of β is a factor such the effective SINR can be mapped onto a lookup table of SNR versus BLER curve precomputed under AWGN channel for a given MCS in order to model BLER [100]. The packet is considered as a successfully decoded packet when γ_{eff} is higher than γ_{th}^{high}. The value of γ_{th}^{high} is the maximum SINR thresholds from the AWGN BLER lookup tables corresponding to the required BLER ϵ_{req} and MCS in which the packet is decoded correctly. In contrast, the received packet is considered as an undecoded packet when γ_{eff} is less than the minimum threshold SINR γ_{th}^{low}. Note that for the case the γ_{eff} is between the two bounds, the probability of errors from the AWGN BLER lookup table is taken. Finally, the likelihood of the

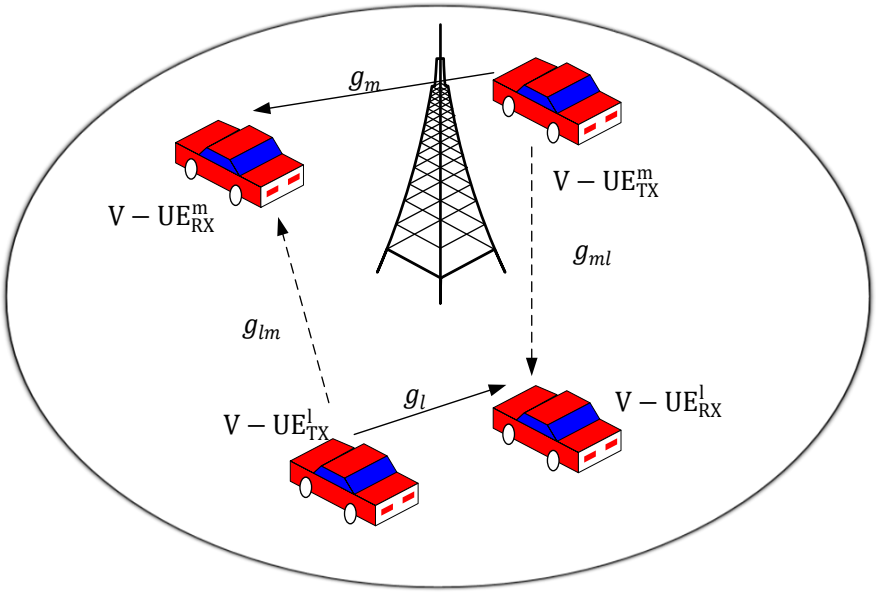

FIGURE 7.1: The system model illustrates an exemplary model with two transmitter V-UEs and two receiver V-UEs wherein $m-th$ and $l-th$ transmitter V2X users from M are transmitting on the same resources when the channel coefficients received from counterpart transmitter V-UEs, g_{ml}, g_{lm} are below a certain threshold.

Table 7.1: List of Notations

Notation	Interpretation
K	Set of sub-channel, $k = 1, ..., K$
M	Set of V2V users, $m = 1, ..., M$
F	Set of available RBs on gNB
B	Number of RBs per sub-channel, $b = 1, ..., B$
X	Allocation indicator
α	Path loss component
μ	Fading component
σ_0	White Gaussian noise
σ	Shadowing
γ	Signal to noise and interference
P_m	Transmit power of $m - th$ V-UE, $m = 1, ..., M$
P_{MAX}	Maximum transmit power
q	Modulation and coding scheme
ϵ_{req}	General term for BLER
T	data transmission time
τ_{MAX}	Maximum transmission delay
τ_s	Sensing window
N_s	Number of sensing samples
τ	Transmission time interval
τ_{proc}	Processing time
τ_a	Resource selection triggering time
E	Energy consumption (Joule)
Q	Priority of packet
L	Traffic density of network

dropped packet ϵ at the receiver V-UE is given by:

$$\epsilon = \begin{cases} 1, & \text{if } \gamma_{eff} < \gamma_{th}^{low}, \\ 0, & \text{if } \gamma_{eff} \geq \gamma_{th}^{high}, \\ \epsilon, & \text{otherwise}, \end{cases} \tag{7.4}$$

As mentioned earlier, when resource selection at transmitter V-UE is triggered, the time resource for transmission of the packet at m-th transmitter V-UE, τ_m, is bounded between triggering time, τ_a, and the maximum packet delay budget, τ_{MAX}:

$$\tau_a + \tau_{proc} < \tau_m \leq \tau_{MAX}. \tag{7.5}$$

where τ_{proc} is a processing time at the transmitter V-UE.

In general, the energy consumption can be represented by the amount of energy dissipated by a circuit block, say P_c, for data transmission time, T^{TX} and total time a V-UE involves its receiver hardware, T^{RX}, to receive the transmitting data. In Mode 2, the sensing procedure also contributes to energy consumption at V-UEs. Let us consider a single-input single-output (SISO), and single-carrier (SC), the energy consumption by

m-th V-UE, E_m is:

$$\begin{aligned} E_m\left(P, N_s\right) = & \sum_{k=1}^{K}\left(T_{mk}^{TX} P_c^{TX}\left(P_{mk}\right) + T_{mk}^{RX} P_c^{RX}\right) + \\ & \sum_{n=1}^{N_s^m} P_s \frac{n}{F_s}, \\ & 0 \leq N_s^m \leq \tau_s, \quad \forall m = 1, .., M, \ \forall k = 1, ...K, \end{aligned} \tag{7.6}$$

where P_s is energy consumption per transmission slot due to processing and buffering of sensing measurement in the unit of watts. N_s denotes the total number of sensing slot, and F_s is the sampling frequency of sensing in a slot. As a result, the sensing duration of a V-UE is given by $\tau_s = \frac{N_s}{F_S}$. The P_c^{TX} and P_c^{RX} indicate the dissipated power in all the circuit block of transmitter and receiver V-UE to operate the device for standard transmission and reception except the sensing measurement. We should also remark that the circuit power P_c^{TX} depends on transmit power P_{mk} (see (7.1)) [98].

Focusing on communication aspect of V2X communication, total number of transmitted packets by m-th transmitter V-UE on a sub-channel k in every transmission interval that can be successfully received by the receiver V-UEs is expressed by sum-rate R_{mk}:

$$R_{mk} = T_m^{RX} K_m B_m \log_2(1 + \gamma_{mk}), \tag{7.7}$$

To achieve more realistic sum-rate, we compute the sum-rate R_m based on the multiplication of the number of RBs within the allocated sub-channels K with MCS q corresponding to SINR and BLER (see (7.2) − (7.4)). Moreover, to relate the RBs and transmitter V-UEs in every transmission time interval τ, we define a mapping variable $X : M \rightarrow K$. The mapping variable, X_{mk} is a binary variable that equals 1 if a resource k is assigned to m-th transmitter V-UEs, and 0 otherwise.

Here, we consider a trade-off between sum-rate and energy consumption. To this aim, the energy efficiency (EE) is defined as a ratio of the sum-rate to corresponding energy consumption, considering the latency and reliability requirements as constraints. The energy efficiency is then cast as a maximization problem as follows:

$$\begin{aligned} & \underset{N_s^m,\ (m,k)\ \in\ C_{M\times K}}{\text{maximize}} \quad EE \\ & = \sum_{m=1}^{M} \frac{\sum_{k=1}^{K} X_{mk} R_{mk}}{\sum_{k=1}^{K}\left(T_{mk}^{TX} P_c^{TX}\left(P_{mk}\right) + T_{mk}^{RX} P_c^{RX}\right) + \sum_{n=1}^{N_s^m} P_s \frac{n}{F_s}}, \end{aligned} \tag{7.8a}$$

subject to

$$X_{mk} \in \{0, 1\} \ \forall\ m = 1, ..., M, \ \forall\ k = 1, ..., K, \tag{7.8b}$$

$$N_s^m \ \in \ [0, \tau_s], \quad \forall\ m = 1, ..., M, \tag{7.8c}$$

$$\sum_{m=1}^{M} X_{mk} = 1, \quad if\ \gamma_m \geq \gamma_{th} \quad \forall\ k = 1, ...K, \tag{7.8d}$$

$$\epsilon_m \leq \epsilon_{req}, \ \forall\ m = 1, ..., M, \tag{7.8e}$$

$$\tau_{a_m} + \tau_{proc} \leq \tau_m \leq \tau_{MAX}, \ \forall\ m = 1, ..., M, \tag{7.8f}$$

$$\sum_{k=1}^{K} P_{mk} \leq P_{MAX}, \ \forall \ m = 1, ..., M, \quad \forall \ k = 1, ..., K, \tag{7.8g}$$

In the problem formulation, X_{mk} is a binary variable that equals 1 when k-th RB is assigned to the m-th transmitter V-UE. It is worth mentioning that all V-UEs are allowed to share the same sub-channels providing that the received signal strength on the sub-channel are below a specific threshold. In constraint (7.8c), the number of sensing instances for every V-UE is determined. Constraint (7.8d) limits the sub-channel sharing when the received signal on the sub-channel is higher than the configured threshold. The constraints (7.8e) and (7.8f) considers the reliability and latency required by the packet in transmission parameters and time-frequency resource selection. The constraint (7.8g) ensures that the maximum transmission power of each V-UE is limited by a specific threshold during the data transmission.

The input to the problem (7.8) consists of the number of the sub-channel K, the number of V-UEs M, the reliability requirement ϵ_{req}, and latency requirement τ_{Max} of the packet. Moreover, the channel gain between vehicular users is given and the corresponding transmission power P_{mk} is allocated through (7.1). The output is represented by X_{mk}, N_s for every V-UEs.

The energy efficiency problem (7.8) is a mixed-integer programming problem and when the number of users is high, the optimal solution might be achieved at the cost of the high number of iterations, making the algorithm intractable or be converged at a sub-optimal solution in a limited time. Therefore, in the following section, we propose a heuristic algorithms as closed-form solutions to the problem mentioned above for specific scenarios.

7.4 Density of Traffic-based Resource Allocation (DeTRA)

As explained earlier, the sensing-based resource selection is chosen as a solution through which radio resources are selected autonomously in NR V2X. However, the algorithm was proposed based on the assumption that a V-UE has no limitation on energy consumption and thus, energy efficiency was not considered in the resource selection procedure. Here, we take the energy efficiency aspects into account and propose a heuristic algorithm by leveraging the sensing-based resource selection procedure. The proposed algorithm could achieve near-optimal solutions in terms of sum-rate to the sensing-based resource selection, while less energy is consumed. This way, the problem (7.8), cast earlier in the previous section, is solved.

This study assumes that the central control unit or a nearby V-UE provides the transmitter V-UE with the channel busy ratio (CBR) measurement information per traffic type, i.e., periodic and aperiodic.

The per traffic CBR measurement is then used to split the configured bandwidth, i.e., resource pool. To be more specific, size of the resource pool is determined based on the traffic density of periodic and aperiodic traffic. This way, a part of the resource pool is configured to be used by the V-UEs generating periodic traffic, and the remaining amount is used for the V-UEs with aperiodic traffic. In addition, the V-UEs with periodic traffic is mandated to perform sensing-based resource selection. In contrast,

the V-UEs with aperiodic traffic are instructed to perform random resource selection within the dedicated resource pool.

In the proposed algorithm, the traffic density of periodic traffic L_P, traffic type of a generated packet at the transmitter V-UE τ_{res}^{tx}, and maximum delay afforded by packet τ_{MAX} and resource selection triggering time τ_a are considered as input parameters. The time difference between resource selection triggering time and maximum packet latency and the processing time is computed. In the case of aperiodic traffic, if the traffic density of periodic traffic is below a certain threshold, the user is mandated to perform a random selection from the dedicated resource pool (see lines $4-8$). For periodic traffic, V-UEs perform the sensing-based resource selection on the corresponding dedicated resource pool (see lines $10-12$), configured for the periodic traffic. When the periodic traffic load is higher than a specific threshold, the V-UE adopts to perform the sensing-based resource selection.

Finally, it is worth mentioning that the proposed algorithm has the same computational complexity as the sensing-based resource selection algorithm.

Algorithm 7.4.1 Density of Traffic-based Resource Allocation

1: **procedure** RESOURCE SELECTION
2: **Input:**$\tau_{res}^{tx}, L_P, L_P^{th}, \tau_{MAX}, \tau_a$
3: $T = \tau_{MAX} - \tau_a - \tau_{proc}$
4: **if** $L_P \leq L_P^{th}$ **then**
5: **if** τ_{res}^{tx} == Aperiodic **then**
6: $N_{Total} \leftarrow \lceil L_p \times K \rceil \times T$
7: Select randomly $k \in [0, K]$ from N_{Total}
8: $X \leftarrow k$
9: **EndIf**
10: **if** $\tau_{res}^{tx} \neq$ Aperiodic **then**
11: $N_{Total} \leftarrow \lceil (1 - L_p) \times K \rceil \times T$
12: Update X through Normal Sensing Procedure
13: **EndIf**
14: **else**
15: *Update X through Normal Sensing Procedure*
16: **EndIf**
17: **Output:** Return X

7.5 Simulation Results and Discussions

We assume a single grid in urban grid model [99] controlled by a gNB, with a carrier frequency centred at 5.9 GHz. All V-UEs perform autonomous resource selection, and the Quadriga tool in [101] is used to generate the channel model characteristics for V2V communication non-line of sight and line of sight in the urban scenarios as defined in [99]. Besides, a high density periodic and aperiodic traffic model in [99] with traffic packet size and packet time interval as shown in Table 7.2 is used. Each V-UE is only allowed to broadcast one of the traffic types during the simulation run. For the transmission parameters, the bandwidth is equally divided into different sub-channels, and each sub-channel comprises 10 physical resource blocks. The transmit power of each

V-UE is computed from (7.1) based on the configured desired received signal, $P0$, and does not change during the simulation run. Note that the transmitter V-UE uses a fixed modulation scheme, i.e., 16QAM-1/2, during its transmission. The energy consumption for transmission, reception, and sensing per transmission time interval (TTI) is set as specified in [98]. In this study, a 3GPP compliant simulator is used, and the simulation is repeated 10 times, where each simulation takes 10s to complete. Further simulation parameters are summarized in Table 7.2.

7.5.1 Performance Metrics

We base our evaluations on the following metrics:

- Energy efficiency (EE): the energy efficiency is defined as fraction of sum-rate over the power consumption in every transmission time. The sum-rate is computed based on (7.7) as explained earlier.
- Average per-user power consumption: the per user energy consumption is obtained from the power consumption model in (7.6).
- Packet reception ratio (PRR): is defined as the average number of successfully received packets from a transmitting V-UE to all receiving V-UEs in a specific range, i.e., [0, 150m] in urban scenario [99].

Table 7.2: Network parameters used in the simulator.

Parameter	**Value**
Frequency, fc and BW, Sub-carrier spacing	5.9 GHz, 20 MHz, 15kHz
Number of V-UEs	50
Velocity of vehicles	60 Km/h (option A in [99])
Gemotery deployment	Urban scenario (1x1 grid, i.e., 433 m x 250 m) in [99]
Channel Model [19]	Large scale parameters (Table 6.2.1-1-Urban) Small scale parameters (Table 6.2.3-1)
Traffic Model	Periodic and Aperiodic: Packet size = 390B, λ = 10ms, $\epsilon_{req} = 10^{-1}$
Power Control	Open Loop ($P0$ = -104 dBm/RB)
Noise Power Density (σ_0)	-174 dBm/Hz
MAX UE TX Power, P_{MAX}	23 dBm
Power consumption of transmission (P_c^{TX})	700 (mwatt) (23dBm) [98]
Power consumption of reception (P_c^{RX})	200 (mwatt) [98]
Power consumption of sensing (P_s)	100 (mwatt) [98]
γ_{th}	-110 dBm
Simulation Time	10s

7.5.2 Results and Discussions

We evaluate the proposed algorithm, i.e., DeTRA, and compare it with available the state of the art, i.e., sensing-based resource selection and random resource selection in terms of PRR. Moreover, the DeTRA algorithm is compared with the sensing-based resource selection in terms of the average energy consumption per user and energy efficiency. Note that the transmitter V-UEs with periodic traffic reserve time-frequency radio resources for the whole simulation run. In contrast, in the case of aperiodic traffic, only one time-frequency radio resource is reserved.

Figure 7.2 compares average PRR for the sensing-based resource selection, the proposed algorithm and random resource selection. Average PRR for different algorithms per traffic type densities, i.e., periodic, is evaluated. From the figure, it is revealed that the PRR of the sensing-based resource selection increases proportionally to the periodic traffic density. In contrast, the PRR of the random resource selection is slightly decreasing with the periodic traffic density increase. Recall that for the periodic traffic, a transmitter reserves whole radio resources needed for its transmission considering the periodicity of the packet. This increases the probability of collision in the random selection. In contrast, for the sensing algorithm, the collision can be mostly avoided employing the sensing procedure explained in the autonomous resource selection, i.e., Mode 2, earlier. It can also be seen when the density of periodic traffic is low; the PRR for random selection is slightly lower than the sensing algorithm. This is mainly because of the reserved radio resources indicated by SCI may not be identified through the sensing window in the sensing algorithm as the aperiodic traffic is randomly generated. The PRR value for the sensing and the proposed algorithm is the same when the periodic traffic density is higher than 70% as it is shown in the figure. The main reason is that the resource pool is split into two parts depending on the traffic density, wherein random selection and sensing algorithm are run in the different dedicated resource pool. This way, the collision from the V-UE with periodic on the nearby V-UEs with aperiodic traffic is avoided. Besides, due to aperiodic traffic sparsity, short sensing at the transmitter V-UEs is not efficient for aperiodic traffic, and thus the probability of collision among the V-UEs is almost similar to the sensing algorithm.

Figure 7.3 compares the PRR value versus distance for all algorithms when 70% of the transmitter V-UEs generate periodic traffic. The PRR value is the same for the sensing algorithm and proposed algorithm. The reason is that the resource pool split per traffic density approach helps avoid the collision between the transmitter V-UEs with aperiodic and periodic traffic. Moreover, due to the sparsity of aperiodic traffic and its low density, the same PRR is achieved for the sensing and the proposed algorithm. The probability of collision for all algorithms increases when the receiver V-UEs are farther from the transmitter V-UEs.

Figure 7.4 compares energy efficiency between the sensing algorithm and the proposed algorithm for a scenario that 70% of V-UEs generates periodic traffic and 30% of V-UEs generates aperiodic traffic. The figure shows the energy efficiency increase by almost 20% applying the proposed algorithm. The reason is that the transmitter V-UEs with aperiodic traffic refrains perform sensing and thus consume less energy than the normal sensing-based algorithm. Moreover, as shown in Figure 7.3, the PRR is the same for the sensing and the proposed algorithms, and thus the overall sum-rate is the same for both algorithms.

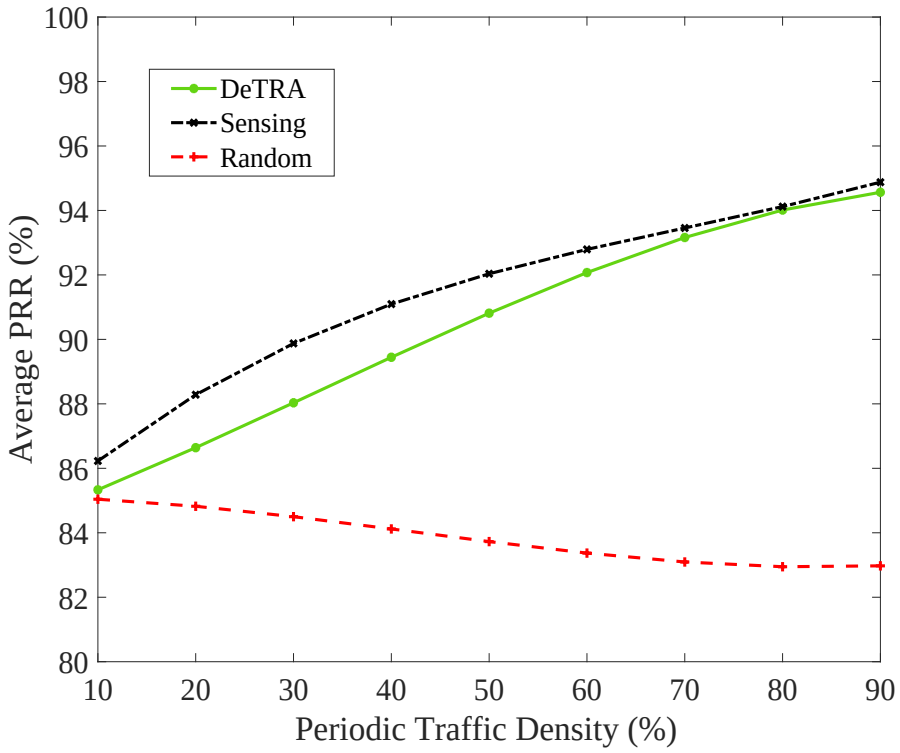

FIGURE 7.2: Illustration of average packet reception ratio of different algorithms when for a scenario with distance range of 100m as defined in [99] for different periodic traffic density.

Figure 7.5 represents average per-user energy consumption for the sensing and the proposed algorithm for a scenario when 70% of the transmitter V-UE generates periodic traffic and the remaining V-UEs have aperiodic traffic. The results show that energy consumption reduces by almost 40% applying the proposed algorithm. As explained before, the transmitter V-UEs with aperiodic traffic refrain perform sensing, resulting in energy consumption reduction.

7.6 Summary

In this chapter, we first formulated the energy efficiency problem as a ratio of the sum-rate to power consumption for the power-saving users subject to their reliability and latency requirements. This problem is a mixed-integer programming problem and becomes intractable when the number of users is high. Therefore, we proposed the heuristic of traffic density based random resource selection on dedicated pool algorithm (DeTRA). In the proposed algorithm, the resource pool is split based on the traffic density per traffic type. The random resource selection is then mandated to be performed on the dedicated resource pool upon arrival of the aperiodic traffic is triggered. Our simulation studies shows that the proposed algorithm achieves the same PRR value as the sensing-based algorithm. Besides, per-user power consumption is reduced, and consequently, the energy efficiency is improved by applying the proposed algorithm. The next chapter gives a high-level summary of the dissertation and discusses some open problems and hints on the other approaches and solutions that can be applied.

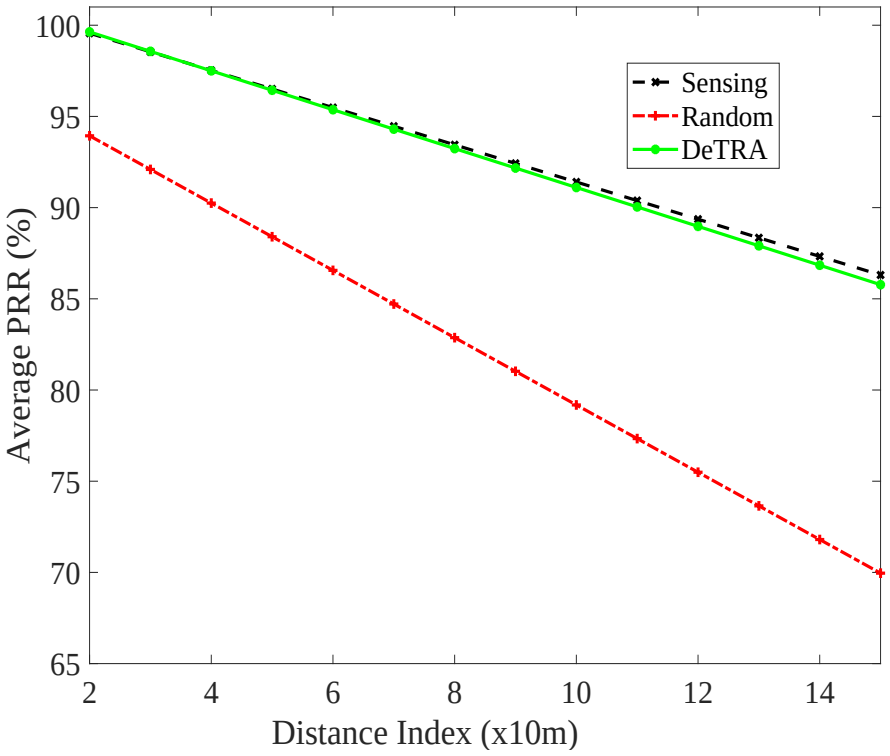

FIGURE 7.3: Average PRR for different distances when 70% of V-UEs generates periodic traffic and 30% of V-UEs generates aperiodic traffic.

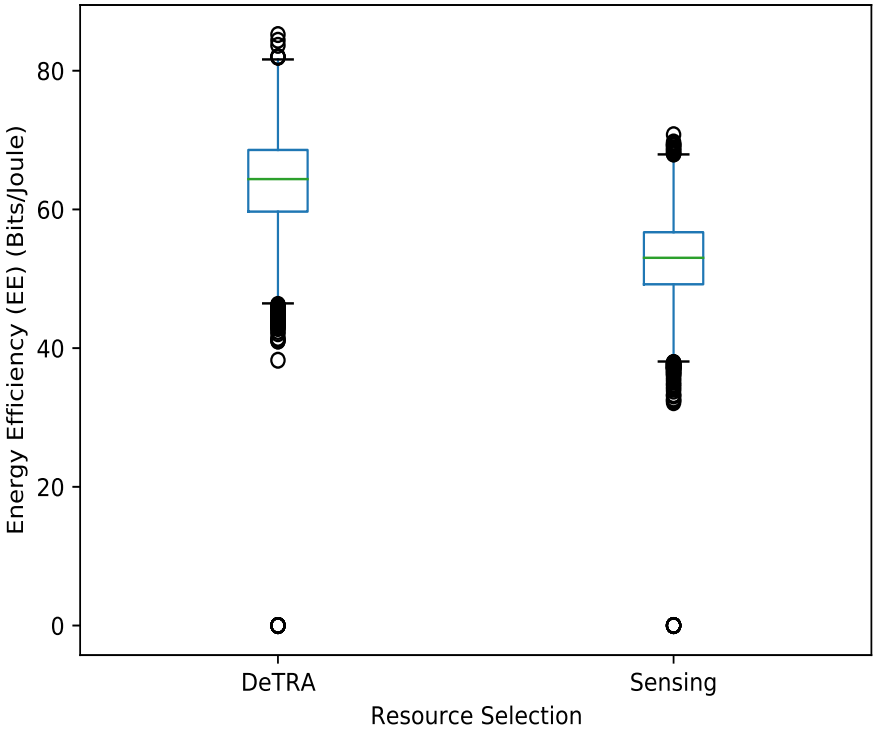

FIGURE 7.4: Energy efficiency comparison in a scenario when 70% of users are generating periodic traffic and resource pool is split based on the traffic density of each type.

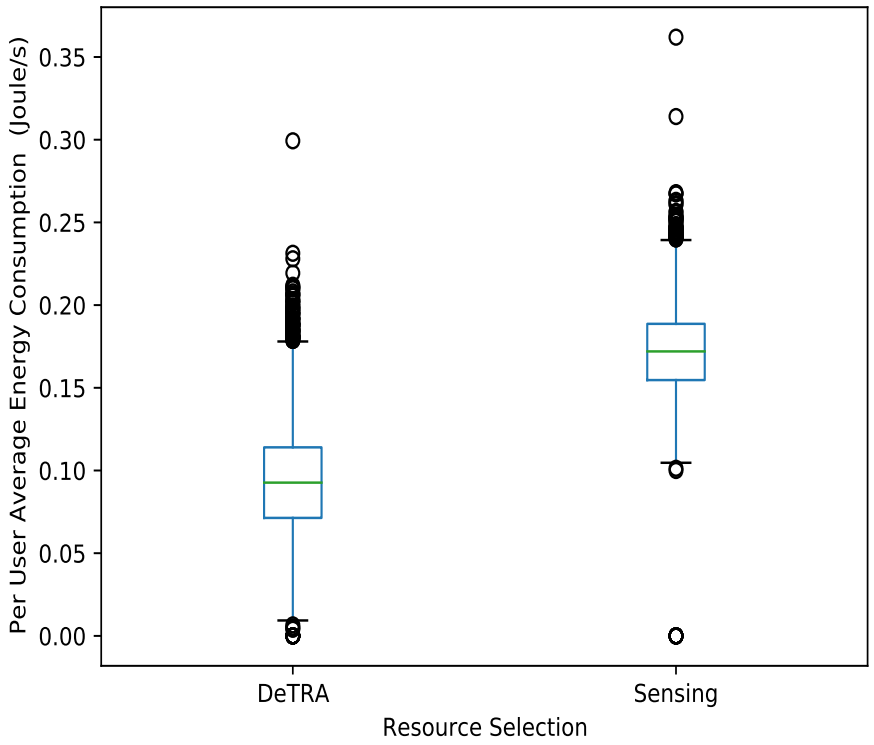

FIGURE 7.5: Average per user energy consumption for all algorithms in a scenario with 70% of the transmitter V-UEs generate periodic traffic and resource pool is split based on the traffic density of each type.

CHAPTER 8

Conclusion and Future Work

Contents

This chapter endeavors to summarize all the works that have been undertaken in this thesis. However, it has no meaning to elaborate all tasks explained in the thesis here, but rather a concept of different ideas and works. Consequently, in the following sections, some limits and constraints are explained, and the corresponding avenues are suggested to address the radio resource selection problem in future vehicular communication.

8.1 Summary

The thesis has studied the problem of radio resource allocation for overlay D2D-based V2V communication in LTE and NR technologies with a particular focus on the applications with high-reliability and low-latency requirements. In LTE, a part of radio resources is reserved in a semi-persistent manner to reduce the delay arising from the radio resource scheduling. However, subframe granularity in the LTE is too coarse to be suitable for new emerging applications characterizing with very small payload size, e.g., machine type communication. Therefore, a part of the allocated radio resource may be wasted. Resource allocation and power control have been the main research topics in V2X communications, where the goal is to optimize spectral efficiency, reliability, latency, and energy efficiency.

In LTE V2X, two resource selection procedures, partial sensing, and random resource selection, were introduced to cater for the power-saving users [19]. Random resource

selection is the procedure where a power-saving UE does not carry out sensing but randomly selects resources for its intended transmission from the configured radio resource pool. Another power-saving resource selection method specified in the LTE V2X is partial-sensing. It allows power-saving UEs to perform resource selection based on fewer sensing measurements than the normal sensing procedure, resulting in energy saving.

In LTE V2X, periodic traffic is considered as a dominant traffic type, and only the traffic types with specific periodicities are supported. Thus, a power-saving UE only needs to perform the sensing at specific time intervals in order to be able to select appropriate radio resources for its own transmission. However, traffic with different periodicities in NR V2X poses a significant challenge to the resource selection strategy for the power-saving users. The problem is intensified by the introduction of aperiodic traffic in conjunction with periodic traffic in NR V2X. Therefore, it is essential to leverage the existing resource allocation procedures in NR V2X considering both periodic and aperiodic traffic types for the power-saving users.

In general, considering the open problems stated above, we have strived to find an answer for three following questions corresponding to LTE and NR based D2D communication throughout the dissertation:

1. that how can we design an inter-coordinated mechanism to share the unused radio resources among different users.
2. how then should a candidate beneficiary users be selected to increase the spectral efficiency.
3. how resources are selected to jointly optimize spectral efficiency and energy consumption for the power-saving UEs in NR V2X communication while considering the reliability and latency requirements.

To ensure even a general reader is able to follow the thesis content, we included a comprehensive literature review on which platform, the dissertation contributions were placed.

The major contributions of this dissertation are three-fold:

1. Sub-granting Radio Resource Scheme:

A sub-granting radio resource scheme was proposed wherein a part of allocated radio resource, but not utilized, is granted to other users. A necessity of changes in the physical layer and MAC layer was discussed to realize the sub-granting scheme. In the physical, a flexible subframe for the sub-granting scheme is devised in which some signaling information is embedded to indicate the free resources in the frequency and time domains. Then, three algorithms are developed for transmitter and receiver at the sub-grant provider and the beneficiary user aiming to exploit the un-utilized radio resources indicated by the sub-granting signaling. The effectiveness of the proposed algorithms are examined by some numerical and simulation studies. Moreover, the sub-granting scheme is compared with other related state-of-art, to further justify the achieved positive performance of the proposed framework to be used in studying beneficiary user selection problem.

2. Beneficiary User Selection in Sub-granting Radio Resource Scheme:

Considering a sub-grant provider as an individual agent that can signal the amount of un-used radio resources to other nearby beneficiary users, it was observed that an appropriately selected beneficiary user would increase spectrum efficiency. To this aim, two algorithms, DSGRR, and OSGRR were proposed, wherein the beneficiary users are selected in centralized and distributed fashions, respectively. For simplicity, a bipartite graph was applied on both algorithms, in which the sub-grant provider and the beneficiary user construct two vertices of the Bipartite graph, and the edges of the graph are weighted by the utilization rate of every beneficiary user. Both algorithms aimed to achieve the maximum matching in the constructed Bipartite graph. In the DSGRR algorithm, to reduce time complexity due to measurement collection, it was proposed to compute an eLA area for each sub-grant provider, wherein a beneficiary user with the highest utilization rate within the eLA is selected. Our observation showed that the DSGRR outperforms other algorithms in a stationary scenario. However, in the case of a dynamic scenario, the collected measurements become obsolete faster that results in degraded performance. To address this problem, it was proposed to select the beneficiary user in a distributed manner applying the auction theory. To this aim, an auction is held, wherein the sub-grant providers are auctioneer, and commodities are the number of free resources promoted by the sub-granting user for sale purpose. Every beneficiary user computes its valuation using a symmetric strategy function and share it valuations, i.e., bids, on the corresponding sub-grant providers that are in the communicating range, with other beneficiary users. This way, all beneficiary users collaborate to select a beneficiary user with the highest utilization rate for a specified selection time interval in a cooperative manner. The observations were shown that the OSGRR algorithm outperforms the DSGRR algorithm in terms of the defined metrics.

3. Density of Traffic-based Resource Allocation (DeTRA) for NR V2V Communication:

The sensing-based resource selection was put forward as a solution for autonomous resource selection based on the assumption that a V-UE has no limitation on energy consumption, and thus, energy efficiency was not considered in the resource selection procedure. We take the energy efficiency aspects into account and propose a heuristic algorithm by leveraging the sensing-based resource selection procedure. The proposed algorithm could achieve a close sum rate to the sensing-based resource selection while less energy is consumed. This way, the problem (7.8), cast earlier in the previous section, is solved. Our study assumed that the central control unit or a nearby V-UE provides the transmitter V-UE with the channel busy ratio (CBR) measurement information per traffic type, i.e., periodic and aperiodic. The per traffic CBR measurement is then used to split the configured bandwidth, i.e., resource pool. To be more specific, the size of the resource pool is determined based on the traffic density of periodic and aperiodic traffic. This way, a part of the resource pool is configured to be used by the V-UEs generating periodic traffic, and the remaining amount is used for the V-UEs with aperiodic traffic. In addition, the V-UEs with periodic traffic are mandated to perform sensing-based resource selection. In contrast, the V-UEs with aperiodic traffic are instructed to perform random resource selection within the dedicated resource pool.

8.2 Future Work and Extensions

This section discusses a number of expansions that can be attempted from this work. We highlight here a few that we consider being completely critical.

As explained before, V2V communication is foreseen as a potential key enabler for different applications. In V2V communication, Multiple Input Multiple Output (MIMO) technology has recently drawn much attention from the researcher as a viable solution that can increase the spectral efficiency and mitigate the interference among the users sharing the radio resources. For example, authors in [102] compared the performance of a multi-antenna receiver with a single antenna receiver for a live cellular signal, wherein the receive beamforming technique outperforms the other techniques, e.g., Maximum Ratio Combining (MRC) in highway and dense urban scenarios. In the sub-granting scheme, the beam steering aids to assign the same sub-granting resource to the different beneficiary users locating in a different direction while maintaining the interference below a certain threshold. Both DSGRR and OSGRR algorithms can be enhanced, taking into consideration the trajectory of vehicles, communication cast type, e.g., unicast, group-cast, geographical area, the minimum communication range of intended V2V communication to avoid the interference arising from selecting undue beneficiary users.

In addition, recently, coordination between two vehicular users, i.e., inter-UE coordination, is discussing in NR V2X in 3GPP Release 17, and foresee to further enhance autonomous radio resource allocation in terms of reliability and resource utilization efficiency in NR V2X communication. In the inter-UE coordination, it is possible that gNB assigns radio resources over time and frequency domain for NR V2X user, wherein the NR V2X can signal not utilized radio resources to other vehicular users. Similar to this, the adaptability and enhancement of the sub-granting approach presented in this thesis with inter-UE coordination feature in NR V2X communication is worth to be investigated in the future.

New emerging enhanced Mobile Broad Band (eMBB) applications are demanding more data rate, and the increasing number of connected devices, for example, the users watching various entertainment videos while sitting inside their cars, will eagerly devour the bandwidth. Therefore, with increasing requests for new emerging services, evolving the existing 5G networks, and designing a new architecture for beyond 5G technology, the so-called 6G, seems vital to satisfy the requirements of the new service. Initiatives and overall overview on use cases and open research topics in the 6G are outlined in [103], [104].

As mentioned earlier, the tremendous growth of applications such as video streaming and increasing the number of connected devices, for example, vehicular communications, increase the demand for higher spectral efficiency. The 6G framework can cater to spectral efficiency to fulfill these requirements. Besides, many previously developed procedures, e.g., resource allocation procedures, need to be improved considering the spectral efficiency and QoS requirements of all users. Furthermore, another aspect is energy efficiency, commonly defined as information bits per unit of energy, which should also be considered in addition to the spectrum efficiency to preserve energy and protect the environment in the future 6G networks.

The carrier frequency and the corresponding bandwidths specified in LTE and NR V2X networks cannot furnish the necessary resources demanding by a tremendous number of

connected vehicular users with new emerging applications. One candidate technology in 6G could be the (sub-) Terahertz (THz) frequency that caters for a higher data rate to be used for faster transmission of big data between the users, for example, inside cars and other nearby users, such as RSU or pedestrian users on a sidewalk or inside other cars at the junction with eMBB applications, through THz-based sidelink communication [105]. However, the significant path loss is an intrinsic factor in THz frequency, which limits the communication range. Therefore, some techniques, such as beam steering, are proposed to reduce the adversary impact of signal attenuation for THz frequency. Besides, the path loss effect would be further reduced for a scenario where the line of sight signal is dominant, e.g., in the junction with low-speed vehicles and pedestrians.

Note that a closed-form solution with a conventional mathematical model is hard to be achieved for new use cases defined in 6G wireless communication. To this purpose, some techniques like machine learning are seen as a promising tool that could help to find optimal solutions for various problems. Particularly, one of the research areas that are worth to be investigated is machine learning-based radio resource allocation techniques over terahertz frequency in V2X communication in 6G wireless communication.

List of Acronyms

BS	Base Station
BER	Block Errors Rate
CRC	Cyclic Redundancy Check
CQI	Channel Quality Index
CSI	Channel State Information
D2D	Device-to-Device
D2I	Device-to-Infrastructure
DMRS	DeModulation Reference Signal
DSGRR	Dedicated Sub-Granting Radio Resource
eMBB	enhanced Mobile Broad Band
eNB	enhanced Node B
eLA	error-Limited Area
gNB	gNodeB
HARQ	Hybrid Automatic Repeat Request
ILA	Interference Limited Area
IoT	Internet of Things
LTE	Long Term Evolution
MAC	Media Access Control
MCS	Modulation and Coding Scheme
MIMO	Multiple Input Multiple Output
MRC	Maximum Ratio Combining
M2M	Machine-to-Machine
MTC	Machine Type Communication
NR	New Radio
OFDM	Orthogonal Frequency Division Multiplexing
OFDMA	Orthogonal Frequency Division Multiple Access

OSGRR	Open Sub-Granting Radio Resource
PRB	Physical Resource Block
PDCP	Packet Data Convergence Protocol
PHY	Physical
PRB	Physical Resource Block
PIMRC	Personal, Indoor and Mobile Radio Communications
ProSe	Proximity Service
PSCCH	Physical Sidelink Control Channel
P2I	Pedestrian to Infrastructure
QoS	Quality of Service
RB	Resource Block
RLC	Radio Link Control
RSSI	Received Signal Strength Indicator
RSU	Road Side Unit
SC-FDMA	Single Carrier Frequency Division Multiple Access
SCFDMA	Single Carrier Frequency Division Multiple Access
SGRR	Sub-Granting Radio Resource
SINR	Signal to Interference and Noise Ratio
SNR	Signal to Noise Ratio
SGRR	Sub-granting Radio Resource
3GPP	3rd Generation Partnership Project
TB	Transport Block
TBS	Transport Block Size
THz	Terahertz
TTI	Transmission Time Interval
UE	User Equipment
uRLLC	ultra Reliable Low Latency Communication
VUE	Vehicular User Equipment
V2X	Vehicle-to-Everythings
V2X	Vehicle-to-Everthings
V2I	Vehicle-to-Infrastructure
V2P	Vehicle-to-Pedestrain
V2N	Vehicle-to-Network
V2V	Vehicle-to-Vehicle

Bibliography

[1] P. Schulz, M. Matthe, H. Klessig, M. Simsek, G. Fettweis, J. Ansari, S. A. Ashraf, B. Almeroth, J. Voigt, I. Riedel *et al.*, "Latency Critical IoT Applications in 5G: Perspective on the Design of Radio Interface and Network Architecture," *IEEE Communications Magazine*, vol. 55, no. 2, pp. 70–78, 2017.

[2] J. Du, W. Zhu, J. Xu, Z. Li, and H. Wang, "A Compressed HARQ Feedback for Device-to-Device Multicast Communications," in *2012 IEEE Vehicular Technology Conference (VTC Fall)*, 2012, pp. 1–5.

[3] N. Pratas and P. Popovski, "Underlay of Low-rate Machine-type D2D Links on Downlink Cellular Links," 06 2014, pp. 423–428.

[4] X. Xiao, X. Tao, and J. Lu, "A QoS-Aware Power Optimization Scheme in OFDMA Systems with Integrated Device-to-Device (D2D) Communications," 09 2011, pp. 1–5.

[5] C.-H. Yu, O. Tirkkonen, K. Doppler, and C. Ribeiro, "Power Optimization of Device-to-Device Communication Underlaying Cellular Communication," in *2009 IEEE International Conference on Communications*, 2009, pp. 1–5.

[6] G. Fodor, "Performance comparison of practical resource allocation schemes for device-to-device communications," *Wireless Communications and Mobile Computing*, vol. 2018, 2018.

[7] 3rd Generation Partnership Project (3GPP), "3GPP TR 22.803: Technical Specification Group Services and System Aspects; Feasibility study for Proximity Services (ProSe) (Release 12)," jun 2013.

[8] 3rd Generation Partnership Project (3GPP), "TS 22.186:5G;Service Requirements for Enhanced V2X Scenarios (Release 16)," Nov. 2020.

[9] S. Xu, H. Wang, T. Chen, Q. Huang, and T. Peng, "Effective Interference Cancellation Scheme for Device-to-Device Communication Underlaying Cellular Networks," in *2010 IEEE 72nd Vehicular Technology Conference - Fall*, Sep 2010, pp. 1–5.

[10] C. Xu, L. Song, Z. Han, D. Li, and B. Jiao, "Resource Allocation using a Reverse Iterative Combinatorial Auction for Device-to-Device Underlay Cellular Networks," in *2012 IEEE Global Communications Conference (GLOBECOM)*, 2012, pp. 4542–4547.

[11] H. Min, J. Lee, S. Park, and D. Hong, "Capacity Enhancement Using an Interference Limited Area for Device-to-Device Uplink Underlaying Cellular Networks," *IEEE Transactions on Wireless Communications*, vol. 10, no. 12, pp. 3995–4000, Dec. 2011.

[12] X. Chen, L. Chen, M. Zeng, X. Zhang, and D. Yang, "Downlink Resource Allocation for Device-to-Device Communication Underlaying Cellular Networks," in *2012 IEEE 23rd International Symposium on Personal, Indoor and Mobile Radio Communications - (PIMRC)*, Sep 2012, pp. 232–237.

[13] S. N. Swain, S. Mishra, and C. S. R. Murthy, "A Novel Spectrum Reuse Scheme for Interference Mitigation in a Dense Overlay D2D Network," in *2015 IEEE 26th Annual International Symposium on Personal, Indoor, and Mobile Radio Communications (PIMRC)*, 2015, pp. 1201–1205.

[14] X. Zhang, Y. Shang, X. Li, and J. Fang, "Research on Overlay D2D Resource Scheduling Algorithms for V2V Broadcast Service," in *IEEE Conference on Vehicular Technology*, 2016, pp. 1–5.

[15] S. Liu, Y. Wu, L. Li, X. Liu, and W. Xu, "A Two-Stage Energy-Efficient Approach for Joint Power Control and Channel Allocation in D2D Communication," *IEEE Access*, vol. 7, pp. 16 940–16 951, 2019.

[16] S. Lin, H. Ding, Y. Fang, and J. Shi, "Energy-Efficient D2D Communications With Dynamic Time-Resource Allocation," *IEEE Transactions on Vehicular Technology*, vol. 68, no. 12, pp. 11 985–11 999, 2019.

[17] A. Asadi, Q. Wang, and V. Mancuso, "A Survey on Device-to-Device Communication in Cellular Networks," *IEEE Communications Surveys Tutorials*, vol. 16, no. 4, pp. 1801–1819, 2014.

[18] J. Liu, N. Kato, J. Ma, and N. Kadowaki, "Device-to-Device Communication in LTE-Advanced Networks: A Survey," *IEEE Communications Surveys Tutorials*, vol. 17, no. 4, pp. 1923–1940, 2015.

[19] 3rd Generation Partnership Project (3GPP), "3GPP TR 37.985:Overall Description of Radio Access Network (RAN) Aspects for Vehicle-to-everything (V2X) based on LTE and NR (Release 16)," Jun. 2020.

[20] ——, "RP-202846 : Work Item Description ; NR Sidelink Enhancement in Release 17," Dec. 2020.

[21] N. H. Mahmood, H. Alves, O. A. López, M. Shehab, D. P. M. Osorio, and M. Latvaaho, "Six Key enablers for Machine Type Communication in 6G," *arXiv preprint arXiv:1903.05406*, 2019.

[22] E. Roth-Mandutz, A. Puschmann, D. Mohammad Soleymani, A. Mitschele-Thiel, and J. Mueckenheim, "Transfer of Access Rights in the Form of Radio Resource Blocks in Wireless Communication Devices," DE Patent 10 2016 10 327, Jul., 2017.

[23] D. M. Soleymani, A. Puschmann, E. Roth-Mandutz, J. Mueckenheim, and A. Mitschele-Thiel, "A Hierarchical Radio Resource Management Scheme for Next Generation Cellular Networks," in *IEEE Wireless Communications and Networking Conference (WCNC)*, Doha, Qatar, Apr. 2016.

[24] D. M. Soleymani, J. Mueckenheimi, M. Harounabadi, A. M. Waswa, Z. Shaik, and A. Mitschele-Thiel, "Implementation Aspects of Hierarchical Radio Resource Management Scheme for Overlay D2D," in *IEEE International Conference on Ultra Modern Telecommunications and Control Systems*, 2017, pp. 154–161.

[25] D. Mohammad Soleymani, A. Matovu-Waswa, J. Mueckenheim, and A. Mitschele-Thiel, "Study on Uplink Throughput of Radio Resource Sub-granting and Shortening TTI Schemes for Overlay D2D," 23. ITG Mobilfunk-Fachtagung, Osnabruck, 2018.

[26] D. M. Soleymani, M. R. Gholami, J. Mueckenheim, and A. Mitschele-Thiel, "Dedicated Sub-Granting Radio Resource in Overlay D2D Communication," in *2019 IEEE 30th Annual International Symposium on Personal, Indoor and Mobile Radio Communications (PIMRC)*, Sep. 2019, pp. 1–7.

[27] D. Mohammad Soleymani, M. R. Gholami, G.Del Galdo, and J. Mueckenheimand A. Mitschele-Thiel, "Open Sub-Granting Radio Resources in Overlay D2D-Based V2V Communications," *EURASIP Journal on Wireless Communications and Networking (in review)*, 2021.

[28] D. M. Soleymani, L. Ravinchandran, M. R. Gholami, J. Del Galdo, and M. Harounabadi, "Energy-Efficient Autonomous Resource Selection for Power-Saving Users in NR V2X," in *2021 IEEE 32th Annual International Symposium on Personal, Indoor and Mobile Radio Communications (PIMRC)*, Sep. 2021, pp. 1–7.

[29] P. Schulz, A. Wolf, G. P. Fettweis, A. M. Waswa, D. Mohammad Soleymani, A. Mitschele-Thiel, T. Dudda, M. Dod, M. Rehme, J. Voigt, I. Riedel, T. Wankhede, W. P. Nitzold, and B. Almeroth, "Network Architectures for Demanding 5G Performance Requirements: Tailored Toward Specific Needs of Efficiency and Flexibility," *IEEE Vehicular Technology Magazine*, vol. 14, no. 2, pp. 33–43, 2019.

[30] A. Matovu Waswa, D. Mohammad Soleymani, Z. Shaik, J. Mueckenheim, and A. Mitschele-Thiel, "D2D Communication Implementation for Future Cellular Networks (5G)," 22. ITG Mobilfunk-Fachtagung, Osnabruck, 2017.

[31] J. Mueckenheim, A. Puschmann, D. Mohammad Soleymani, E. Roth Mandutz, A. Matovu Waswa, and A. Mitschele-Thiel, "On D2D-Communication for Resource Efficient Data Transmission of Delay-Critical Service," 21. ITG Mobilfunk-Fachtagung, Osnabruck, 2016.

[32] PIRMC Conference, "International Workshop on Beyond 5G Support for the Future Vehicular Networks," https://pimrc2021.ieee-pimrc.org/international-workshop-on-beyond-5g-support-for-the-future-vehicular-networks/, Sep. 2021.

[33] A. M. Waswa, D. M. Soleymani, S. Mwanje, J. Mueckenheim, and A. Mitschele-Thiel, "Multiple Resource Reuse for D2D Communication with Uniform Interference in 5G Cellular Networks," in *2017 IEEE 28th Annual International Symposium on Personal, Indoor, and Mobile Radio Communications (PIMRC)*, 2017, pp. 1–7.

[34] E. Roth-Mandutz, K. Shawky Hassan, S. Bhadauria, M. Leyh, D. Mohammad Soleymani, and B. Niemann, "Method and Apparatus for Zone Adaptation in a Network," EP Patent EP3 731 554A1, Jul., 2019.

[35] K. Shawky Hassan, D. Mohammad Soleymani, M. Leyh, S. Bhadauria, and E. Roth-Mandutz, "Radio Resource Management to Enhance Reliability in Mobility Scenarios," EP Patent WO2 021 004 622A1, Jul., 2019.

[36] D. Mohammad Soleymani, K. Shawky Hassan, E. Roth-Mandutz, S. Bhadauria, and M. Leyh, "NR Sidelink Control Message Design," EP Patent WO2 021 028 387A1, Aug., 2019.

[37] S. Bhadauria, D. Mohammad Soleymani, M. Leyh, K. Shawky Hassan, and E. Roth-Mandutz, "Enhanced Exceptional Pool Design for NR V2X Sidelink," EP Patent WO2 021 004 621A1, Jul., 2019.

[38] D. Mohammad Soleymani, M. Leyh, E. Roth-Mandutz, and S. Bhadauria, "User Devices for a Wireless Communication System and Methods for Communicating in a Wireless Communication system," EP Patent WO2 021 064 135A, Oct., 2019.

[39] TDoc R1-2008817, "NR Sidelink Resource Allocation for UE Power Saving," Fraunhofer, Tech. Rep., Oct. 2020.

[40] Haroundabadi, Mehdi, Mohmmad Soleymani, Dariush, Bhadauria, Shubhangi, Leyh, Martin, Roth-Mandutz, Elke, "V2X in 3GPP Standardization: Sidelink in Rel-16 and Beyond," *IEEE Wireless Communication Magazine*, vol. 1, no. 3-4, pp. 187–197, 2020.

[41] C. Hoymann, D. Astely, M. Stattin, G. Wikstrom, J. Cheng, A. Hoglund, M. Frenne, R. Blasco, J. Huschke, and F. Gunnarsson, "LTE Release 14 Outlook," *IEEE Communications Magazine*, vol. 54, no. 6, pp. 44–49, June 2016.

[42] G. Durisi, T. Koch, and P. Popovski, "Toward Massive, Ultrareliable, and Low-Latency Wireless Communication with Short Packets," *Proceedings of the IEEE*, vol. 104, no. 9, pp. 1711–1726, 2016.

[43] J. Li, H. Sahlin, and G. Wikstrom, "Uplink PHY Design with Shortened TTI for Latency Reduction," in *2017 IEEE Wireless Communications and Networking Conference (WCNC)*, March 2017, pp. 1–5.

[44] 3rd Generation Partnership Project (3GPP), "3GPP TS 36.814: Evolved Universal Terrestrial Radio Access (E-UTRA);Further Advancements for E-UTRA Physical Layer Aspects (Release 9)," Oct. 2015.

[45] J. Li, H. Sahlin, and G. Wikstrom, "Uplink PHY Design with Shortened TTI for Latency Reduction," in *Wireless Communications and Networking Conference (WCNC)*, Mar. 2017.

[46] 3rd Generation Partnership Project (3GPP), "3GPP TS 36.211: Evolved Universal Terrestrial Radio Access (E-UTRA);Physical layer and modulation (Release 15)," Sep. 2019.

[47] I. Aktas, M. H. Jafari, J. Ansari, T. Dudda, S. A. Ashraf, and J. C. Arenas, "LTE Evolution-Latency Reduction and Reliability Enhancements for Wireless Industrial Automation," in *2017 IEEE 28th Annual International Symposium on Personal, Indoor, and Mobile Radio Communications (PIMRC)*. IEEE, 2017, pp. 1–7.

[48] 3rd Generation Partnership Project (3GPP), "3GPP TS 36.321: Evolved Universal Terrestrial Radio Access (E-UTRA); Medium Access Control (MAC) (Release 12)," oct 2015.

[49] 3rd Generation Partnership Project (3GPP), "Digital cellular telecommunications system (Phase 2+) (GSM);Universal Mobile Telecommunications System (UMTS);LTE;5G;Release description;," Jan. 2020. [Online]. Available: https://www.3gpp.org/specifications

[50] J. Lianghai, B. Han, M. Liu, and H. D. Schotten, "Applying Device-to-Device Communication to Enhance IoT Services," *IEEE Communications Standards Magazine*, vol. 1, no. 2, pp. 85–91, 2017.

[51] A. Orsino, G. Araniti, L. Militano, J. Alonso-Zarate, A. Molinaro, and A. Iera, "Energy Efficient IoT Data Collection in Smart Cities Exploiting D2D Communications," *Sensors*, vol. 16, no. 6, p. 836, 2016.

[52] A. Nauman, M. A. Jamshed, Y. Ahmad, R. Ali, Y. B. Zikria, and S. Won Kim, "An Intelligent Deterministic D2D Communication in Narrow-band Internet of Things," in *2019 15th International Wireless Communications Mobile Computing Conference (IWCMC)*, June 2019, pp. 2111–2115.

[53] B. Kaufman and B. Aazhang, "Cellular Networks with an Overlaid Device to Device Network," in *2008 42nd Asilomar Conference on Signals, Systems and Computers*, Oct 2008, pp. 1537–1541.

[54] T. Peng, Q. Lu, H. Wang, S. Xu, and W. Wang, "Interference Avoidance Mechanisms in the Hybrid Cellular and Device-to-Device Systems," in *2009 IEEE 20th International Symposium on Personal, Indoor and Mobile Radio Communications*, Sep 2009, pp. 617–621.

[55] P. Janis, V. Koivunen, C. Ribeiro, J. Korhonen, K. Doppler, and K. Hugl, "Interference-Aware Resource Allocation for Device-to-Device Radio Underlaying Cellular Networks," in *VTC Spring 2009 - IEEE 69th Vehicular Technology Conference*, April 2009, pp. 1–5.

[56] A. M. Waswa, "Multiple Resource Reuse for Device-to-Device Communication in Future Cellular Networks," Ph.D. dissertation, Dec 2020. [Online]. Available: https://www.db-thueringen.de/receive/dbt_mods_00047388

[57] B. Zhou, H. Hu, S. Huang, and H. Chen, "Intracluster Device-to-Device Relay Algorithm With Optimal Resource Utilization," *IEEE Transactions on Vehicular Technology*, vol. 62, no. 5, pp. 2315–2326, Jun 2013.

[58] J. C. F. Li, M. Lei, and F. Gao, "Device-to-Device (D2D) Communication in MU-MIMO Cellular Networks," in *2012 IEEE Global Communications Conference (GLOBECOM)*, Dec 2012, pp. 3583–3587.

[59] G. Fodor, E. Dahlman, G. Mildh, S. Parkvall, N. Reider, G. Miklos, and Z. Turanyi, "Design Aspects of Network Assisted Device-to-Device Communications," *IEEE Communications Magazine*, vol. 50, no. 3, pp. 170–177, March 2012.

[60] X. Zhang, Y. Shang, X. Li, and J. Fang, "Research on Overlay D2D Resource Scheduling Algorithms for V2V Broadcast Service," in *2016 IEEE 84th Vehicular Technology Conference (VTC-Fall)*, Sep. 2016, pp. 1–5.

[61] S. Feki, A. Masmoudi, A. Belghith, F. Zarai, and M. S. Obaidat, "Swarm Intelligence-based Radio Resource Management for D2D-based V2V communication," *International Journal of Communication Systems*, p. e3817, 2018.

[62] 3rd Generation Partnership Project (3GPP), "3GPP TS 22.185: LTE;Service Requirements for V2X Services(Release 14)," Jul. 2018.

[63] ——, "3GPP TS 36.213: Evolved Universal Terrestrial Radio Access (E-UTRA);Physical layer procedures(Release 12)," Oct. 2015.

[64] ——, "3GPP TS 38.212: 5G; NR; Multiplexing and Channel Coding (Release 16)," Jan. 2021.

[65] 3rd Generation Partnership Project (3GPP), "TS 38.214:NR; Physical Layer Procedures for Data (Release 16)," Sep. 2020.

[66] W. Sun, E. G. Ström, F. Brännström, K. C. Sou, and Y. Sui, "Radio Resource Management for D2D-based V2V Communication," *IEEE Transactions on Vehicular Technology*, vol. 65, no. 8, pp. 6636–6650, 2015.

[67] G. Nardini, A. Virdis, C. Campolo, A. Molinaro, and G. Stea, "Cellular-V2X Communications for Platooning: Design and Evaluation," *Sensors*, vol. 18, no. 5, p. 1527, 2018.

[68] T. Sahin and M. Boban, "Radio Resource Allocation for Reliable Out-of-coverage V2V Communications," *arXiv preprint arXiv:1904.12710*, 2019.

[69] Y. Jeon, S. Kuk, and H. Kim, "Reducing Message Collisions in Sensing-Based Semi-Persistent Scheduling (SPS) by Using Reselection Lookaheads in Cellular V2X," *Sensors*, vol. 18, no. 12, p. 4388, 2018.

[70] J. Yang, B. Pelletier, and B. Champagne, "Enhanced Autonomous Resource Selection for LTE-based V2V Communication," in *2016 IEEE Vehicular Networking Conference (VNC)*, Dec 2016, pp. 1–6.

[71] B. Kang, S. Jung, and S. Bahk, "Sensing-based Power Adaptation for Cellular V2X Mode 4," in *2018 IEEE International Symposium on Dynamic Spectrum Access Networks (DySPAN)*. IEEE, 2018, pp. 1–4.

[72] G. Cecchini, A. Bazzi, B. M. Masini, and A. Zanella, "MAP-RP: Map-based Resource Reselection Procedure for Autonomous LTE-V2V," in *2017 IEEE 28th Annual International Symposium on Personal, Indoor, and Mobile Radio Communications (PIMRC)*, Oct 2017, pp. 1–6.

[73] U. A. Khan and S. S. Lee, "Three-Dimensional Resource Allocation in D2D-based V2V Communication," *Electronics*, vol. 8, no. 9, p. 962, 2019.

[74] G. P. W. NBA, J. Haapola, and T. Samarasinghe, "A Markov Perspective on C-V2X Mode 4," in *2019 IEEE 90th Vehicular Technology Conference (VTC2019-Fall)*. IEEE, 2019, pp. 1–6.

[75] F. Jameel, W. U. Khan, N. Kumar, and R. Jaentti, "Efficient Power-Splitting and Resource Allocation for Cellular V2X Communications," *IEEE Transactions on Intelligent Transportation Systems*, pp. 1–10, 2020.

[76] C. Zheng, D. Feng, S. Zhang, X. Xia, G. Qian, and G. Y. Li, "Energy Efficient V2X-Enabled Communications in Cellular Networks," *IEEE Transactions on Vehicular Technology*, vol. 68, no. 1, pp. 554–564, 2019.

[77] H. W. Kuhn, "The Hungarian Method for the Assignment Problem," *Naval research logistics quarterly*, vol. 2, no. 1-2, pp. 83–97, 1955.

[78] W. Sun, E. G. Strom, F. Brannstrom, Y. Sui, and K. C. Sou, "D2D-based V2V Communications with Latency and Reliability Constraints," in *2014 IEEE Globecom Workshops (GC Wkshps)*, Dec 2014, pp. 1414–1419.

[79] L. F. Abanto-Leon, A. Koppelaar, and S. H. de Groot, "Graph-based Resource Allocation with Conflict Avoidance for V2V Broadcast Communications," in *2017 IEEE 28th Annual International Symposium on Personal, Indoor, and Mobile Radio Communications (PIMRC)*, Oct 2017, pp. 1–7.

[80] L. Liang, G. Y. Li, and W. Xu, "Resource Allocation for D2D-Enabled Vehicular Communications," *IEEE Transactions on Communications*, vol. 65, no. 7, pp. 3186–3197, July 2017.

[81] X. Gu and Y. Ding, "A Dynamic Geo-based Resource Selection Algorithm for LTE-V2V Communications," *EURASIP Journal on Wireless Communications and Networking*, vol. 2018, no. 1, p. 186, 2018.

[82] V. Krishna, *Auction Theory*, 01 2002.

[83] N. Tadayon and S. Aissa, "Radio Resource Allocation and Pricing: Auction-Based Design and Applications," *IEEE Transactions on Signal Processing*, vol. 66, no. 20, pp. 5240–5254, Oct 2018.

[84] L. Song, D. Niyato, Z. Han, and E. Hossain, "Game-theoretic Resource Allocation Methods for Device-to-Device Communication," *IEEE Wireless Communications*, vol. 21, no. 3, pp. 136–144, June 2014.

[85] M. Hasan and E. Hossain, "Distributed Resource Allocation in D2D-enabled Multi-tier Cellular Networks: An auction Approach," in *2015 IEEE International Conference on Communications (ICC)*, June 2015, pp. 2949–2954.

[86] C. Xu, L. Song, Z. Han, Q. Zhao, X. Wang, X. Cheng, and B. Jiao, "Efficiency Resource Allocation for Device-to-Device Underlay Communication Systems: A Reverse Iterative Combinatorial Auction based Approach," *IEEE Journal on Selected Areas in Communications*, vol. 31, no. 9, pp. 348–358, Sep. 2013.

[87] J. Huang, Z. Han, M. Chiang, and H. V. Poor, "Auction-based Resource Allocation for Cooperative Communications," *IEEE Journal on Selected Areas in Communications*, vol. 26, no. 7, pp. 1226–1237, Sep. 2008.

[88] 3rd Generation Partnership Project (3GPP), "3GPP TS 36.300: "Evolved Universal Terrestrial Radio Access (E-UTRA) and Evolved Universal Radio Access Network (E-UTRAN); Overall description; Stage 2 (Release 12)," Mar 2015.

[89] A. Frotzscher, U. Wetzker, M. Bauer, M. Rentschler, M. Beyer, S. Elspass, and H. Klessig, "Requirements and Current Solutions of Wireless Communication in Industrial Automation," in *IEEE International Conference on Communications Workshops (ICC)*, Jun. 2014, pp. 67–72.

[90] 4G Americas, "Recommendations on 5G Requirements and Solutions," oct 2014. [Online]. Available: www.5gamericas.org/index.php/download_file/view/513/162/

[91] 3rd Generation Partnership Project (3GPP), "TR 36.881: Study on Latency Reduction Techniques for LTE (Release 13)," Sep. 2015.

[92] E. Dahlman, S. Parkvall, and J. Skold, *4G: LTE/LTE-Advanced for Mobile Broadband*. Academic press, 2013.

[93] N. Johansson, Y.-P. Wang, E. Eriksson, and M. Hessler, "Radio Access for Ultra-Reliable and Low-Latency 5G Communications," in *IEEE International Conference on Communication (ICC)*, Jun. 2015, pp. 1184–1189.

[94] A. J. Goldsmith and S.-G. Chua, "Variable-Rate Variable-Power MQAM for Fading Channels," *IEEE Transactions on Communications*, vol. 45, no. 10, pp. 1218–1230, 1997.

[95] M. Goemans, K. Jansen, J. D. Rolim, L. Trevisan *et al.*, "Approximation, Randomization and Combinatorial Optimization: Algorithms and Techniques," 2001.

[96] 3rd Generation Partnership Project (3GPP), "3GPP TS 23.003:Technical Specification Group Core Network and Terminals;Numbering, addressing and identification (Release 15)," Sep. 2019.

[97] ——, "3GPP TS 36.213:Evolved Universal Terrestrial Radio Access (E-UTRA);LTE Positioning Protocol (LPP) (Release 15)," Jul. 2018.

[98] ——, "3GPP TR38.840: Study on User Equipment (UE) Power Saving in NR (Release 16)," Jun. 2019.

[99] 3rd Generation Partnership Project (3GPP), "TR 37.885: Study on Evaluation Methodology of new Vehicle-to-Everything (V2X) Use Cases for LTE and NR (Release 15)," Jun. 2019.

[100] K. Brueninghaus, D. Astely, T. Salzer, S. Visuri, A. Alexiou, S. Karger, and G. . Seraji, "Link Performance Models for System Level Simulations of Broadband Radio Access Systems," in *2005 IEEE 16th International Symposium on Personal, Indoor and Mobile Radio Communications*, vol. 4, 2005, pp. 2306–2311 Vol. 4.

[101] S. Jaeckel, K. Raschkowski, K. Borner, L. Thiele, F. Burkhardt, and E. Eberlein, "QuaDRiGa-Quasi Deterministic Radio Channel Generator, User Manual and Documentation, Fraunhofer Heinrich Hertz Institute," Tech. Rep. v1. 4.8-571, Tech. Rep., 2016.

[102] T. Izydorczyk, F. M. Tavares, G. Berardinelli, M. Bucur, and P. Mogensen, "Performance Evaluation of Multi-antenna Receivers for Vehicular Communications in Live LTE Networks," in *2019 IEEE 89th Vehicular Technology Conference (VTC2019-Spring)*. IEEE, 2019, pp. 1–6.

[103] E. Calvanese Strinati, S. Barbarossa, J. L. Gonzalez-Jimenez, D. Ktenas, N. Cassiau, L. Maret, and C. Dehos, "6G: The Next Frontier: From Holographic Messaging to Artificial Intelligence using Subterahertz and Visible Light Communication," *IEEE Vehicular Technology Magazine*, vol. 14, no. 3, pp. 42–50, 2019.

[104] W. Saad, M. Bennis, and M. Chen, "A Vision of 6G Wireless Systems: Applications, Trends, Technologies, and Open Research Problems," *IEEE Network*, vol. 34, no. 3, pp. 134–142, 2020.

[105] S. Mumtaz, J. M. Jornet, J. Aulin, W. H. Gerstacker, X. Dong, and B. Ai, "Terahertz Communication for Vehicular Networks," *IEEE Transactions on Vehicular Technology*, vol. 66, no. 7, 2017.

Erklärung

Ich versichere, dass ich die vorliegende Arbeit ohne unzulässige Hilfe Dritter und ohne Benutzung anderer als der angegebenen Hilfsmittel angefertigt habe. Die aus anderen Quellen direkt oder indirekt übernommenen Daten und Konzepte sind unter Angabe der Quelle gekennzeichnet.

Weitere Personen waren an der inhaltlich-materiellen Erstellung der vorliegenden Arbeit nicht beteiligt. Insbesondere habe ich hierfür nicht die entgeltliche Hilfe von Vermittlungs- bzw. Beratungsdiensten (Promotionsberater oder anderer Personen) in Anspruch genommen. Niemand hat von mir unmittelbar oder mittelbar geldwerte Leistungen für Arbeiten erhalten, die im Zusammenhang mit dem Inhalt der vorgelegten Dissertation stehen.

Die Arbeit wurde bisher weder im In- noch im Ausland in gleicher oder ähnlicher Form einer Prüfungsbehörde vorgelegt.

Ich bin darauf hingewiesen worden, dass die Unrichtigkeit der vorstehenden Erklärung als Täuschungsversuch bewertet wird und gemäß § 7 Abs. 10 der Promotionsordnung den Abbruch des Promotionsverfahrens zur Folge hat.

Erlangen, 21.09.2021 Dariush Mohammad Soleymani